IMPROVE CONTROL STRATEGY FOR POWER SHARING IN ISLANDED MICROGRID

2021
MASTER THESIS
ELECTRICAL & ELECTRONICS ENGINEERING

AIMEN M. ALSHIREEDAH

THESIS ADVISOR
Assoc. Prof. Dr. Ziyodulla YUSUPOV

IMPROVE CONTROL STRATEGY FOR POWER SHARING IN ISLANDED MICROGRID

Aimen M. ALSHIREEDAH

T.C.

Karabuk University

Institute of Graduate Programs

Department of Electrical & Electronics Engineering

Prepared as

Master Thesis

Thesis Advisor

Assoc. Prof. Dr. Ziyodulla YUSUPOV

KARABUK

April 2021

I certify that in my opinion the thesis submitted by Aimen M. ALSHIREEDAH titled "IMPROVE CONTROL STRATEGY FOR POWER SHARING IN ISLANDED MICROGRID" is fully adequate in scope and in quality as a thesis for the degree of Master of Science.

Assoc. Prof. Dr. Ziyodulla YUSUPOV .....
Thesis Advisor, Department of Electrical-Electronics Engineering

This thesis is accepted by the examining committee with a unanimous vote in the Department of Electrical & Electronics Engineering as a Master of Science thesis. April 9, 2021

Examining Committee Members (Institutions)	Signature
Chairman : Assist. Prof. Dr. Ozan GÜLBUDAK (KBU)	.....
Member : Assoc. Prof. Dr. Ziyodulla YUSUPOV (KBU)	.....
Member : Assist. Prof. Dr. Adem DALCALI (BANU)	.....

The degree of Master of Science by the thesis submitted is approved by the Administrative Board of the Institute of Graduate Programs, Karabuk University.

Prof. Dr. Hasan SOLMAZ .....
Director of the Institute of Graduate Programs

"I declare that all the information within this thesis has been gathered and presented in accordance with academic regulations and ethical principles and I have according to the requirements of these regulations and principles cited all those which do not originate in this work as well."

Aimen M. ALSHIREEDAH

ABSTRACT

M. Sc. Thesis

IMPROVE CONTROL STRATEGY FOR POWER SHARING IN ISLANDED MICROGRID

Aimen M. ALSHIREEDAH

Karabük University
Institute of Graduate Programs
The Department of Electrical and Electronic Engineering

Thesis Advisor:
Assoc. Prof. Dr. Ziyodulla YUSUPOV
April 2021, 84 pages

Distributed energy resources are expected to play a vital role to meet the future energy demand response in power system and for the development of Microgrid concept. In the last years, Microgrid as basic part of Smart Grid is being more attractive. It is becoming not only an addition but also an alternative for low and medium distribution network of conventional power systems. Unlike to conventional power systems microgrid operates in two modes, i.e., grid-connected and island modes. Therefore, control strategies of microgrid differs from power systems, too.

The modeling, control design and stability analysis for parallel inverters in the islanded microgrid are considered in this research work. Primary control strategy of microgrid is studied and based on investigations parallel connected inverters technique is proposed to improve microgrid control strategy for island mode operation.

The differences in the type of output impedance (inductor/resistor) of parallel inverters can affect the accuracy of power-sharing and thus destabilize the system. The dissertation studies this phenomenon by utilizing the Bode plot technique. The controller based on virtual impedance is proposed to enhance the stability of the system.

This thesis proposes improved method of controlling reactive power-sharing. The results of the simulation are implemented in MATLAB/Simulink to verify the validity of the theoretical analysis, robustness and efficiency of the proposed controllers. The results of proposed method have compared with a conventional method.

Key Words : Microgrid, distributed generation, reactive power sharing, droop control, island mode, virtual impedance.

Science Code : 90502

ÖZET

Yüksek Lisans Tezi

ADA MİKRO ŞEBEKEDE GÜÇ PAYLAŞIMI İÇİN KONTROL STRATEJİSİNİN GELİŞTİRİLMESİ

Aimen M. ALSHIREEDAH

Karabük Üniversitesi
Lisansüstü Eğitim Enstitüsü
Elektrik ve Elektronik Mühendisliği Anabilim Dalı

Tez Danışmanı:
Doç. Dr. Ziyodulla YUSUPOV
Nisan 2021, 84 sayfa

Gelecekte güç sisteminde enerji talebinin karşılanması ve Mikro Şebeke konseptinin geliştirilmesi için dağıtılmış enerji kaynaklarının hayati bir rol oynaması beklenmektedir. Son yıllarda, Akıllı Şebekenin temel parçası olan Mikro Şebeke daha çekici hale gelmektedir. Geleneksel güç sistemlerinin düşük ve orta dağıtım ağları için sadece bir ek değil, aynı zamanda bir alternatif haline gelmektedir. Geleneksel güç sistemlerinden farklı olarak mikro şebeke iki moda çalışır, yani şebekeye bağlı ve ada modları. Bu nedenle, mikro şebekenin kontrol stratejileri de güç sistemlerinden farklıdır.

Ada mikro şebekedeki paralel eviricilerin modellemesi, kontrol tasarımı ve kararlılık analizi bu araştırma çalışmasında dikkate alınmıştır. Mikro şebekenin birincil kontrol stratejisi incelenmiştir ve araştırmalara dayalı olarak, ada modu işletimi için mikro

şebeke kontrol stratejisini iyileştirmek için paralel bağlı invertörler tekniği önerilmiştir.

Paralel eviricileri çıkış empedansının (indüktör /direnç) tipindeki farklılıklar, güç paylaşımının doğruluğunu etkileyebilir ve böylece sistemi kararsız hale getirebilir. Tezde Bode diagramini kullanarak bu fenomen incelenmiş. Sanal empedansa dayalı bir kontrolör mikro şebeke sisteminin kararlılığını artırmak için önerilmiştir.

Bu tez, reaktif güç paylaşımını kontrol etmek için geliştirilmiş bir yöntem önermektedir. Simülasyonun sonuçları, önerilen kontrolörlerin teorik analizinin, sağlamlığının ve verimliliğinin geçerliliğini doğrulamak için MATLAB/Simulink'te uygulanmış. Önerilen yöntemin sonuçları geleneksel bir yöntemle karşılaştırıldı.

Anahtar Kelimeler : Mikro şebeke, dağıtılmış üretim, reaktif güç paylaşımı, düşüş kontrolü, ada modu, sanal empedans.

Bilim Kodu **:** 90502

ACKNOWLEDGMENT

Firstly, I would like to express my sincere gratitude to my supervisor Assoc. Prof. Dr. Ziyodulla YUSUPOV for his continued support to me to finish my master's degree, thanks for his motivation, enthusiasm, patience, also always his door was open to me for any trouble or question related to my research and he steered me in the right direction for writing my thesis paper.

My sincere thanks also to my parents, children, and my family, and I must express my profound gratitude to my wife for the unfailing support to me throughout my years of study. This fulfillment would not have been possible without them.

CONTENTS

Page

Page

Page

LIST OF FIGURES

Page

Page

LIST OF TABLES

Page

PART 1

INTRODUCTION

1.1. CONCEPT OF MICROGRID

The attention to distributed generation systems (DG) is growing rapidly, as enormous power plants have become less viable due to increased fuel prices, its finite availability and knowledge of the adverse effects of burning fossil fuels on humans and the environment also rigid environmental regulations [1]. Furthermore, the latest technological advances to small generators, energy storage devices and power electronics offered new opportunities related to distributed energy resources in distributed level. There are several disadvantages to the traditional central power generation system. First, power plants rely significantly on fossil fuels, which increases carbon dioxide emissions and wastes heat. Second, a big amount of electricity is generated in one place and transmitted using expensive transmission lines and transformers. Third, these latter because several problems including voltage droop and power loss. Fourth, traditional centralized power generation cannot provide economically appropriate solutions to supply electricity poor and remote communities. Integration of renewable energy (like wind, solar energy) help reduce carbon dioxide emission from energy sources dependent on fossil fuels, reduce losses in transmission, reduce voltage variance, mitigate peak loads and improve supply reliability. On the other hand, excess penetration to DG sources (especially in distribution networks) can cause issues like voltage rising, voltage and frequency instability, and lack of coordination between protection [2,3]. These problems are mitigated by combining multiple DG sources and loads and implementing a controller on them, and this is called a microgrid (MG), as shown in Figure 1.1.

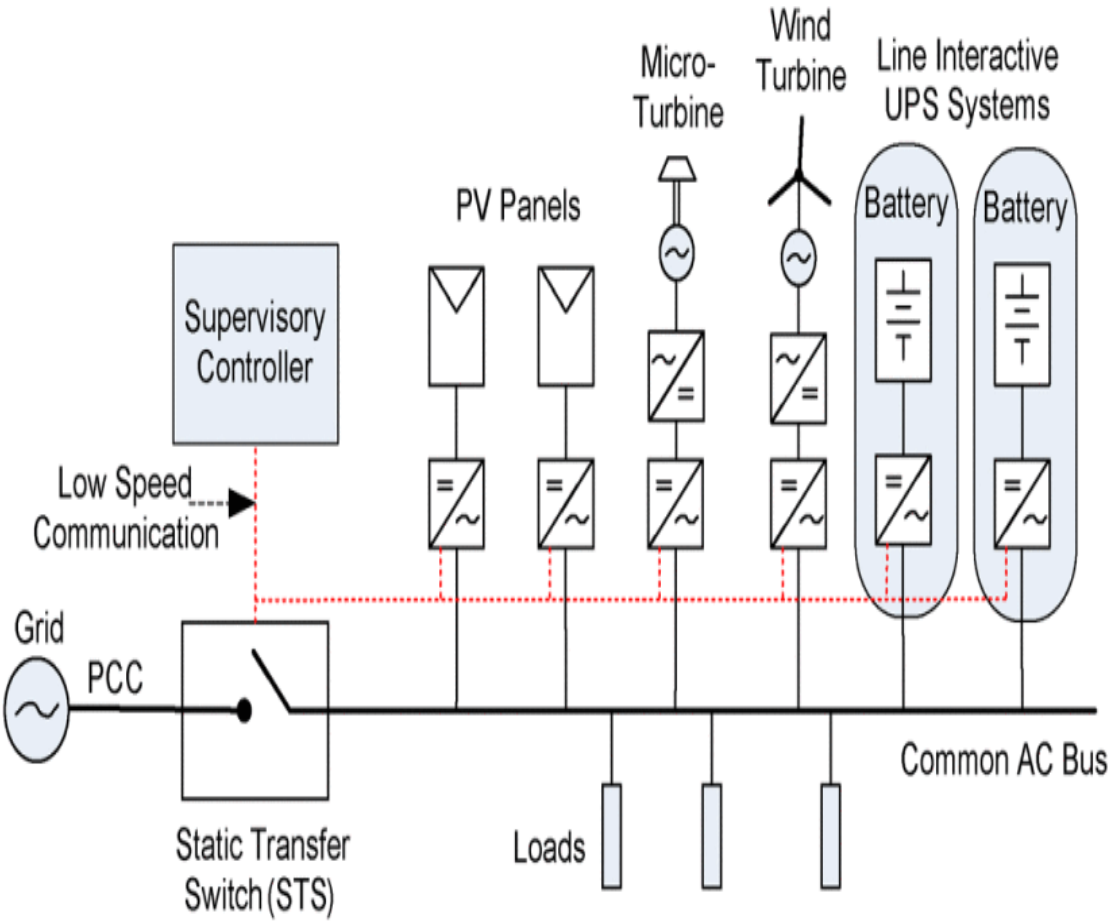

Figure 1.1. Microgrid structure [4].

There are several advantages to the MG, such as high reliability, high controllability and high-power quality. MG is a small power system where the generation and distribution of electricity to the consumer execute locally [5].

MG includes DG sources like photovoltaic modules (PV), wind turbine, gas microturbines, and also energy storage systems (battery, flywheel, supercapacitors) to provide power for loads [6]. These DG sources cannot be easily connected with the utility grid in direct current (PV and batteries) or in alternating current with variable frequency (wind turbine/gas microturbines). Electronic power converters therefore necessary to link these DGs with the grid. Network interface inverters are connected to an AC bus in parallel, which will be connected to a utility grid through a static transfer switch. The load is tied to a microgrid side through the static transfer switch (STS). The MG is operating in two modes: grid connecting mode and an island (stand-alone mode). While the MG is in on-grid mode, is able to export or import electricity

from the grid, which acts as a manageable source or load. Further, the grid defines MG's apparent power flow to minimize imported electricity from the main grid. In the other mode (island mode), the MG is designed to operate in an isolated mode, when the grid is isolated (STS open) because of emergencies, fault, or natural disasters, all electricity is supplied by power sources that are locally available in the MG [7].

A vital part of any MG is the inverter, which is founded on power electronics consisting of semiconductor components with high-frequency switching and low-pass filter as seen in Figure 1.2. An inverter input is a direct current which is produced via the DC coupling capacitor, whereas the output is alternating current, which is generated at the inverter output. The switching devices, Insulated-gate bipolar transistor (IGBT), that through a voltage regulator, it receives control signals, then generates pulse width modulation signal (PWM) which is associated with a reference voltage. The switching tool's AC output produces several harmonic signals that arise from switching so the LCL filter was used to minimize harmonics and generate the power signal of the sine wave.

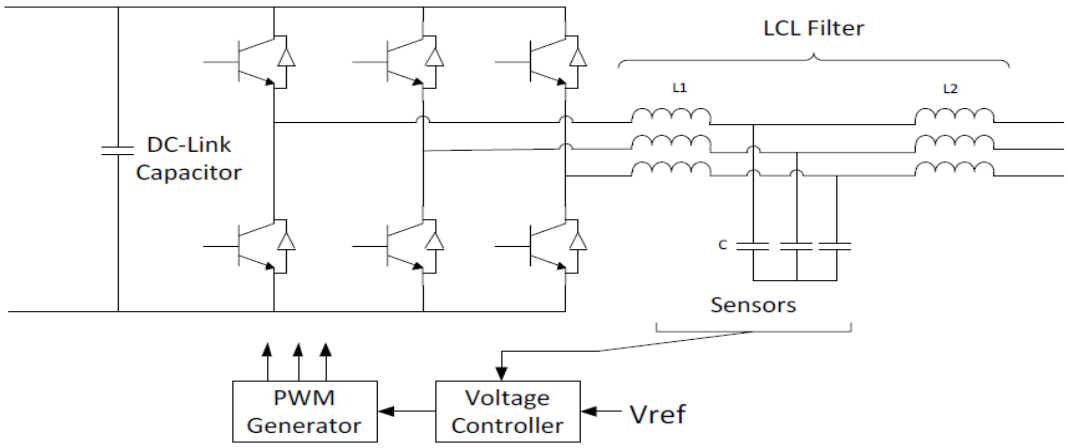

Figure 1.2. Inverter structure including 6 IGBT and LCL [8].

The major emphasis of this study is to improve control strategy technics for droop control-based inverters in island position that shape a microgrid. High reliability, stability and robustness should be supported by the control system against the sudden change in load and also the unequal output impedance between DG units due to the difference of cables length among all paralleled inverters), that lead to inaccurate

droop control, especially with regard to reactive power-sharing (*Q*). Frequency and voltage stabilization must be maintained, so the accuracy of power-sharing among all paralleled inverters is important to reach high stability. Inaccuracy power-sharing could get to undesirable circulating power flow. Also since the power-sharing is load-dependent, thus the total power of the parallel inverters have to be more than or equal to the demanded load in order for to stability is achieved [9]. Using traditional droop control, accurate active power-sharing could easily be accomplished since the frequency of the system could be viewed as virtual communication bond among the inverters. *Q*-sharing in island microgrid, however, rely on output voltages that may differ from point to point relying on interconnecting cables' impedances and the place each inverter. Prior research has shown that the communication bond among inverters and the supervisory controller, through sensing those voltage nodes, has an essential role to maintain precise reactive power-sharing. The lack of this contact, however, could get to instability. Some literature addressed the effect of the difference in the type of output impedances of parallel inverters and revealed that this could generate resonance and make instability. However, the emphasized effect of various feedback signals of the loop of voltage control on the shape of output impedances is not clarified well thus for getting robust controllers against this issue, further work is still required.

1.2. THE RESEARCH PROBLEM

A natural problem for inverters operates in parallel in the islanded microgrid is how to accurately share the load between them. In paralleled inverters, the droop control was invariably the first option. When using this traditional technique against the sudden change in load and also the unequal output impedance between DG units, although real power-sharing in island MG is usually accurate, it is inaccurate for reactive power-sharing so causes instability [10]. In addition, the different nature of the output impedances of paralleled inverters that relies on different voltage controllers of inverters has shown that these may perform resonance and thus to instability.

1.3. THESIS OBJECTIVES

This dissertation is concerned on basic study of techniques for controlling island MG based on droop-control. The dissertation also presents the investigation of equal shared use of reactive / active power among inverters. Moreover, developing a conventional droop control element, demonstrating its strengths and weaknesses, and implementing some feasible solutions such as virtual impedance.

1.4. CONTRIBUTION

The major contribution of this dissertation is designing a controller for a group of connected inverters in parallel in island mode, where the droop control technic is applied to realize power-sharing in the island mode. Adding an improvement to traditional droop control through proposed control makes accuracy reactive power-sharing thus maintaining stability. In addition, Investigations into virtual impedance influence on the stability of inverters connected in parallel. Moreover, the study on the different output impedance natures that affect stability is developed. To improve system stability, voltage controllers with double loops are offered.

1.5. THESIS ORGANIZING

Part 1 presents an introduction to the microgrid. Part 2 introduces the architecture and properties of microgrids. Literature review related to power-sharing techniques; particularly drooping control is presented in Part 3. Part 4 studies the impact virtual impedance on the stability of inverters connected in parallel. Moreover, studies the influence the different nature of the output impedance that relies on different voltage controller of inverters. In Part 5, the inaccuracy of reactive power-sharing is illustrated in island mode, and the controller is proposed to improve system operation. Chapter 6 offers conclusion and future works.

PART 2

THE ARCHITECTURE AND PROPERTIES OF MICROGRID

2.1. INTRODUCTION

The idiom microgrid (MG) points to the notion of singular subsystems for electrical power that are connected to a number of DERs with a bunch of loads [11]. Renewable energy sources integration help reduce carbon dioxide emission from fossil fuel-based energy sources, reduce transmission losses, reduce voltage variance, mitigate peak loads and improve supply reliability. On the other hand, excess penetration to DG sources (especially in distribution networks) can cause issues like voltage rising, voltage and frequency instability, and lacking coordination between protection. These issues are mitigated by combining multiple DG sources and loads and implementing a controller on them, and this is called a microgrid. In another meaning, the microgrid could be a small power system where creates, distributes, and adjusts the flow of electricity from local DERs to local loads which allows it to connect with the grid or work as stand-alone as shown in Figure 2.1. In the Table 2.1, the properties of MG are compared to the conventional power grid.

Table 2.1. Comparison of MG properties with conventional power grid.

Microgrid	Conventional Grid
bidirectional	One directional
A lot of Sensors	Few sensors
Digital	Electromechanical
Pervasive control	Limited control
Distributed generation	Centralized generation
Self-healing	Manual restoration
Self-monitoring	Manual monitoring

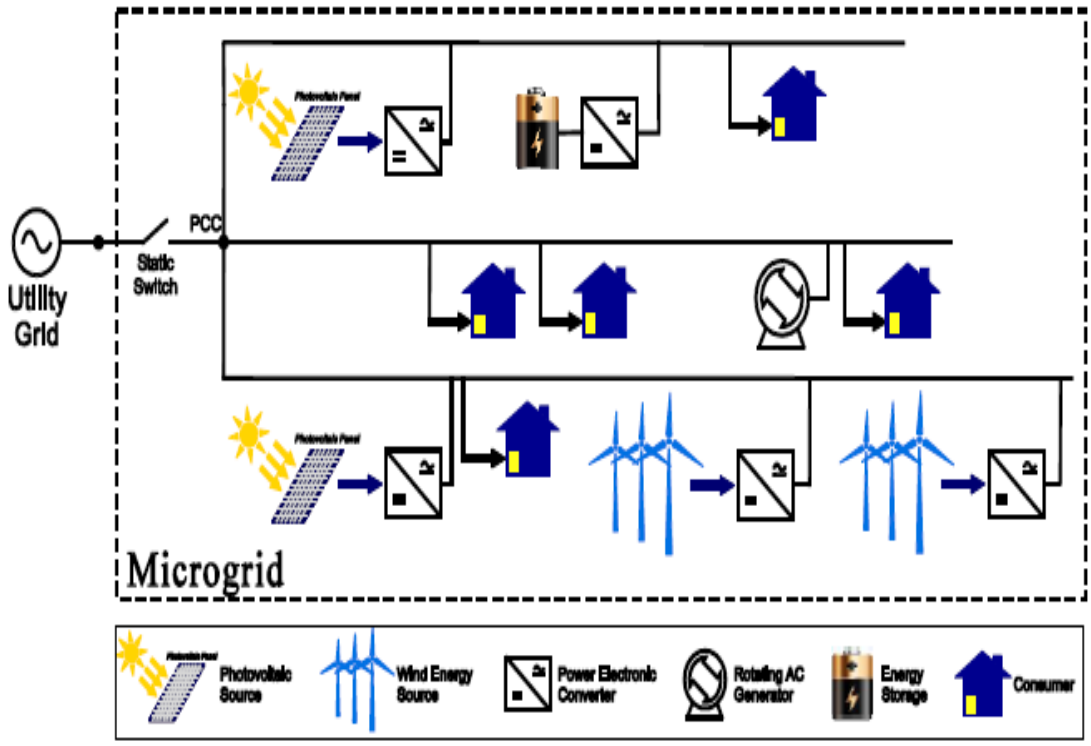

Figure 2.1. An instance of the microgrid [12].

2.2. THE ARCHITECTURE OF MICROGRID

The fundamental architecture of MG is illustrated in Figure 2.2. This shows that MG systems usually constituted of distributed generation sources, storage systems, distribution systems, communication systems, control and loads. The capacity of MG to connect and disconnect a utility grid a utility grid and work independently and efficiently when needed to support local loads. It is strategically important to design a flexible and suitable architecture of the MG system that functions efficiently in isolated and networked methods [13]. From a grid perspective, the principal feature of MG is it is dealt with as controlled within the electrical system that could act as the single load. From the customer's perspective, MG is advantageous because it can meet their need for electricity and heating locally, deliver uninterrupted electricity and improve electricity quality.

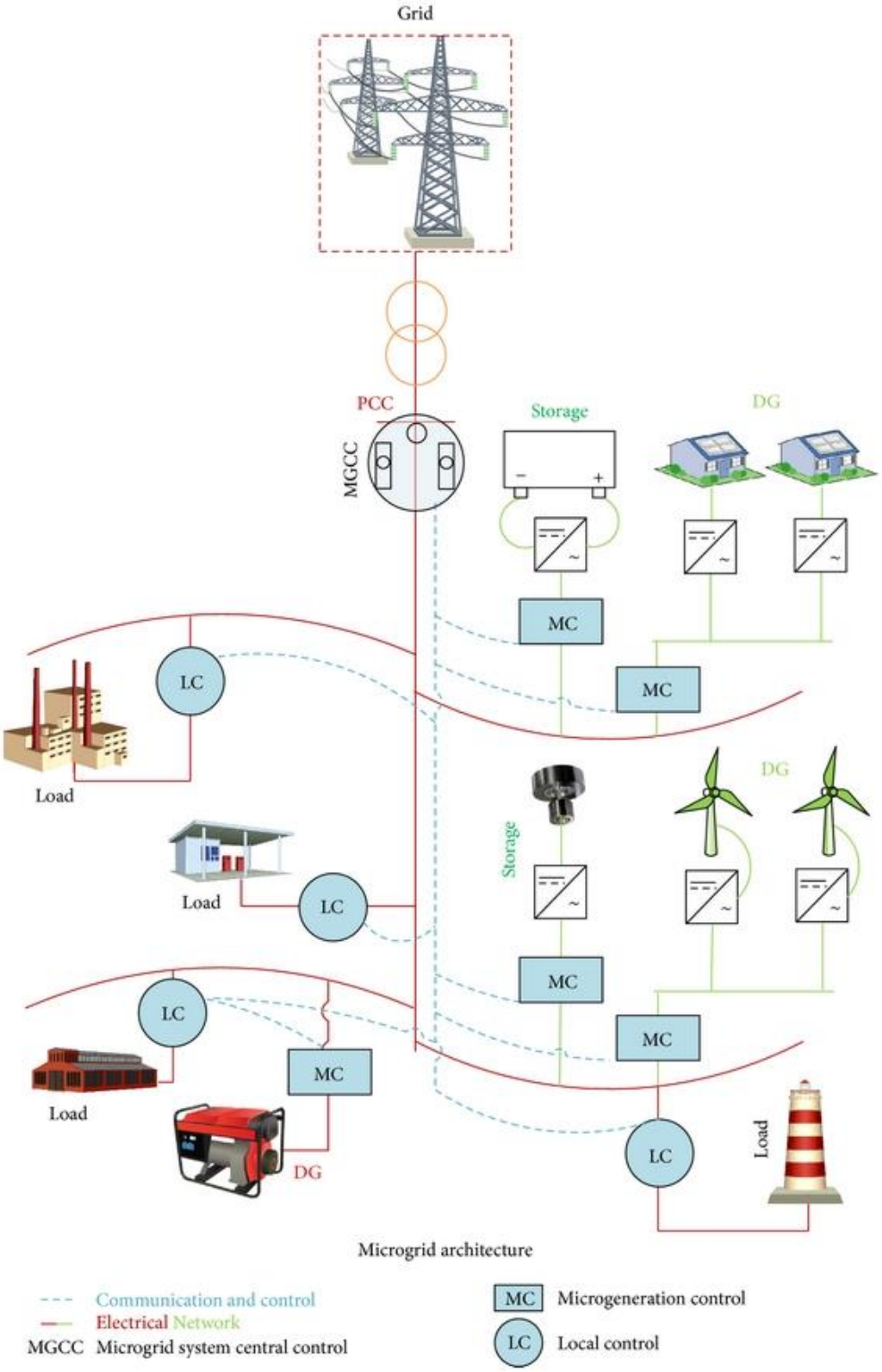

Figure 2.2. Microgrid architecture [11].

2.3. OPERATION MODES OF THE MICROGRID

One of the microgrid's characteristics is that it is running in two modes: connected to the grid and an island (stand-alone mode). Moreover, it can go from one run mode to another one smoothly. This section describes the characteristics of the two modes of operation.

2.3.1. Island Mode

During the MG is not connected to the utility grid due to open STS is opened, it indicates that it is in island mode. This mode requires DERs being sent within the MG in a coordinated manner in order that regulates voltage and frequency. Successful operation on the island also requires the power demand management execution to balance the generation load. Island mode has two situations: intentional and unintentional. The intended island is created based on a pre-planned decision and opens STS at a predetermined time. Typically, preventive measures are undertaken to bring the intended transition from connected to unconnected mode as smoothly as possible. However, the unintentional island may occur due to the sudden failure in the grid. In this case, by continuously monitoring the network condition, STS recognizes the exceptional state and separates MG from the grid, ensuring continuity of supply of local loads and protection of distributed generators and energy storage units consequently, it improves MG reliability.

2.3.2. Connected to Grid

Under this mode, the MG is in on-grid mode, is able to export or import electricity from the grid, which acts as a manageable source or load. Further, the grid defines MG's apparent power flow to minimize imported electricity from the grid. In the other mode (island mode), the MG is designed to operate in an isolated mode, when the grid is isolated (STS open) because of emergencies, fault, or natural disasters, all electricity is supplied by power sources that are locally available in the MG.

2.4. THE COMPONENTS OF THE MG

Although the complexity of MG, it can determine its basic components namely prime movers, energy storage system (ESS), load, and control unit, resulting in Figure 2.3.

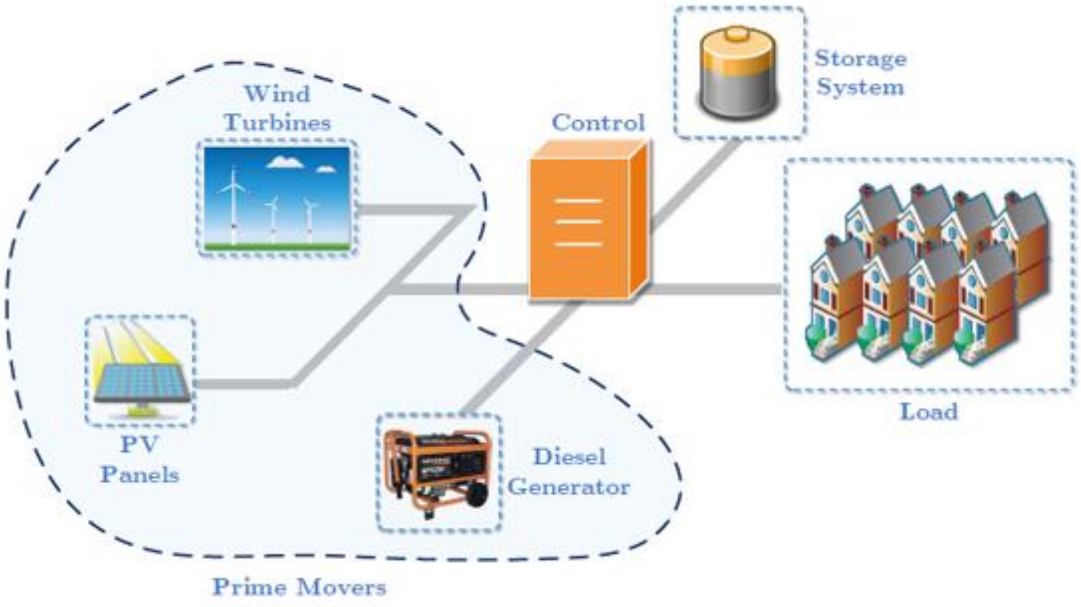

Figure 2.3. Components of the MG [14].

2.4.1. Distributed Generators

MG contains various kinds of generation resources in their range, enabling them to utilize available resources such as sun, wind, water, biomass, etc., and some other DGs are conventional. Another type of source is utilized in combine heat and power (CHP) systems like microturbines. Table 2.2 displays some of the standard characteristics of generally utilized DG sources. DG can act as current source (CSI) or voltage source inverter (VCI) depending on mode that it operates in. VSI is mainly utilized for energy storage system, while CSI is used for wind turbines or photovoltaic cells, requiring maximum power tracking algorithm [15].

Table 2.2. Typical characteristics for common DG sources [11].

Characteristics	Solar	Wind	Microhydro	Diesel	CHP
Availability	Geographical location dependent	Geographical location dependent	Geographical location dependent	Any time	Dependent on source
Output power	DC	AC	AC	AC	AC
GHG emission	None	None	None	High	Dependent on source
Control	Uncontrollable	Uncontrollable	Uncontrollable	Control lable	Dependent on source
Typical interface	Power electronic converter (DC-DC-AC)	Power electronic converter (AC-DC-AC)	Synchronous or induction generator	None	Synchrono -us generator
Power flow control	MPPT&DC link voltage controls (+P,±Q)	MPPT, pitch & Torque control (+P,±Q)	Controllable (+P,±Q)	Control lable (+P,Q)	AVR and governor (+P,±Q)

At the MG level, various technologies are ordinarily installed that contribute efficiently to electricity generation when consumers demand an environmentally friendly production system at reasonable prices. Therefore, renewable energy resources (RERs) are seen as the best means for generating electricity to ride local load demands with less comparable transmission costs and losses, involving the environmental influence on electricity generation.

2.4.2. Storage Systems

Energy storage is modern technology and plays a vital role at MG, it is considered to be one important factor for the succeeded operation of MG, where it balances power demand with generation. Therefore, the system with a number of micro-sources that are designed for operation in island mode should provide storage options for insuring the power balance. Storage devices such as batteries, super capacitors, and flywheels are very significant to compensate for disturbances in the power grid and large load changes [16]. In the event of sudden changes in a grid system, these appliances could conduct as voltage sources. Therefore, a grope of batteries with wind turbines, solar

PV, biomass and microturbine are generally installed to store energy. Likewise, hydroelectric and fuel cell plants incorporate flywheel and supercapacitor bank techniques to store power within off-peak times. Table 2.3 presents characteristics of energy storage devices.

Table 2.3. Basic storage devices' characteristics [11].

Basic features	**Battery**	**Flywheel**	**Super capacitor**
Continuous power (W/kg)	50-100	200-500	500-2000
Typical backup time	5-30 min	10-30 sec	10-30 sec
Losses at standby	Very low	Variable	High
Environmental impact	Medium-high	Low	Low
Maintenance	1/year	1/5 year	None
Charging efficiency (%)	75-95	90	85-95
Current energy price ($/kWh)	150-800	3000-4000	4000-5000
Service life (year)	5	20	>10

2.4.3. Loads

Consumers in MG can be classified into several types of loads, they may be industrial or residential. Furthermore, there is another way to distinguish the loads, which is the need for continuity of electricity in terms of the importance of the loads. These loads could be non-critical or critical, such as hospitals and monitoring rooms, so that these services include priority for critical load and thus ensure the continuity power for them, which increases the reliability factor. Another criterion for rating loads is their linearity. In fact, when the impedance of the load changes with the voltage applied to it, it is classified as non-linear such as rectifier and also motor loads, which causes harmonics in the current and causes distortions in the voltage wave.

2.4.4. Control Unit

It is necessary to coordinate the interaction amongst all components in the system so MG can meet the limitations, especially when the transfer process between the two modes to achieve stability and power quality. That is the role of the controller. MG is joined to the network via STS, which is controlled via the MG central control unit (MGCC) and can also denote it as a supervisor unit. The control of each DG unit also contains an overlapping control loop, which together offers stability as well as precise control of active power and also reactive power for both modes.

2.5. TYPES OF MICROGRID

MGs are classified based on a common bus and distributed power of MG (DC, AC (line frequency) or a combination of AC-DC – hybrids microgrids).

2.5.1. AC Microgrid

By leveraging the existing infrastructure of the AC network such as transformers, distribution and protections AC type of MG is more effortless to implement and design. Numerous MG projects around the world have developed depend on that concept. A typical AC MG structure is illustrated in Figure 2.4. AC bus is used near PCC that is usually designated as a power interface between MG and the utility grid. MG is able to be connected in both modes, relying on the operation needs [17]. This type of MG offers the possibility of integrating DG into the network in a simple manner without major changes. Moreover, the wide range of protective devices on the markets enables a high ability for fault management. Furthermore, voltage levels can easily be edited with low frequency transformers. However, AC architecture has certain disadvantages, such as the requirement of synchronization by the DGs also the circulation of reactive power which makes some losses into the network [14]. In this project, the focus is on the AC MGs.

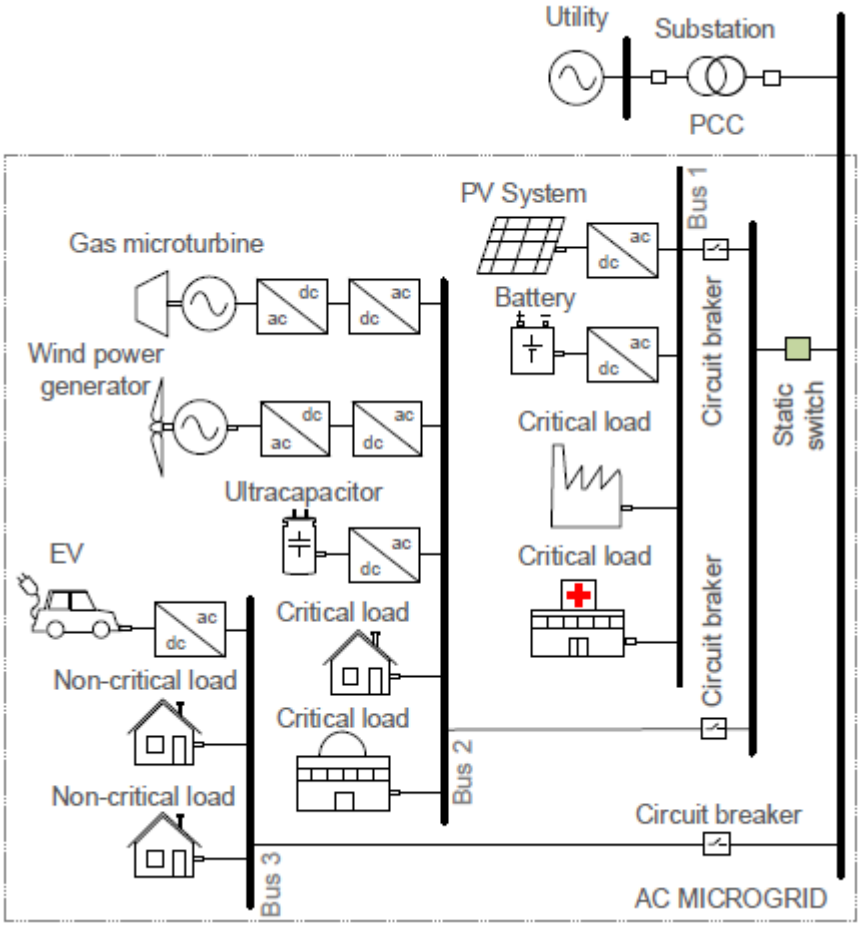

Figure 2.4. AC MG with critical and non-critical loads [18].

2.5.2. DC Microgrid

Figure 2.5, illustrates the DC MG structure. In this architecture, the DC MG is connected with the grid at the PCC node by a two-way electronic converter called interlinking converter (IC) that allows power exchange in both directions. Most DERs operated usually with DC or have the intermediate circuit dc-link at their electronic power interface, while the endpoint connection of ESSs is exclusively direct current. Furthermore, many electricity consumer loads are supplied with direct current. Consequently, integrating these devices into DC microgrids via DC-DC converters is considered a good choice in terms of increasing efficiency, because fewer converting stages required and there is no reactive power generation. In addition, no synchronization operation is required for the DGs connection. The cons of this type are the requirement for DC conversion to AC at the connection point to the grid. Another issue is the protection part for the DC MG network.

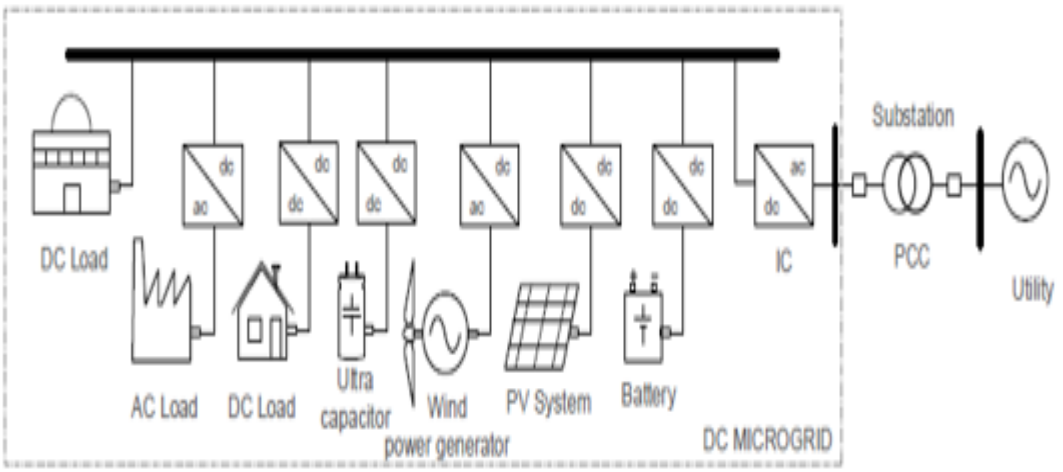

Figure 2.5. DC microgrid [18].

2.5.3. Hybrid Microgrid

A sample hybrid MG structure is illustrated in Figure 2.6. It consists of DC and AC networks, and they are interconnected through a two-way main two-way AC-DC main converter. This structure enables loads to be installed on the DC feeder together with the loads installed on the AC feeder [19]. Hybrid MG collects the advantages both of DC and AC MG and has an Exclusive network for each kind. The cons of this type are the protection aspect of DC MG poses a problem. In addition, the management of this structure is also more complex Because of hardware control requirements associated with DC and AC MGs [20].

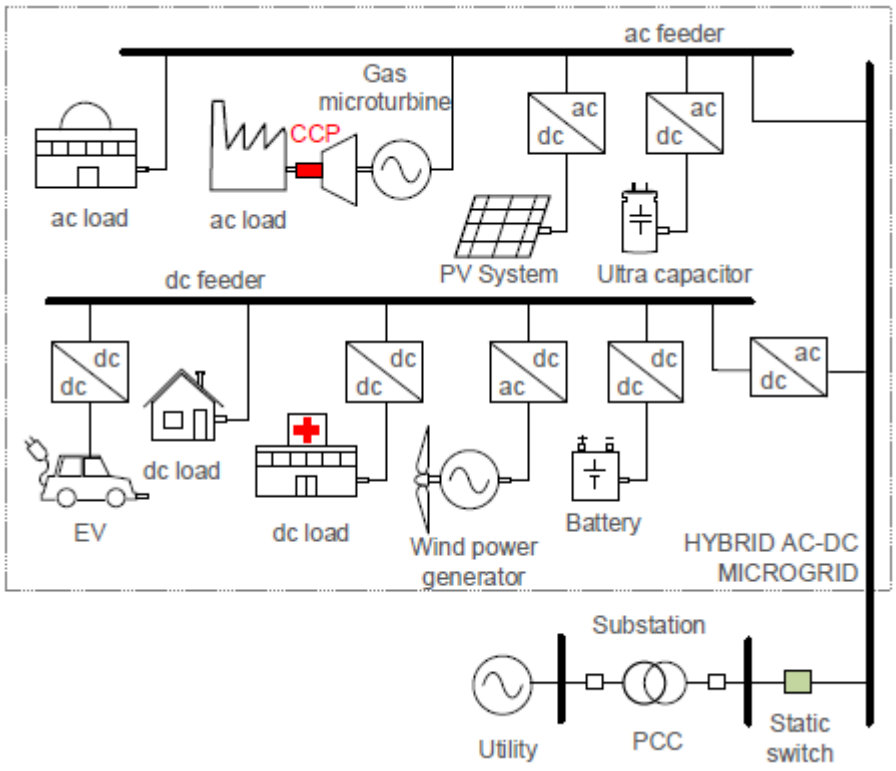

Figure 2.6. Hybrid microgrid [18].

2.6. CONCLUSION

Renewable energy source integration help reduce carbon dioxide emission from fossil fuel-established energy sources, reduce transmission line losses, reduce voltage variance, mitigate peak loads and improve reliability. On the other hand, excess penetration to DG sources (especially in distribution networks) can cause issues like voltage rising, voltage and frequency instability, and lacking coordination between protection. These issues are mitigated by combining multiple DG sources and loads and implementing a controller on them, and this is named a microgrid. In another meaning, the microgrid could be a small power system where creates, distributes and adjusts the flow of electricity from local DERs to local loads which allows it to connect with the grid or work as stand-alone. The microgrid architecture and components are discussed in depth in this chapter. The majority of current systems are AC, but technological advancements will enable hybrid microgrid architectures to emerge.

PART 3

INVERTER BASED MICROGRID CONTROL TECHNIQUES

3.1. HIERARCHICAL CONTROL OF MICROGRID

To develop a flexible and reliable microgrid, the control tasks of MG is divided over levels, namely the primary, secondary and tertiary. These levels separate the control features and create the management system to restore frequency & voltage, compensate reactive power, mode transfer, regulate voltage and share power. In Figure 3.1 the overall hierarchical control shape is introduced, along with a concise overview main tasks of every controller's level [21].

1. Primary control. It performs to maintain voltage and stabilizes frequency of microgrid following the islanding procedure. It is also responsible for regulating *V* and *I* according to a specific reference.
2. Secondary control. This level control compensates the deviations in frequency and voltage in the MG distribution network. It offers a mechanism for synchronization to logically bind or disconnect the MG on the grid. In secondary control the MG's voltage/frequency values are tested and the nominal values are restored. However, this control reacts more slowly than the level of primary control. The secondary level is classified as centralized & distributed (decentralized) control, which is discussed in [22].
3. Tertiary Control. Tertiary control is highest level of hierarchical control responsible for improving the operation of the MG and interacting with the distribution.
4. Network to provide a reference of reactive & active power for the units. This level controls the flow of energy between the MG and the utility. It is responsible for the importing/exporting power for MG [23].

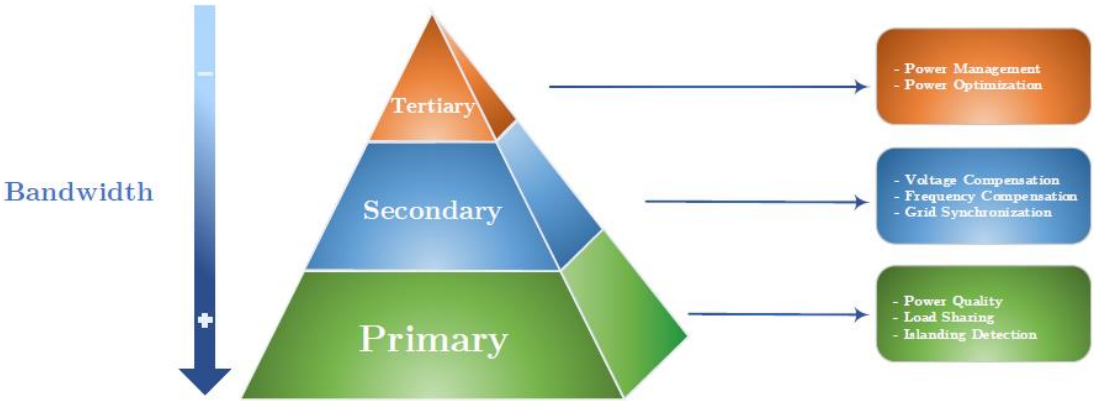

Figure 3.1. Hierarchical control structure of MG [21].

In [21], a PI controller was proposed to carry out secondary, tertiary control after voltage *V*, current *I* and frequency ω were sensed on two sides of the STS, then sent over a low-bandwidth communication. With this type of control level, a smooth transition is made to decrease circulation currents flows. Further work is proposed in [4,24,25] for the management of these tasks.

The actuality that MG has several DGs units that can work in the two modes, this poses several problems that can cause challenges, especially when transferring between operation modes. This section reviews the literature to spotlight key challenges for MG development and recent results of related studies. The work focuses on control strategy, especially on island mode, in relation to voltage regulators, power-sharing, modeling, and stability problems.

Figure 3.2 shows single-line MG diagram, which contains PV system, wind turbine (WT) system, and ESS. The inverter has interfaced with the PCC bus via a power converter and wires. Via the STS which could be operated by the MG central controller (MGCC) and can rather be denoted as a supervisor unit, the MG is associated to the grid. It also sends all DGs configurations and *V*, ω, and power setpoints over communication's low bandwidth channel. Moreover, it has the option of deciding the mode transfer of the process from connected to the island-mode as well as vice versa. The control loops of each unit are nested, which offer stability and precise control of power in the two-mode. It should be noted here DC sources are supposed to have a reliable, controlled output in all distributed generators that can be ready for use via

DC/AC converters. Within this work, the regulation of direct current sources will not be discussed.

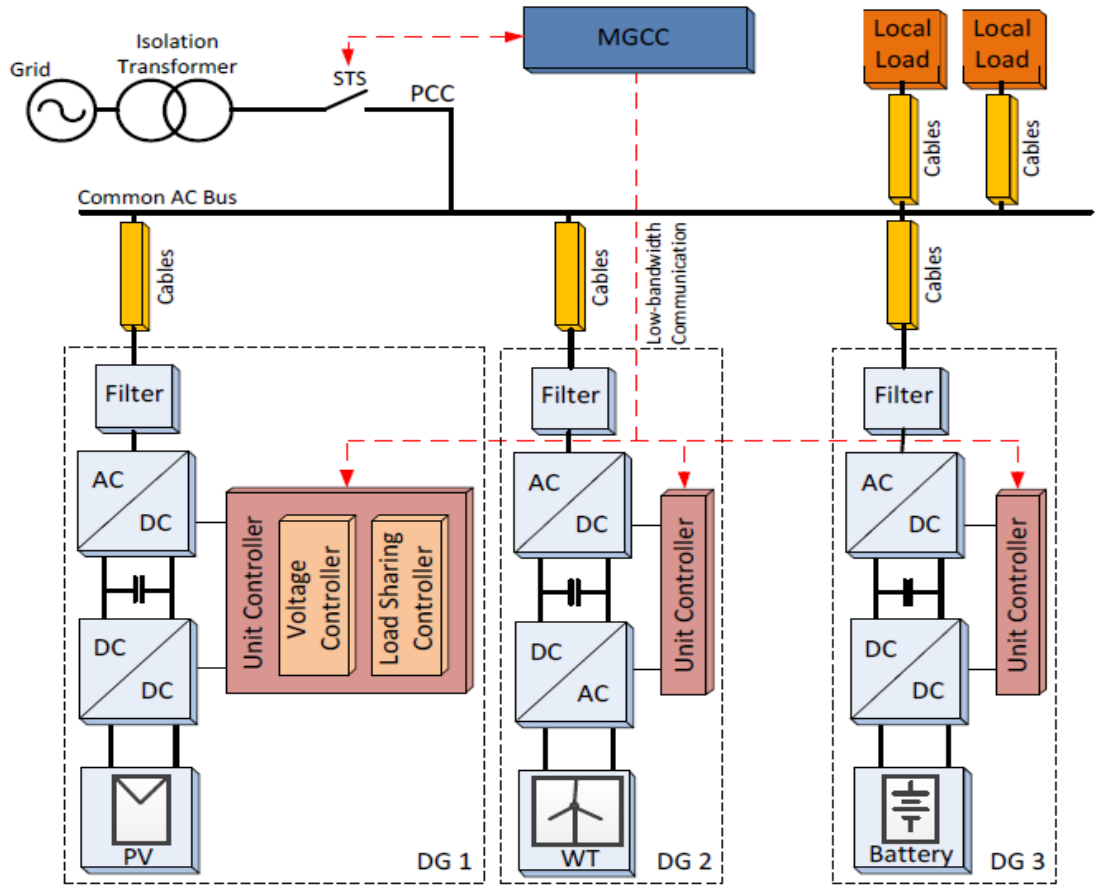

Figure 3.2. The Microgrid control structure [10].

3.2. CONCEPT OF DROOP CONTROL

In island mode, the goal of MG control is to realize precise power sharing while accurately regulation of the voltage amplitude & frequency. To attain the above objectives, two control methods can be followed:

1. Master – slave control [26, 27]. In order to realize precise power sharing, this control system utilizes high-speed communication among inverters by having one inverter play the master role of VCI to control ω and V of the MG, while other inverters work as CCI (Figure 3.3). The main drawback of this method is to utilize a high-speed communication that is expensive and reduces the

system's reliability. Since the entire system will fail if the master unit fails. In addition, a transition between both modes does not smooth [4].

2. Wireless methods that rely on droop control [27–29]. The wireless name is displayed because this method does not require communication among the inverters.

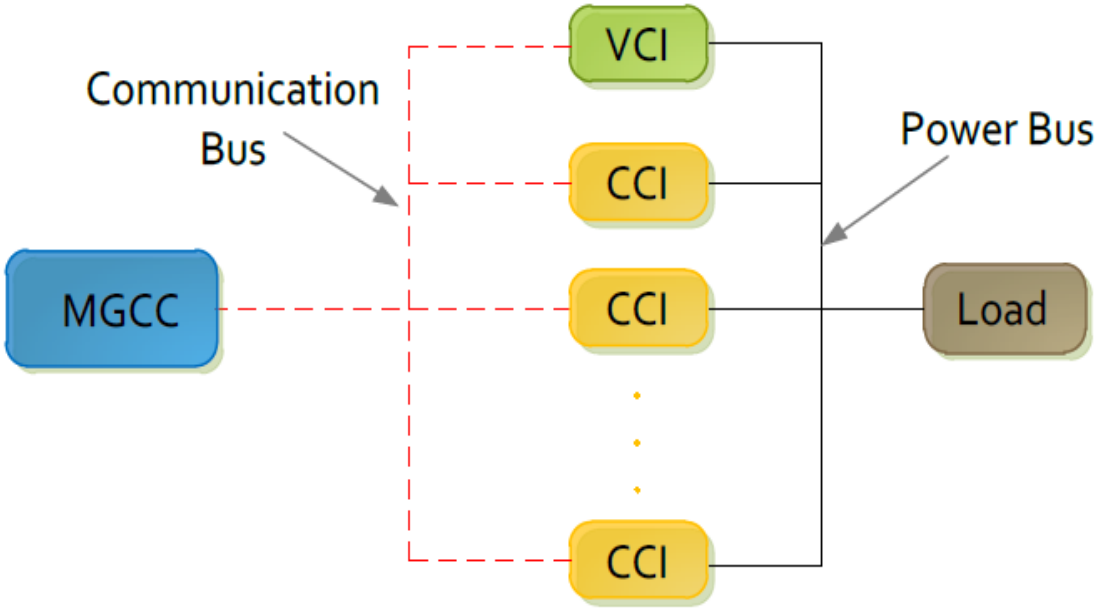

Figure 3.3. Schematic diagram of master-slave control.

In our work we are used droop control wireless method. The parallel wireless architecture relies on the inverter's ability for regulating both the output V and ω at the same time sharing the requirements for apparent power. The droop control is a key of wireless technology [30,31] which is commonly used in traditional systems of power generation. The benefit of this method is no external mechanism of communication between each device and the central monitoring controller may still be utilized for surveillance and administrative problems. Furthermore, the simple implementation allows plug-and-play operation, which simply relies on the local voltage and current. Therefore, the ease of system is increasing.

As mentioned above, the droop control in island mode does not require the communication. The strong of droop control emerges when all inverters need to share power with no need to connect with others according to their rating. The power flow

supply system between two inductor-separated voltage sources is shown in Figure 3.4. It shows how the P can be regulated through the phase angle between the voltage signals and the Q by adjusting the amplitude difference between these sources. In practice, since a resistance value can influence performance inductive, output impedance cannot be strictly inductive.

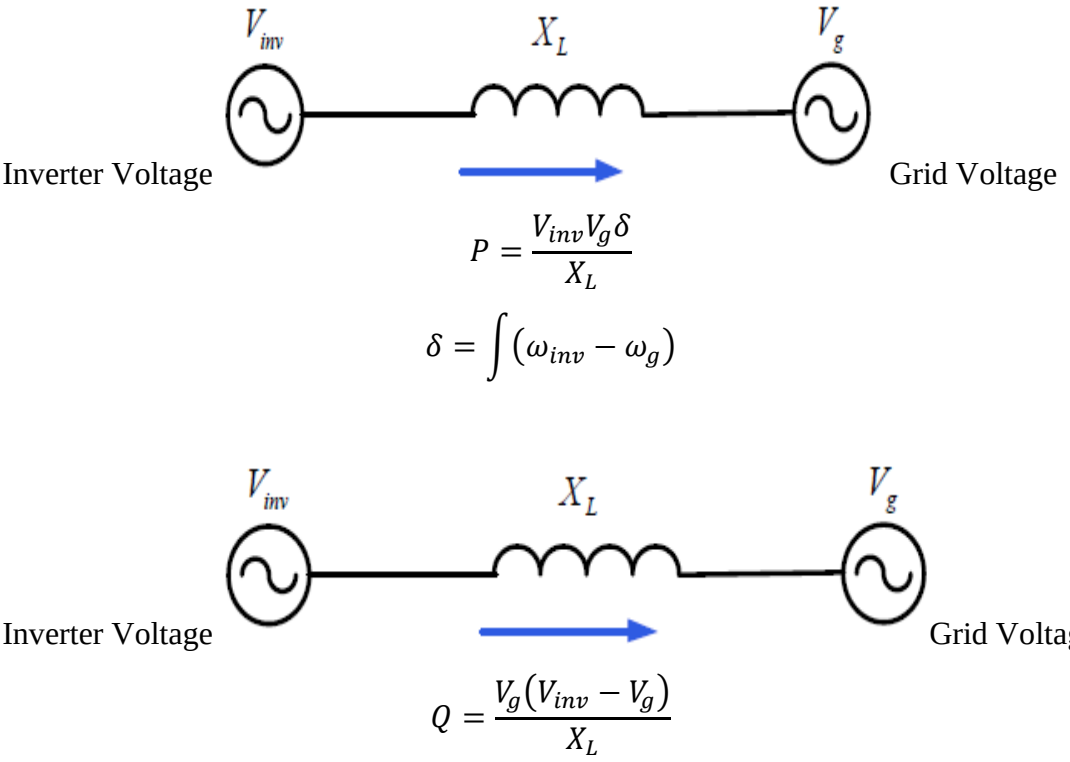

Figure 3.4. Control of power flow between two nodes.

Figure 3.5 shows two parallel inverters that sharing load. Both inverters are jointed to load via the output impedance. Both the reactive & active power exported by each inverter can be done in one of two ways relying on the type of output impedance.

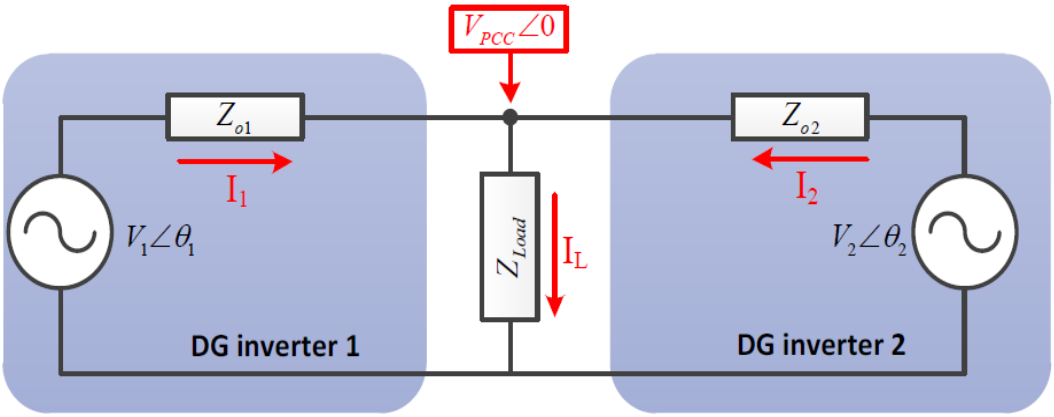

Figure 3.5. The connection two inverters with the load in island-mode.

Output impedance may be either mostly resistive or inductive, which determines how an inverter will control with exporting power. If output impedance of inverter was entirely inductive, P produced relies on phase difference (θ) between each inverter output voltage V and V_{pcc}, while Q, it relies on magnitude variance (V-V_{pcc}). The status will reverse if system impedance is entirely resistive (see Table 3.1).

Table 3.1. Active /reactive power in paralleled inverters [32].

System's Impedance	**Mainly Inductive** $\boldsymbol{Zo=jX}$	**Mainly Resistive** $\boldsymbol{Zo=R}$
Active Power	$P \cong \frac{V_{pcc}\, V\, \theta}{Z_\circ}$	$P \cong \frac{V(V - V_{pcc})}{Z_\circ}$
Reactive Power	$Q \cong \frac{V(V - V_{pcc})}{Z_\circ}$	$Q \cong \frac{-V_{pcc} V\, \theta}{Z_\circ}$

The output impedance in its natural shape is the inductive state in 3-phase lines. This also applies to a single-phase line if an additional grid inductor (long feeder of the grid-side inductor) is used [15]. Therefore, P is controlled pursuant to the phase angle, while Q is controlled via voltage difference as indicated above. Figure 3.6 displays the relationships Q-V and P-ω.

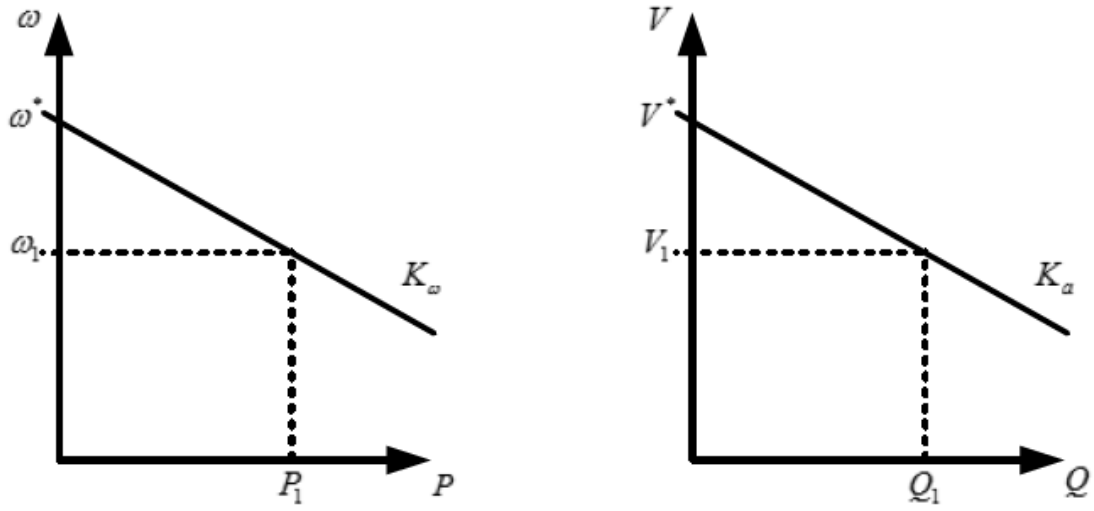

(I) Frequency droop characteristic. (II) Voltage droop characteristic.

Figure 3.6. Relationships Q-V and P-ω

The function of droop control is evident in achieving good power sharing between inverters by regulating the output power in island-mode, while accurately control the power injection into a grid in the connected mode. Hence, the droop control equations for both modes are as follows:

- **Island Mode:**

$$\omega = \omega^* - K_\omega P \quad (3.1)$$

$$V = V^* - K_a Q \quad (3.2)$$

Where: $V^*,\ \omega^*$ – voltage & frequency setpoints.

K_a, K_ω – Voltage and frequency droop coefficients, respectively.

P, Q – active power & reactive power.

- **Grid-Connected Mode:**

$$\omega = \omega^* - K_\omega (P - P^*) \quad (3.3)$$

$$V = V^* - K_a (Q - Q^*) \quad (3.4)$$

Where P^*, Q^* – the setpoints of exported active / reactive power. These parameters are sent via MGCC, P and Q are measured through a cycle of the essential frequency. This could be done with a low-pass filter by reduced bandwidth [33]. Figure 3.7 displays a droop controller block diagram with measuring filters.

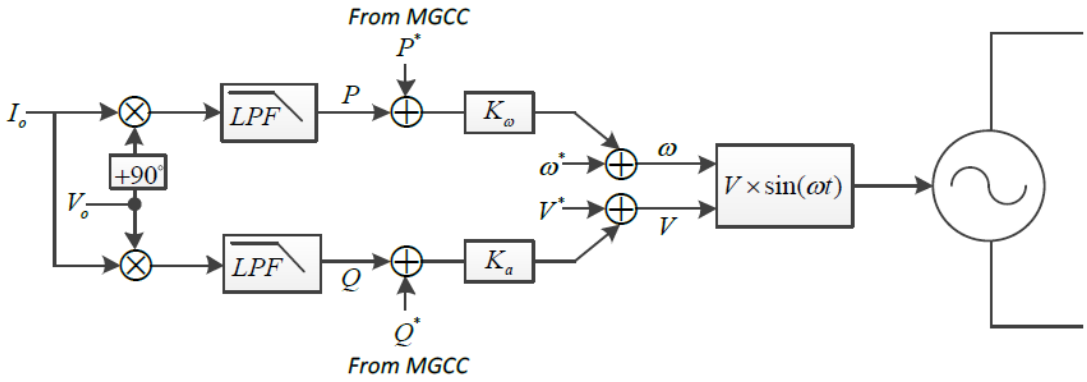

Figure 3.7. Block diagram of droop controller.

While non-communicational way control is the traditional droop form, which lets it further reliable, there are the following drawbacks that restrict its applications [21,34]:

- By utilizing the drooping curve of Figure 3.6 it is illustrated by adjusting the drooping slope to share the reactive force. If we increase it, it will improve the reactive energy sharing but will negatively affect the voltage regulation. Vice versa, there is often trade off since it presents ω and V deviations that are proportional to the Q and P output power.
- Although the dynamics of sharing of power depends on the coefficients of droop control, it also depends on the way of calculating the power as there are low pass filters which lead to additional limits.
- Prior switching back to grid-connected mode, frequency & voltage drop caused by droop control requires a restoration process that reduces seamless transfer mode.
- The droop control uses a purely inductive or purely resistant output impedance assumption, that one in practice is not much precise. Output impedance may be a mixture of the two. This will weaken the decoupling of control loops between reactive & active power since each pure type of output impedance

provides a different form of drop control equation, this is also related to distribution network kind (Table 3.2) [35].

- The conventional droop is non-effective if the units provide non-linear load since it is no supportive sharing of harmonic signals.

Table 3.2. Impedance values of the typical lines.

Line kind	***r [Ω/Km]***	***x [Ω/Km]***	***r / x***
High voltage	0.06	0.192	0.32
Medium voltage	0.162	0.18	0.84
Low voltage	0.641	0.084	7.6

3.3. DROOP CONTROL IMPROVEMENTS

Many researchers have been motivated by the significance and value of droop control in MG to work on improving droop control and implementing various solutions to issues caused via their limitations. Some issues on improving droop regulation are considered in this research.

3.3.1. Sharing of the Load

The load sharing in droop control is classified into the following:

- Power-sharing dynamic
- Power calculation
- The load sharing accuracy

3.3.1.1. Power-Sharing Dynamic

Solutions have been suggested in various publications [36–38] to improve active & reactive power-sharing transient response in island and grid-connected modes. A unit PID controller was suggested by Guerrero et al. [33] as an alternative on a simple

proportional controller in order to enhance dynamic response. Similarly, in order to dampen the transient peak and reduce the circulation currents among inverters, Avelar et al. [39] suggested additional phase loop.

3.3.1.2. Power Calculation

In several studies [39–41], the low-pass filter is also used. Its delayed response, however, affects totality transient of circulation currents and the sharing of power, especially in island-mode. In [4,42] substitute methods were proposed which contain better dynamics, a fast reaction, and less ripple. Moreover, the comparison of many methods is also investigated in [43].

3.3.1.3. The Load Sharing Accuracy

The good accuracy of the power control in the grid connected-mode is achieved thanks to the benefit of the PI controller [4], which removes active & reactive power's steady-state errors. Conversely, in the island's microgrid, this is not easy to execute. The complexity arises from the trade-off between load sharing accuracy and regulation of voltage/frequency. Increasing the gains in droop coefficient to get more precise sharing could degrade control and destabilize a system. A droop control and pair of droop coefficients have proposed to maintain island mode stability at high and low loads in [44]. The new droop controller have been introduced in [45] that makes the droop ratio both P-ω and Q-V non-linear to minimize the drops in voltage and frequency during large load delivery. Moreover, [46] proposed the adaptive droop behavior against large and small loads of steps. Although the high gains needed for better load sharing, an additional loop [38] has suggested to achieve the system's stability. Regulation of the decoupling of virtual (P) and (Q) power by transforming the frame was proposed in [47]. Some researchers have introduced other proposals like [48] that used the generalized integrator of second-order to value the impedance of the grid to replace it in droop control also robust decoupling between (P) and (Q).

3.3.2. Regulating Frequency and Voltage

PCC's voltage & frequency mismatch the MG setpoints in island-mode. Therefore, restoration and regulatory processes are required when the MG reconnects with the grid. In [29,47], the secondary loop was suggested using a PI controller for restoring the needed precise values. The secondary control level is utilized to compensate both frequency & voltage deviations that are caused by primary control in the MG. This control serves to keep the frequency deviations and voltage deviations near-zero or at specified boundaries. However, this control reacts more slowly than the level of primary control [49]. The secondary level is classified as centralized & distributed (decentralized) control, is discussed in [22]. The secondary control' classify ways is clarified in Figure 3.8. The phase drop control was used in [48,49], which lets the frequency is independently on load to be set over time. Furthermore, the authors of [50] enable the operator, via adding an integral gain to real power controller, to tune its controller without affecting frequency control.

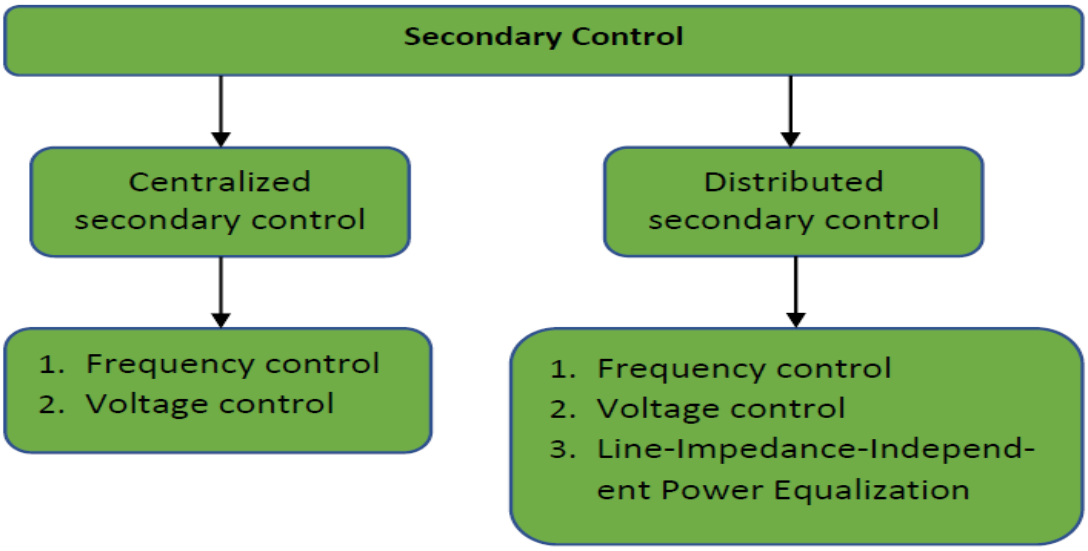

Figure 3.8. Structuring secondary control.

3.3.3. Virtual Impedance

The output impedance considers very essentially for good droop control. As mentioned above, when it is no certainty of being purely resistive or inductive or in between, however, it has a negative effect on the decoupling of the *P* and *Q*.

The purpose of using virtual impedance technique is to solve the power coupling problem owing to the high ratio of *R/X* in low voltage network [4,50]. This is done by increasing the resistance /inductive of the inverter output impedance without the need to use additional physical resistors/inductors, which adding these physical quantities increases the cost and size. Therefore, the impact of line impedances and network on droop control is reduced. Literature shows recent research to develop a concept of virtual impedance. In [51] a parallel linked virtual resistance impedance control technique is suggested to sharing the current in island-mode. It offers the benefits of a damped system with regard to automatic harmonic sharing and resonance. Inductive virtual impedance is utilized in [33]. A problem for the virtual inductance control scheme, however, is the calculation of the inductor voltage drop that includes differentiation of the line's current. Differentiation could cause high frequency noise amplification, which leads to destabilizing the control scheme of inverter voltage, particularly during the transient. Moreover, virtual impedance reduces the impact of the circulating current between inverters as it supports the soft start process so that it maintains a big impedance in the start and later reduces it to the nominal value in a stable condition [32].

Owing to high load requirements, the inverters should work in parallel, this offers the system redundancy besides the high reliability needed for a flexible MG structure. The powerful design of every inverter so that it can operate in parallel together without disturbances in the system is a parallel inverters' major concern. In general, droop control is executed for the wireless sharing of power among the inverters. However, the different output impedance affects the stability and accuracy of power-sharing. The literature suggests numerous control strategies to address such challenges [4,52–55] However, the emphasized effect of various feedback signals of the loop of voltage control on the shape of output impedances is not clarified well. In this thesis, the voltage controllers for single and double loops and their effect on stability will be studied. In addition, System behavior will analyze by utilizing the Bode plot technique when the capacitor and inductance currents are used as feedback. Furthermore, the differing output impedances of parallel-connected inverters impair stability. A virtual impedance has therefore proposed for stabilizing system and unifying the nature of output impedances.

3.3.4. Sharing Current Harmonics

In particular, when providing nonlinear loads in island mode, a method was proposed to deal with nonlinear load-sharing as in [32] by adjustment output voltage bandwidth with supplied harmonic power utilizing the band-pass filter bank, after that, harmonic components of the current signal are extracted and then is re-injected them again in the network. In certain applications, like the UPS system [56], the ohmic output impedance could be a positive for sharing linear and non-linear loads. In [57] a rapid control loop is used, which adjusts the inverters output impedance of in the closed control loop to ensure resistance behavior and to correctly share the harmonic current. In natural output impedance, the impedance of inductive output tends to be more common [32]. In [58], The complex output impedance was shown in which a different design was proposed for a virtual output impedance consisting of a virtual resistor with an HPF-connected virtual inductor. After all, at a nominal frequency, it behaves like an inductor and reflects resistance activity at harmonic frequencies.

3.3.5. Power-Sharing

One of the main concerns of inverters working in parallel is the issue of load sharing. Many techniques used methods based on communication [59–62] to achieve precise load sharing, but those methods require high communication infrastructure bandwidth among all inverters that raises costs and reduces reliability, in addition absence plug-and-play capability. The droop control technique that simulates same synchronous generators behavior [39], introduced the solution so that the inverters work in parallel with no communication mechanism. Accurate active power-sharing could be easily realized utilizing conventional droop control due to parallel inverters are synchronous and have a constant output frequency. On the other hand, to be able the droop controller sharing the reactive power precisely, inverters working in parallel must contain similarly output impedance involving cable impedance and generate similarly output voltage. Even so, in practice, because of the tolerance of parameters in the LC output filter of the inverter, the different lengths of the connection cables, and the inaccuracy of the output voltage control, this cannot be assured. For that reason, conventional drop

control has known for its weak *Q*-sharing performance. Therefore, emphasis will be placed on the reactive power-sharing problem.

A lot of strategies are proposed for improving *Q*-sharing. An algorithm which is dependent on the injection of an additional control signal has suggested in [63]. The suggested method injects signals at various frequencies (90 Hz, 130 Hz) to transmit information over the same distribution lines about the power shared between the inverters, but this would increase the complication of the control method (Figure 3.10).

.

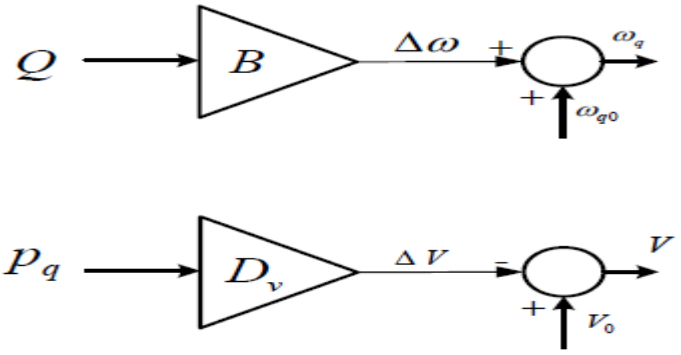

(a)

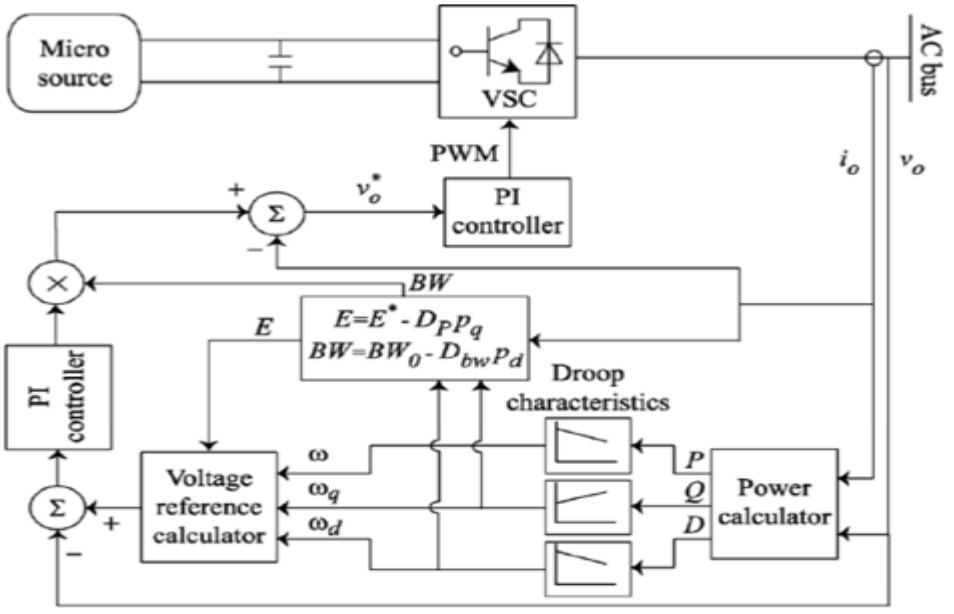

(b)

Figure 3.9. Block diagram of small-signal injection technique.

Chia et al. [64] suggested a technique for compensation of mismatch of lines' impedances, wherein the *Q* is regulated into proportion with derivative of voltage. Despite minimizing errors in *Q*-sharing, this method did not realize an even sharing and increases the complication of the system (Figure 3.11).

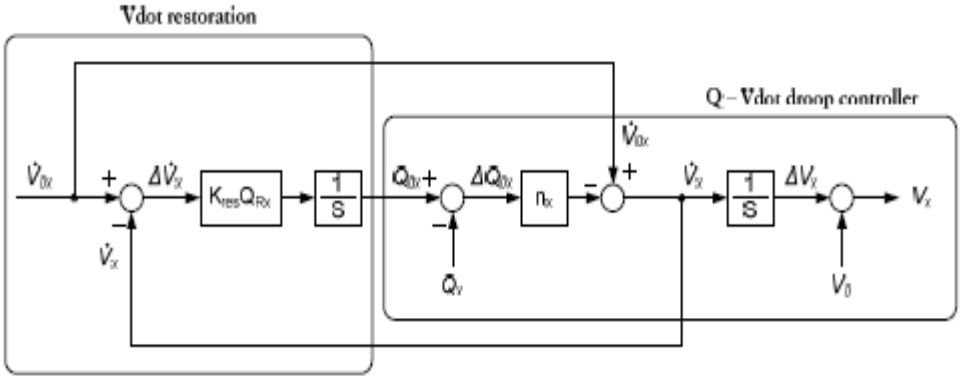

Figure 3.10. Proposed the Q-V dot controller.

A centralized controller to compensate voltage drop using droop control is suggested in [65]. The entire process, however, is performed in MGCC, and a communication link is used to send all parameters. Losing this communication would result in conventional droop control constraints.

Li et al. [66] suggested an online voltage drop value which happened because of the transmission lines until that improve the gain of the droop control to achieve a precise *Q*-sharing in island-mode but the method requires that inverters first work in on-grid mode to get an appropriate estimate for calculating the new droop gain. Furthermore, the complexity of the controller increases as there are local loads that impact the estimation processes. (Figure 3.12).

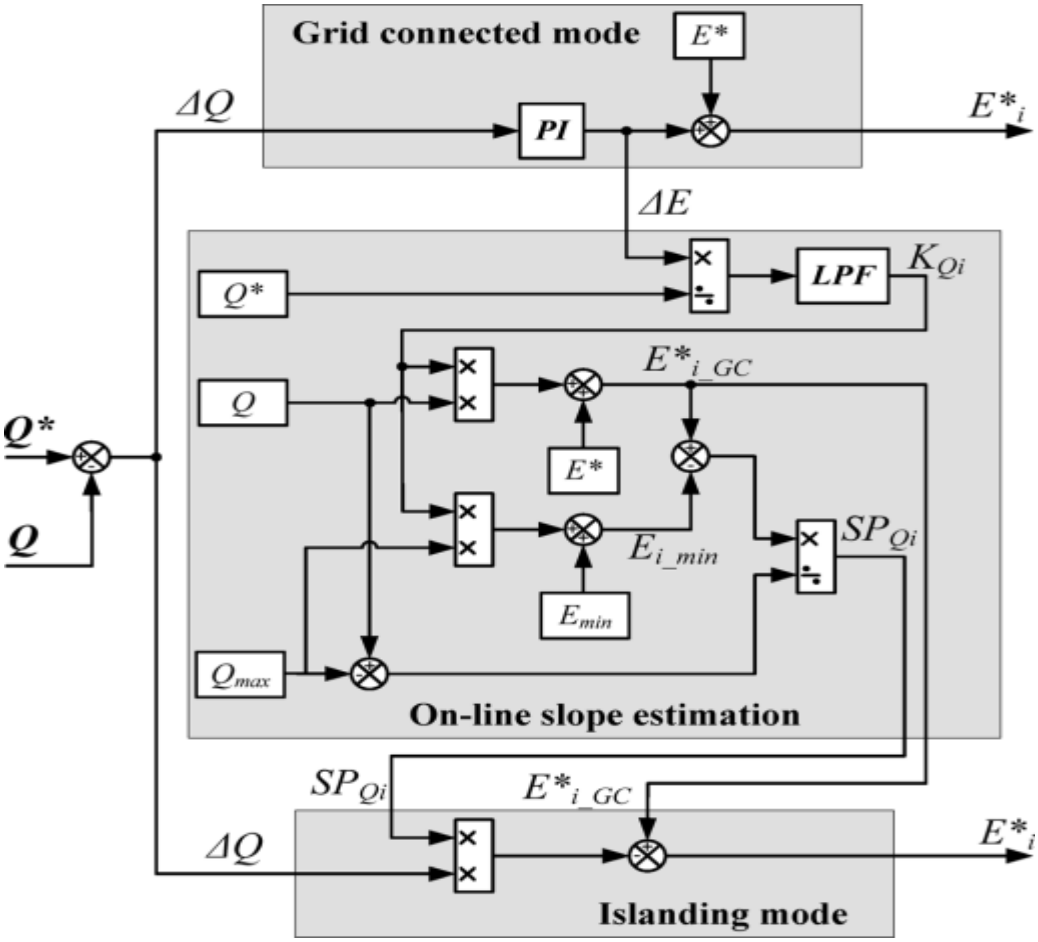

Figure 3.11. Reactive power-sharing by using online voltage drop value.

Zhong (2013) proposes another control system which is strong against errors in calculation and mismatching of components. The control's accuracy does not rely on the impedance of the output. Via a cable link, it continuously tests the load voltage and calculates the variance between this measurement and locally output voltage. In order to obtain an exact sharing of the *Q*-power, this variance is the input to integrated control system, but this method only acts precisely for inverters and local loads near each other. A wireless connection could be used among the inverters for a remote load point or long distances and any interruption of the communication bond, until for a short time, could cause instability owing to the presence of an integrated controller. In addition, the cable impedances which lead to inaccuracy sharing when the localized output voltage returns are not considered by the controller (Figure 3.13).

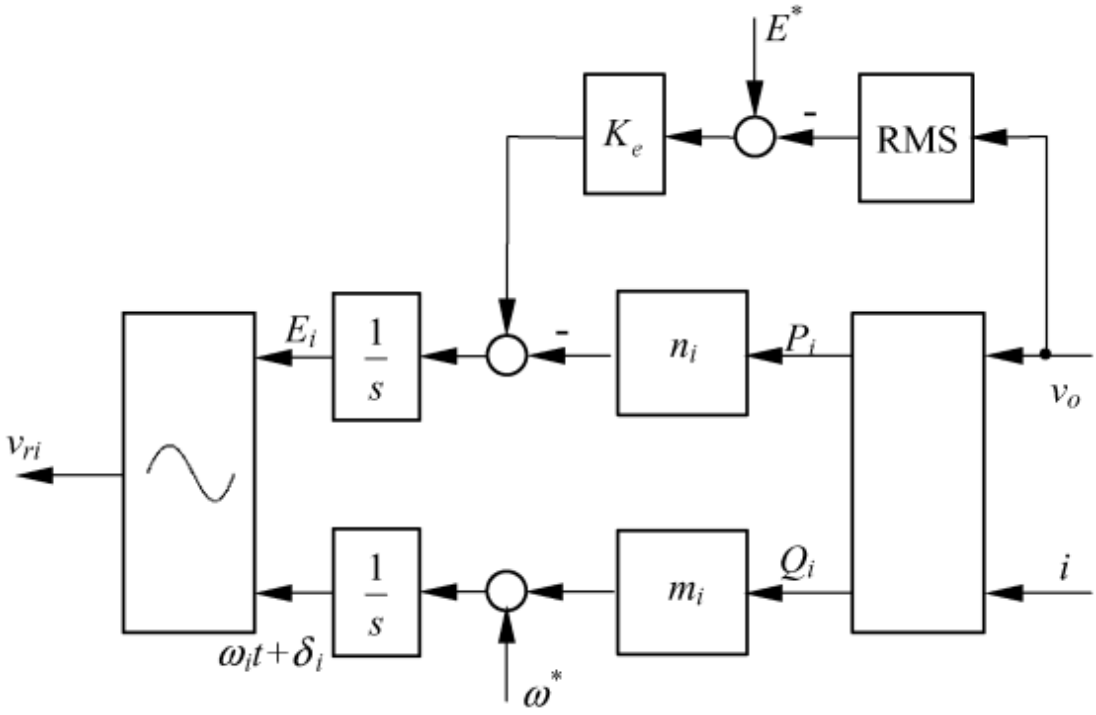

Figure 3.12. Proposed robust droop controller against calculation errors and components mismatch.

Jincwei et al. [68] suggested the synchronized technique that correctly instructs all units for *Q*-sharing by using the *Q* measured in the equation of frequency. This purposely disturbs, however, the precision of *P*-sharing. Furthermore, the sharing accuracy deteriorates for each load fluctuation after compensation, and therefore the technique must be performed again.

The same authors suggested an online evaluation technique for line impedance in [69, 70] , utilizing PCC voltage and line current harmonics to control the virtual impedance and improve the accuracy of *Q*-sharing. Even so, both the complexity of the controller and the reliance on harmonic calculations that presume the presence of nonlinear loads during estimation time are increasing.

3.4. CONCLUSION

In this chapter, the latest technologies for the interfacing between renewable energy and technologies of microgrid control in island mode have overviewed. Several techniques adopted communications-based methods to realize good power sharing

among parallel inverters but losing this link could be very harmful to the controller performance. The literature review exposed that the droop control technique is a popular method of power-sharing recently without depending on communication link among parallel inverters in island mode. However, it has many deficiencies and is being improved by researches work. It also showed that unifying the type of output impedance among parallel inverters considers very essential for supporting droop control. When it is no certainty of being purely resistive or inductive or in between, however, it has a negative effect on the decoupling of the P and Q power so this can affect the accuracy of power-sharing and thus destabilize. In this thesis, a virtual impedance is therefore proposed to reach the system stability and power-sharing.

PART 4

THE EFFECT OF VIRTUAL IMPEDANCE ON INVERTER'S CONTROL TOPOLOGIES

4.1. INTRODUCTION

When making a design for the microgrid control system, it is necessary to achieve stability for each unit in addition to the stability for the entire MG in various conditions of load and system. MG uses inverters to create a connection between distributed generation units (DG) and loads/grid [71,73]. In practical, owing to high load requirements, the inverters should work in parallel, as illustrated in Figure 4.1. This offers the system redundancy besides the high reliability needed for a flexible MG structure. A major challenge of parallel inverters is the robust design of each inverter so that it can operate in parallel together without disturbances in the system. In general, droop control is executed for sharing power wirelessly among the inverters. Nonetheless, unequal output impedance between DG units (due to the difference of cables length among all paralleled inverters) affects the stability and accuracy of power-sharing. The literature suggests numerous control strategies to address such challenges [4,52–55]. However, the emphasized effect of various feedback signals of the loop of voltage control on the shape of output impedances is not clarified well. In this chapter, the voltage controllers for single and double loops and their effect on stability are studied. System behavior is analyzed by using the Bode plot technique when the capacitor and inductor currents are utilized as feedback. Furthermore, differences in the type of output impedance (inductor/resistor) of parallel inverters can affect the accuracy of power-sharing and thus destabilize the system. A virtual impedance has proposed to reach the system stability by unifying the nature of output impedance. Simulation's results are introduced for showing control strategy validity.

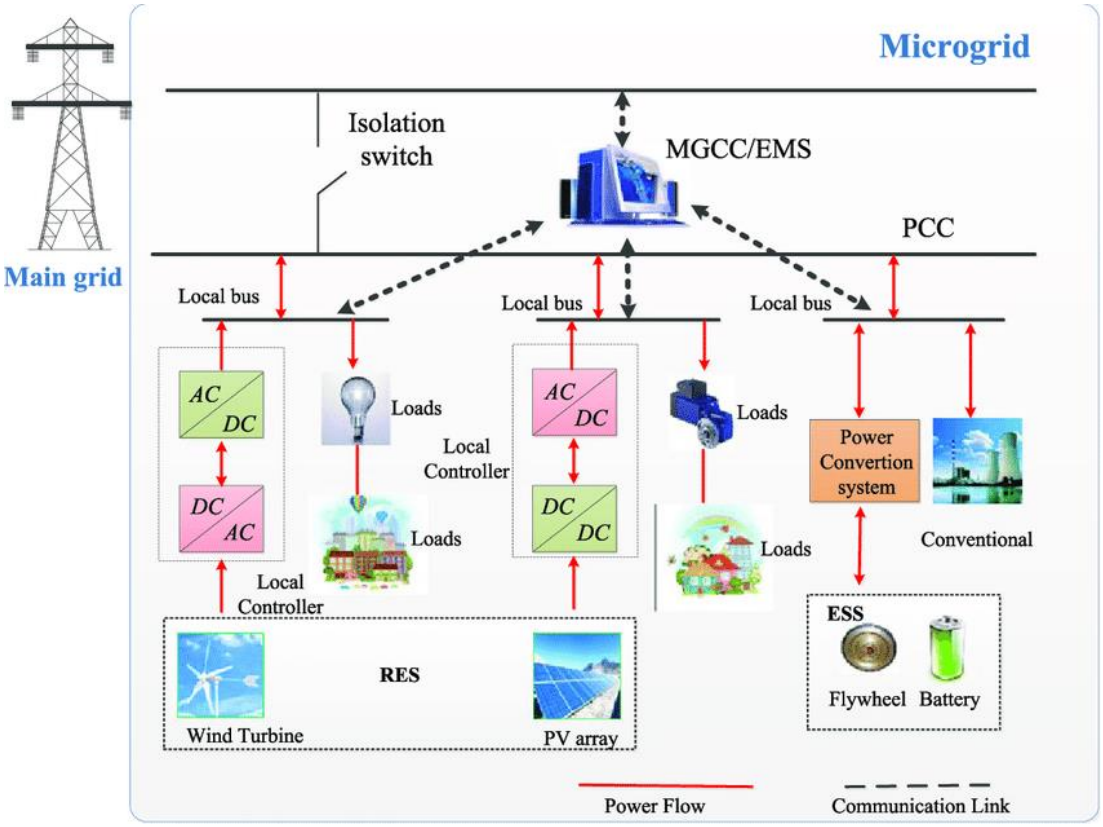

Figure 4.1. General microgrid structure.

4.2. VOLTAGE AND CURRENT CONTROL LOOPS

4.2.1. Outer Voltage Control Loop

Figure 4.2 reveals the proportional controller-based outer voltage controller loop utilized to compensate error signal of voltage V_{error} between reference voltage signal and output voltage signal of inverter for regulation and optimal stability. The voltage-compensated error signal is considered the reference current control *Iref* for the current control loop.

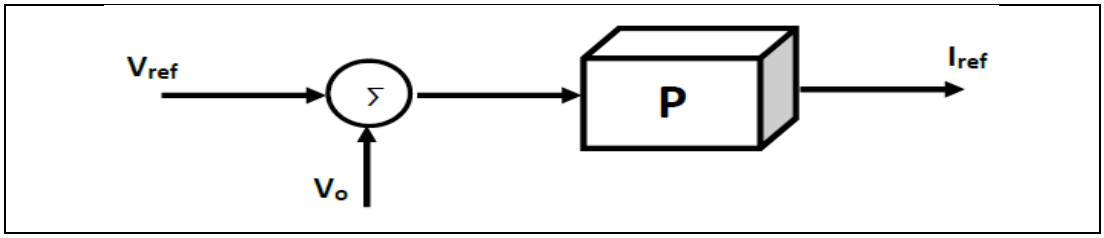

Figure 4.2. Outer voltage control loop.

4.2.2. Inner Current Control Loop

Figure 4.3 reveals the internal current control loop based on the PI controller. Reference current I_{ref} is compared with output current Io to produce an error current Ierror signal which assigned with a PI controller producing PWM signal for full-bridge inverter driving. The benefit of designing an inner loop is having a short settling time and fast harmonic tracking.

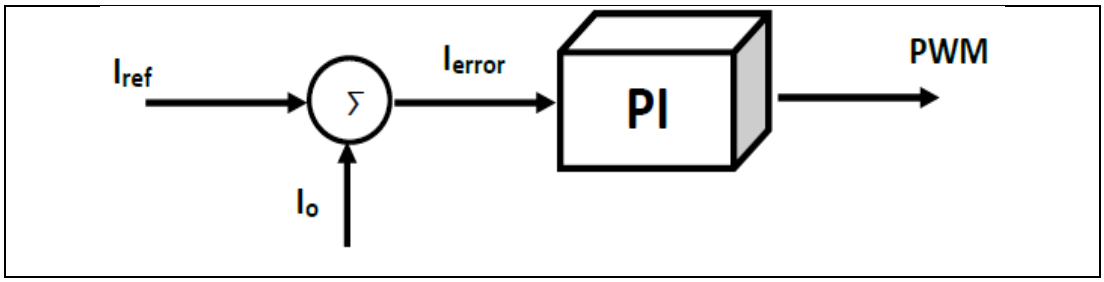

Figure 4.3. The inner current control loop.

Slower than the current internal loop is the outer voltage loop. The structure of the double control loop is revealed in Figure 4.4.

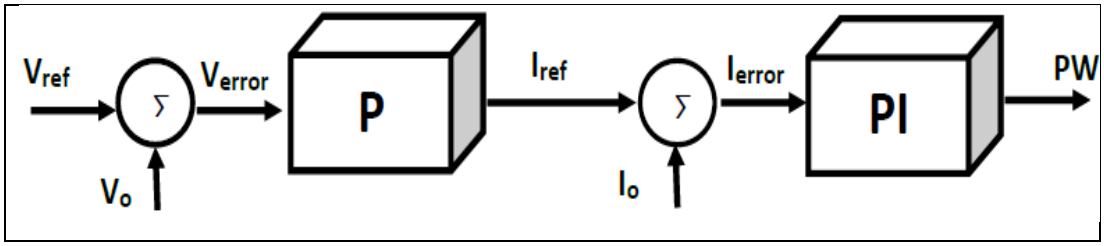

Figure 4.4. Voltage and current control loops

The controller must produce a similar voltage setpoint for the inverters using the frequency and voltage droop's characteristics, with the assumption all inverters connected in parallel have the same output impedance so that they can do load Sharing exactly in proportion with their nominal powers. Figure 4.5 reveals the control block of each inverter module.

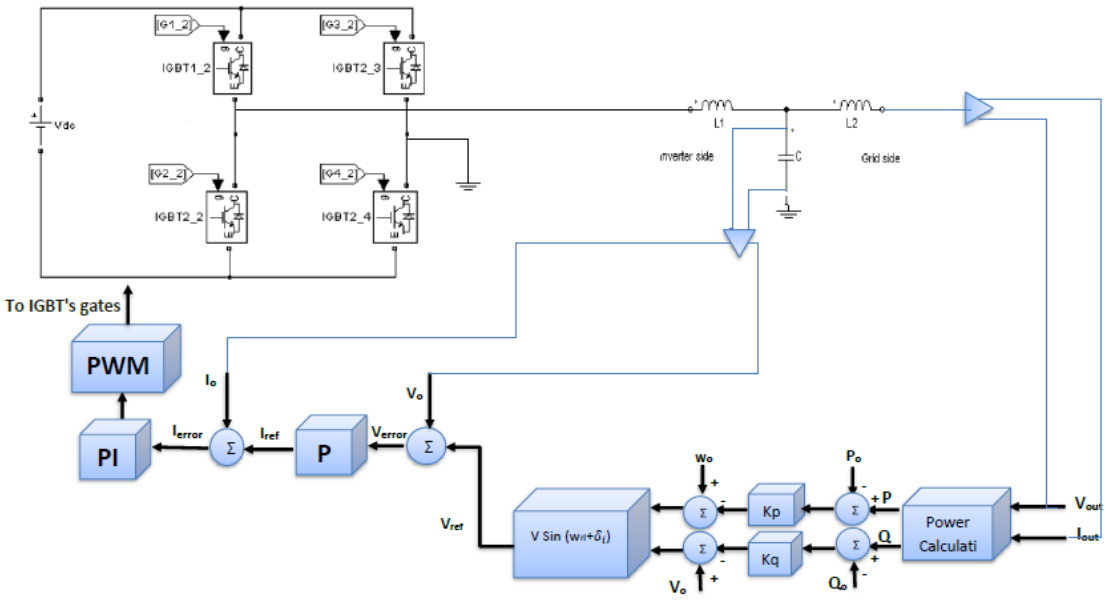

Figure 4.5. Control block of each inverter module.

4.3. SINGLE-LOOP VOLTAGE CONTROLLER

As mentioned above, the inverter is the linkage between the power sources and loads. Figure 4.6 depicted the general configuration of the inverter with IGBT switches that get modulated sinusoidal wave signals (MSWS) from the unit of voltage controller. The pulse width modulation (PWM) method is common in getting a correct sine wave signal (Figure 4.7). The signal duty cycle produced could somehow be modulated so that the average voltage signal complies with a pure sinusoidal wave utilized in switching control. With sine signal fundamental frequency, this generates high-frequency harmonics (Figure 4.8).

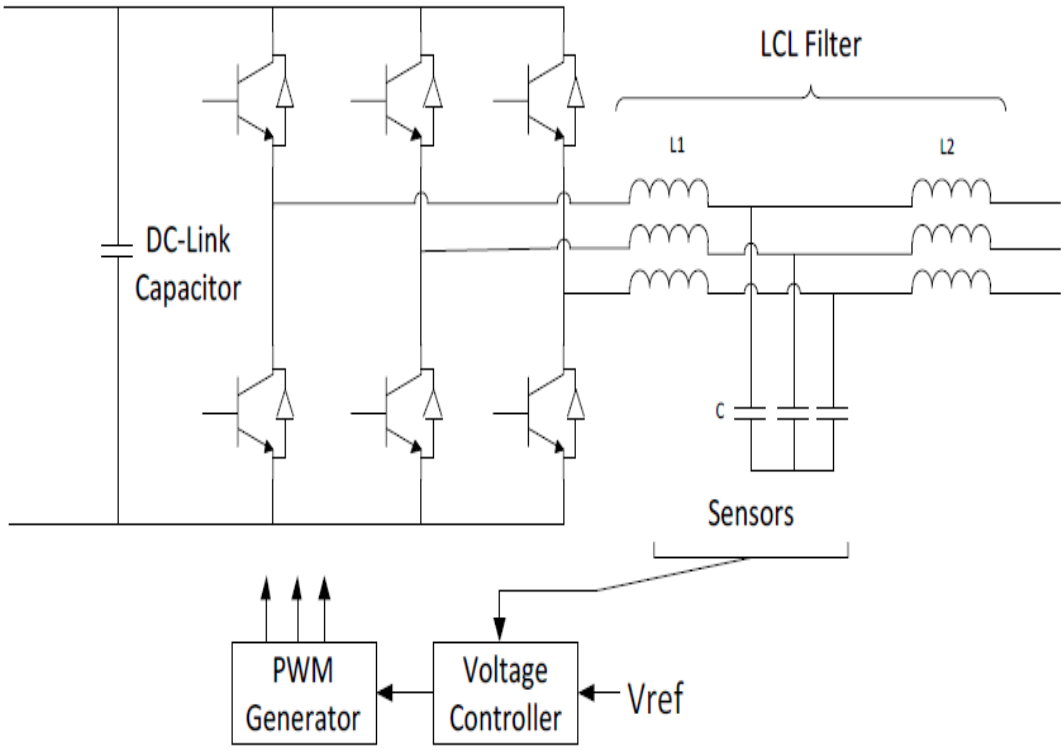

Figure 4.6. The general structure of the inverter, including the LCL filter.

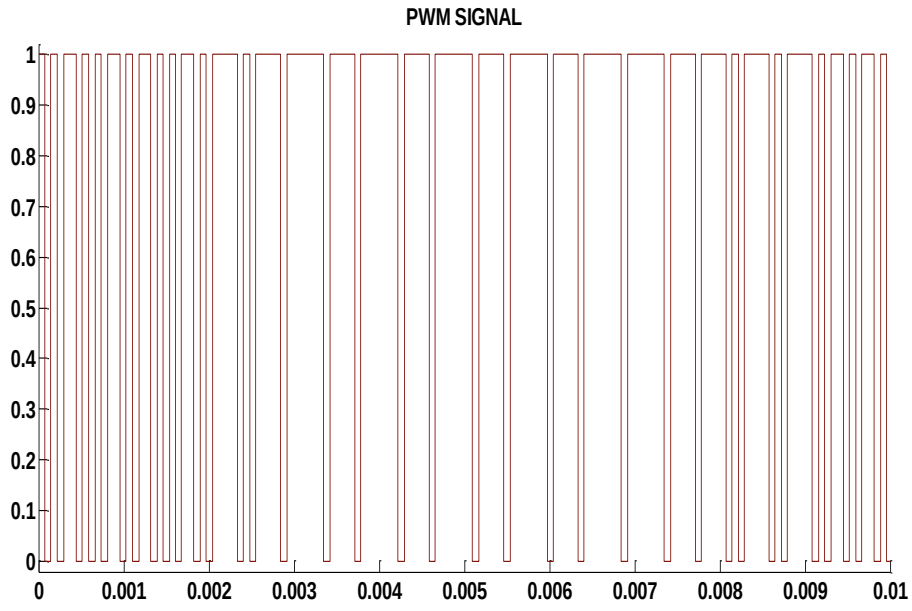

Figure 4.7. SPWM Signal.

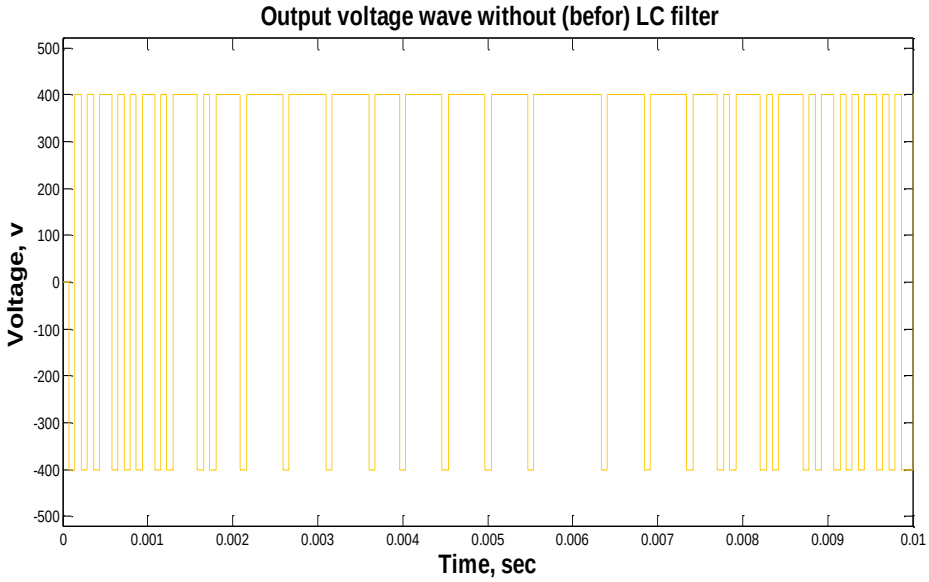

Figure 4.8. The output sinusoidal voltage waveform is divided before filtering.

LCL filter is utilized to dampen harmonics produced and provide the load with a high-quality signal with low harmonic power (Figure 4.9).

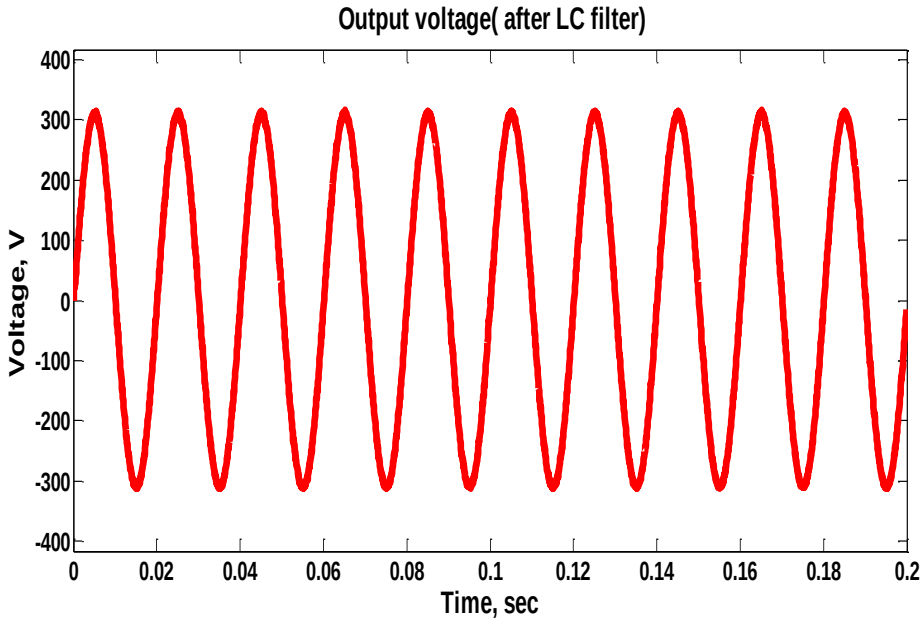

Figure 4.9. Sinusoidal output voltage waveform with high-quality (using LC Filter).

Also, the output current waveform is similar to that of the sinusoidal voltage waveform (see Figure 4.10).

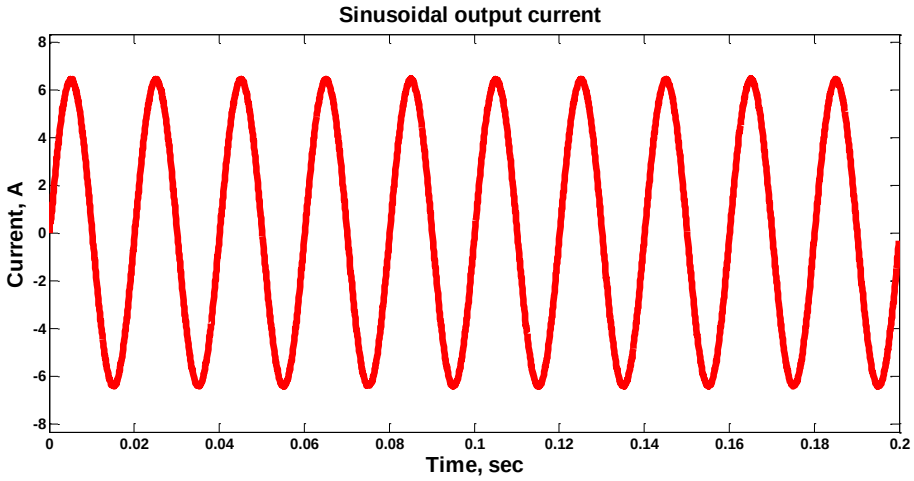

Figure 4.10. The output current waveform.

A voltage control loops are utilized in VSI for tracking the input signal desired and also to decrease error between the previous signal desired and output voltage measured as revealed in Figure 4.11.

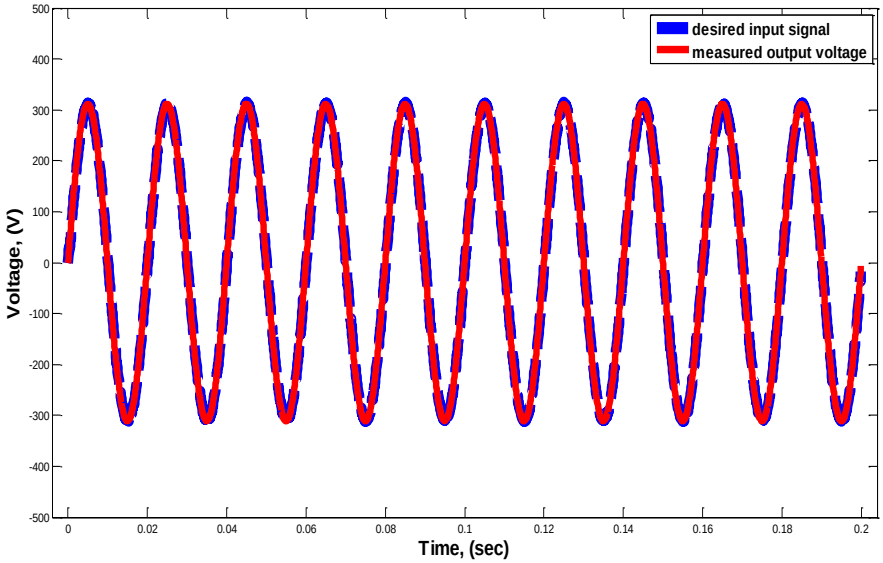

Figure 4.11. Minimizing the error between the signal desired and output voltage measured.

The proportional controller; kv; is used in this chapter, propped by the feedforward loop. This loop reduces steady-state errors plus enables a larger bandwidth control. Figure 4.12 displays the LCL filter (physical system) model and the loop for voltage controller. On filter capacitor's terminals, voltage feedback is measured and then

compared to a setpoint. The controller then produces the control signal for the PWM. This appears from Figure 3.8 which will be determined output voltage as follows:

$$V_o(s) = G(s) * V^*(s) - Z_o(s) * I_o(s) \tag{4.1}$$

Where $G(s)$ – Transfer function of closed-loop system which links *V** and V_0.

Zo – Output impedance of closed-loop system.

then$G(s)$, is given by

$$G(s) = \frac{K_v + 1}{L_1 C s^2 + K_v + 1} \tag{4.2}$$

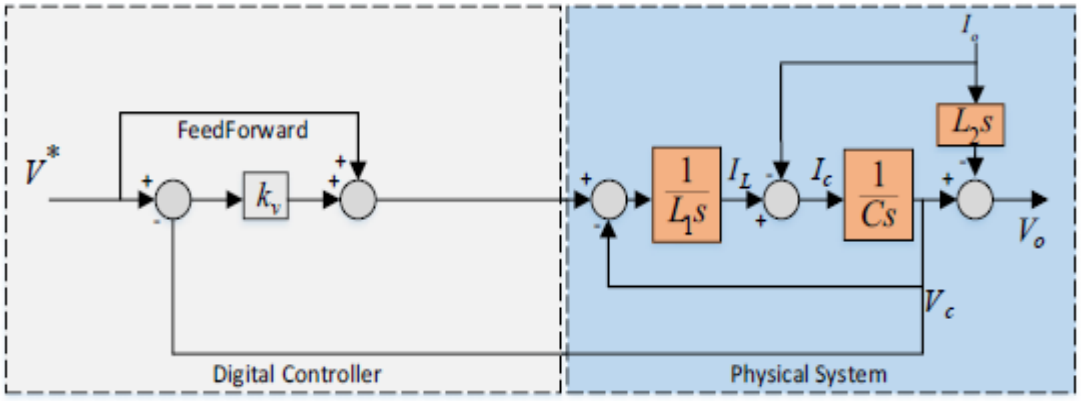

Figure 4.12.The basic single-loop voltage controller model.

It is clear from transfer function that term damping; *s* is null so this could create a resonance that leads to system destabilizing and devalues the quality of the output signals. It is depicted in Figure 4.13 through the bode plot of *G(s)*. At 500 Hz, the peak shown in Figure 4.13 refers to resonance. This frequency can be easily excited by any harmonic signal or interference and disturbances. This signal is amplified by the significant loop gain and hence leads to destabilizes or distort the output. If a larger proportional gain is utilized, the resonance is not damped, but resonance frequency is shifted to little higher values.

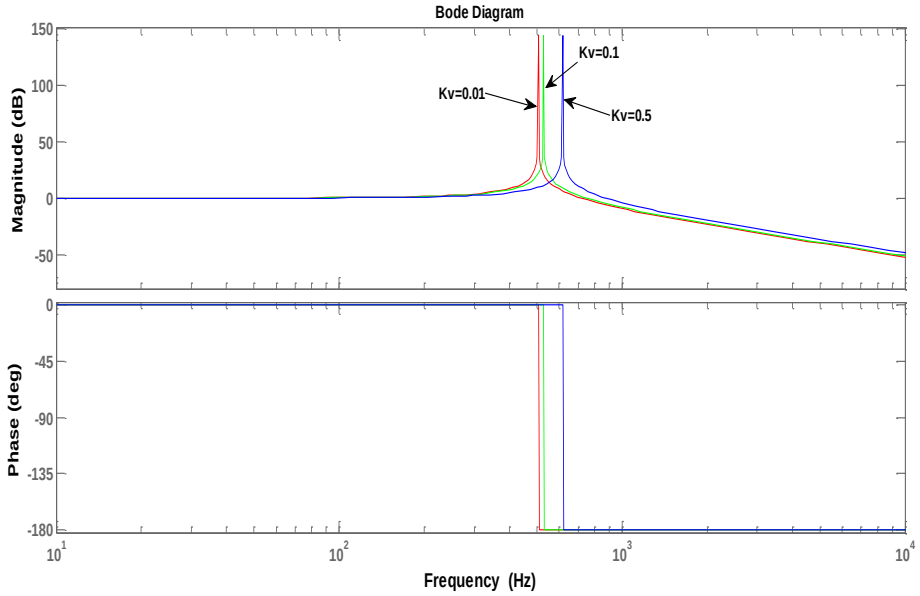

Figure 4.13. Bode-plot of the single-loop voltage controller.

4.4. DOUBLE-LOOP VOLTAGE CONTROLLER

A double control has recently been used in literature to dampen the resonance of output filter [74–76]. The first loop adopts feedback voltage from the output voltage. The second internal loop adopts feedback current from the inductor *L1* or capacitor *C*, such depicted in Figure 4.14. The damping could be effectively realized in both situations. In this thesis, however, the effect of choosing each one of them is discussed in the shape of output impedance.

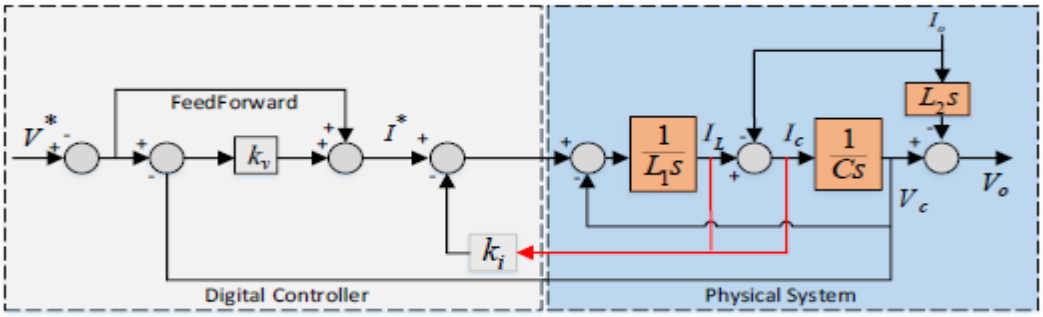

Figure 4.14. The basic double-loop voltage controller model.

As shown in Figure 4.14 transfer function *G(s)* will be indicated as:

$$G(s) = \frac{K_v + 1}{L_1 C s^2 + K_i \mathrm{C} s + K_v + 1} \tag{4.3}$$

The addition of the feed-back loop is expressed in (4.3) via term "s", that supplied damping. The Bode plot diagram in Figure 4.15 reveals the voltage loop behavior with various current feedback gain values (ki). More extra gain leads to provide additional damping.

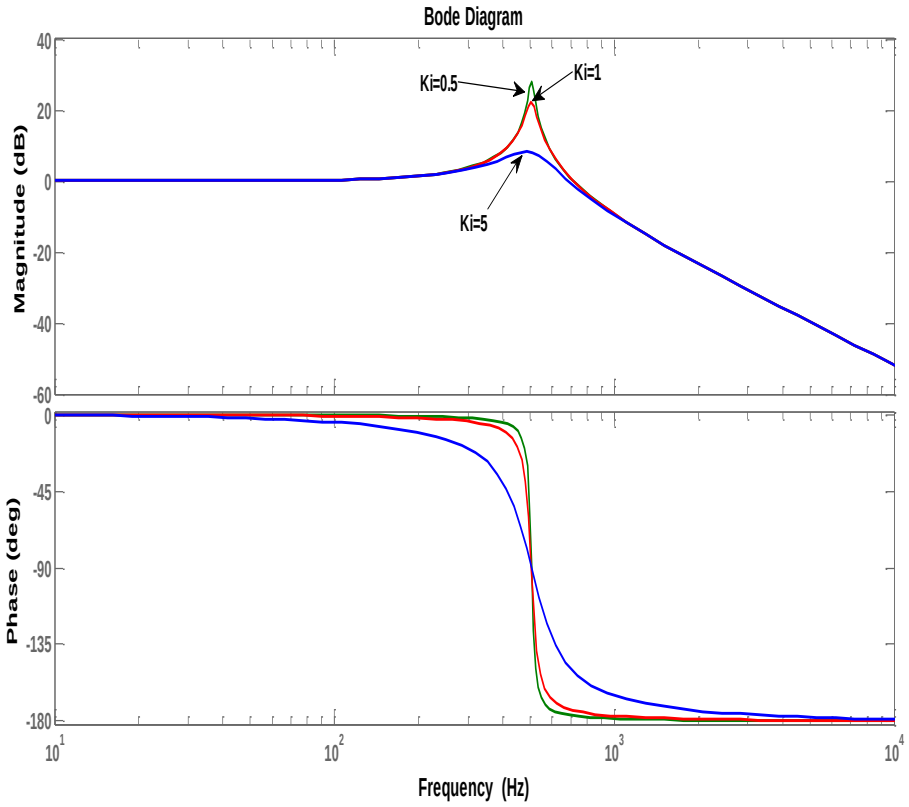

Figure 4.15. Double loop voltage controller's Bode plot.

It should be noted, that every current feedback selection (I_C or I_L) produces the same G (s). Regarding Z_o (s), there are two versions of the internal loop feedback situation (I_c and I_L). If the controller takes over I_L, It is possible to obtain Zo (s) as (4.4) and describe it as Zo_L(s).

$$Z_{\circ_L}(s) = \frac{K_i + L_1 s}{L_1 C s^2 + K_i C s + K_v + 1} + L_2 s \tag{4.4}$$

If I_C is adopted by the controller, Zo(s) can be gotten as (4.5) and identified as Zo_C (s).

$$Z_{\circ_C}(s) = \frac{L_1 s}{L_1 C s^2 + K_i \mathrm{C s} + K_v + 1} + L_2 \mathrm{s} \tag{4.5}$$

Figure 4.16 describes output impedance's Bode plot diagram gotten from (4.4) and (4.5). If I_L is adopted, output impedance's behavior round fundamental frequency (50 Hz) will be resistive, that refers to a nearly fixed gain across of extended frequency range. In the scenario of I_C, however, with the rise in frequency, the output impedance serves as an inductor that adds more impedance. There has been a resonance just at a natural frequency in both scenarios, but due to the internal current loop, it was dampened.

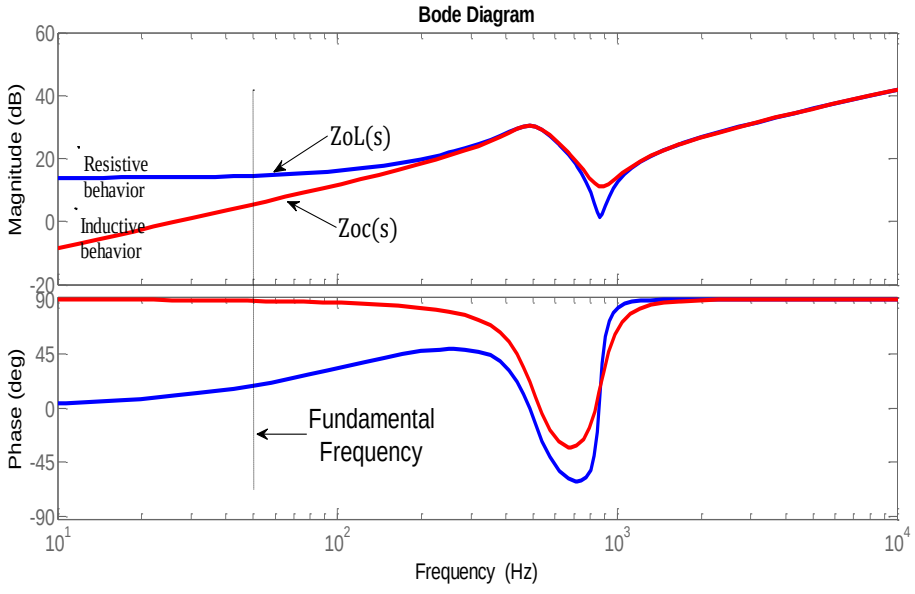

Figure 4.16. Output Impedance Bode plot with IL and IC as feedback.

4.5. DROOP CONTROL BLOCK DIAGRAM

The inverter output voltage & current waveforms V and I are used to calculate the active & reactive power via power calculations Simulink block. The calculated powers are compared with the rated values and the result multiplied with the droop coefficient m_p and n_q. The result is compared with the nominal frequency and voltage amplitude values to generate the reference frequency & voltage amplitude w and v for reference waveform generation. The phase δ is generated as other aspects ωt input (see Figure 4.17).

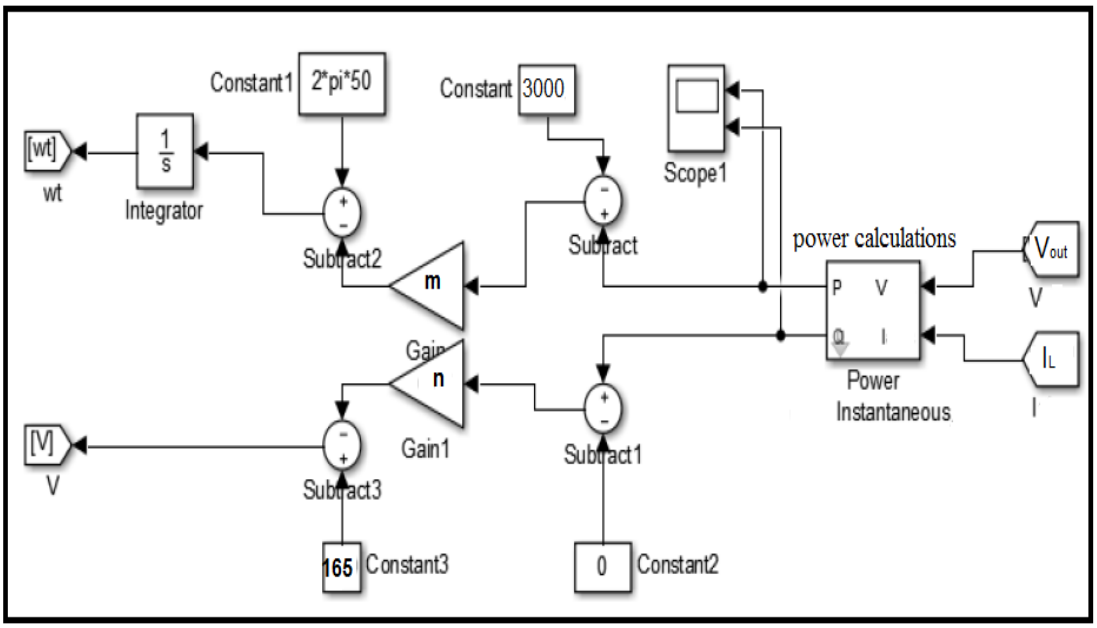

Figure 4.17. Droop control block diagram.

Droop control is performed while the inverters are running in parallel in the island-mode. It can be implemented while the inverters are running in parallel in order to also keep each inverter from overloads to realize better power sharing. This technique supposed that the impedance of output was predominantly resistive or inductive. Depending on this, the droop controller operation differs (Figure 4.18 and Table 4.1).

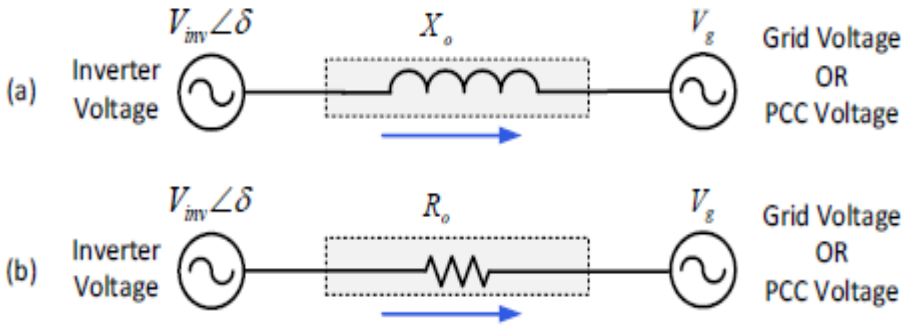

Figure 4.18. Cases of the supposition of output impedance for droop control (a) inductive, (b) resistive.

Table 4.1. Characteristics of Droop controller for active / reactive power.

System's Impedance	**Net Inductive** $\boldsymbol{Zo=jX}$	**Neal Resistive** $\boldsymbol{Zo=R}$
P equation	$\omega = \omega^* - m_p * P$	$V = V^* - n_p P$
Q equation	$V = V^* - n_q * Q$	$\omega = \omega^* + m_q Q$

Where: V^* and ω^*– the nominal output voltage and the frequency of inverter, respectively.

Q and P – the measured active & reactive output power, respectively.

n and m – the droop coefficients.

When inverters work together in parallel for good sharing power, they must have similar droop's equations. It could be done if only Z_{out} has a similar type of nature of inductive or resistive. The working under various nature for Z_{out} without consideration precautions will lead to degenerate the accuracy and stability of the shared performance.

4.6. PROPOSING OF THE VIRTUAL IMPEDANCE

Until when load terms are off-balance, conventional P/f & Q/E control is enough for better MG performance. Nevertheless, we require an additional advanced system of control when it regards to competence. The virtual impedance control (Z_v) can be utilized to modify setting the output impedance of the inverter. Figure 4.19 illustrates a block diagram for Virtual Impedance with droop control.

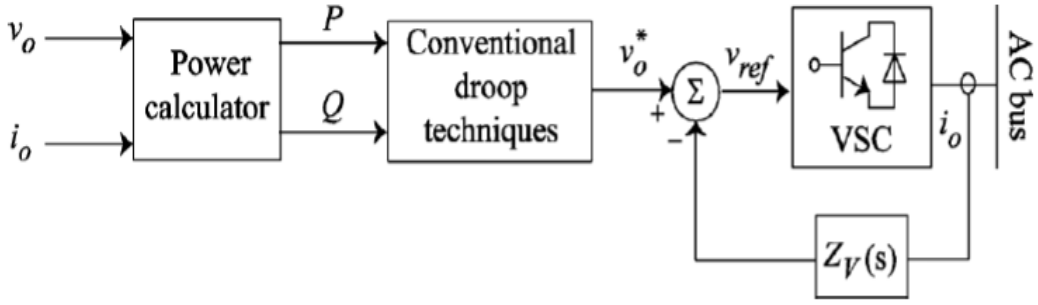

Figure 4.19. Block diagram of Virtual Impedance with droop control.

In order to compute the voltage reference for the inverter, the Z_v(s) effect is possible to see via the next equation,

$$V_{ref} = v_\circ^* - Z_v(s) \times i_\circ \tag{4.6}$$

Where (s) is the output virtual impedance that may be either resistive or inductive. A virtual impedance principle is used in this chapter for unifying the nature of output impedances for inverters that operate in parallel. This impedance in a software simulates the conduct of the resistor or inductor. Utilizing a programmable impedance instead of a physical impedance reduces losses and costs. Moreover, programmability represents an adaptive process and improves the robustness of the inverter toward network impedance fluctuations. Figure 4.20 illustrates the voltage controller block diagram including virtual impedance $Z_v(s)$.

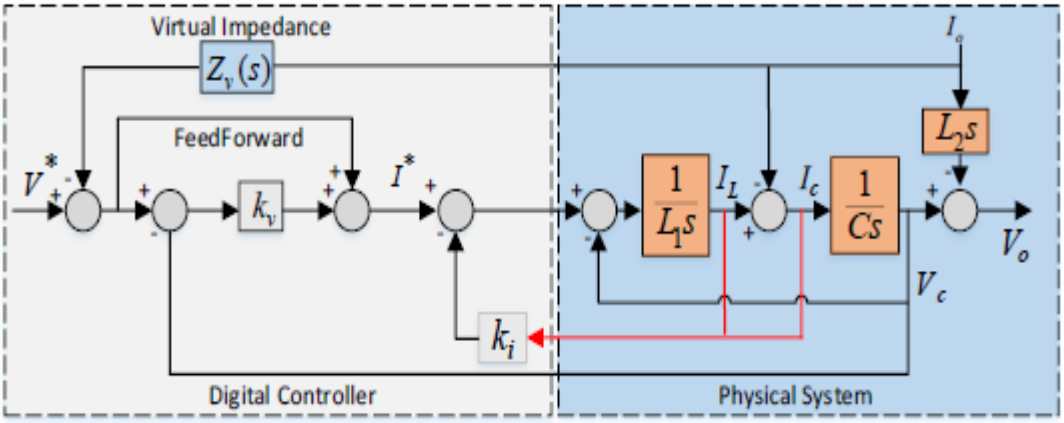

Figure 4.20. Dual-loop voltage controller model including virtual impedance.

Then, newly output impedance will be derived as follows, including virtual impedance,

$$Z_{ov}(s) = Z_o(s) + G(s)Z_v(s) \tag{4.7}$$

The kind of nature of Z_v can be selected to be inductive as,

$$Z_v(s) = \frac{s}{\tau_v s + 1} L_v \tag{4.8}$$

Here L_v is a virtual impedance inductance and τ_v is a high pass filter time constant, with which the transfer function derivative is approximated to perfect virtual inductance$Z_v = sL_v$.

Or it could be resistive as,

$$Z_v(s) = R_v \tag{4.9}$$

As mentioned above, when parallel inverters work together for sharing power, they must have the same droop's equations to realize accuracy. It can be done if only output impedances have the same type of nature of being inductive or resistive, so the difference in the type of nature of the output impedance of parallel inverters impairs stability. A virtual impedance has therefore proposed to reach system stability by

unifying the nature of output impedances. System behavior is analyzed by using the Bode plot technique in MATLAB program.

The influence of Z_{ov} upon this old output-impedance of Figure 4.15 is illustrated in Figure 4.21. The Z_v of the resistive type is utilized in Figure 4.21(a) to transform the inductive characteristics into the dominant resistance nature. Likewise, the Z_v of the inductive type is utilized in Figure 4.21(b) to transform the resistive characteristics into the dominant inductive nature.

Virtual impedance is concluded to have a major impact on the impedance of output and could dominate at high values. The results appear that the important role of virtual impedance is to support the operation of droop control and maintain stability.

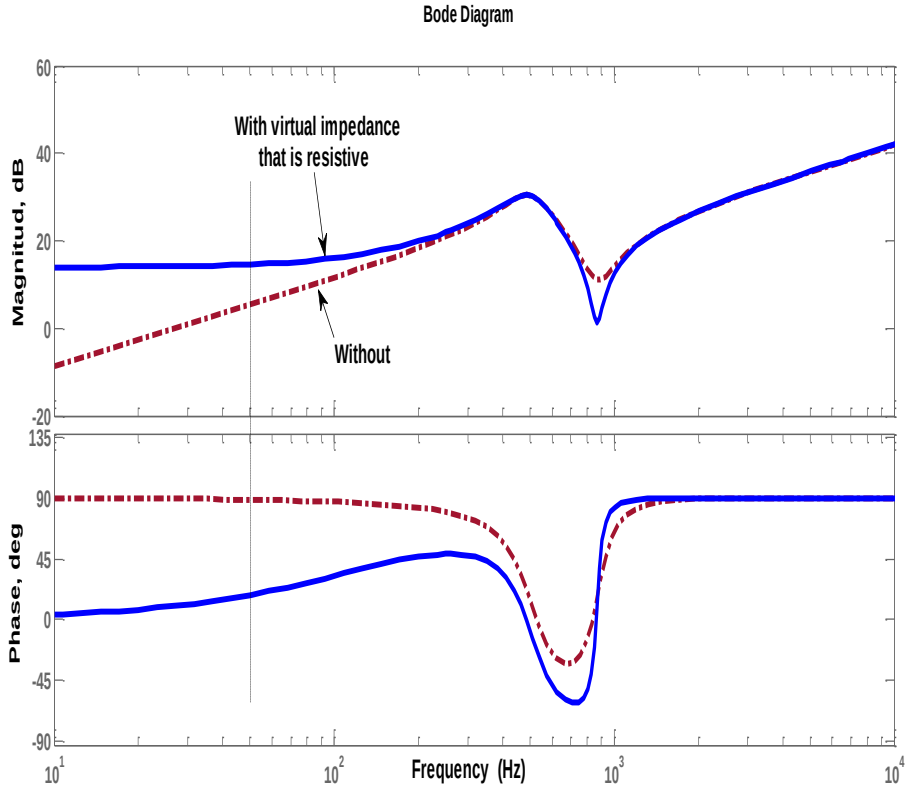

(a) Resistive Z_v

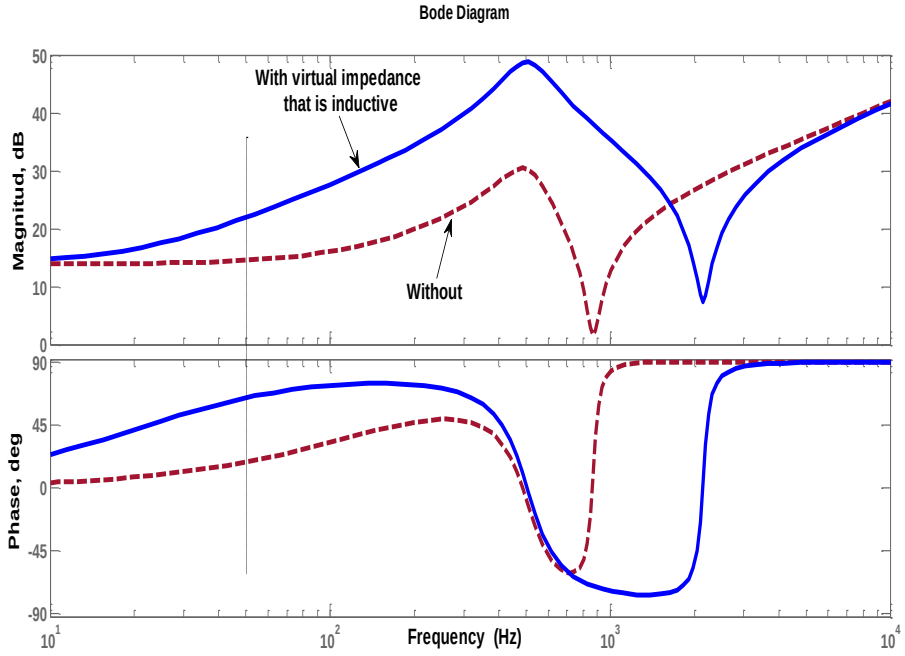

(b) Inductive Z_v

Figure 4.21. Bode plot for output impedance using: (a) – Resistive Zv; (b) – Inductive Zv.

The network's impedance in the low voltage MG network is predominantly resistive. Thus, droop control is specified in this chapter for the resistive network. Nevertheless, each inverter's output impedance is undergone to the feedback and control strategies implemented. Rather than being net resistive, it may be a mixed impedance. In addition, to a certain degree, the inductor of Grid-Side or a transformer utilized in output may alter output impedance. The concept of Z_v is utilized for supporting output impedance resistivity, its own could be selected to be two times or more than existing reactance as the generic base to regard for dominance.

4.7. SIMULATION RESULTS

Single line diagram of parallel inverters of MG is demonstrated in Figure 4.22. Constructed model of this diagram in MATLAB/Simulink is presented in Figure 4.23. MG system parameters are given in Table 4.2. I_L is utilized as feedback by Inverter 1, whereas I_C is used by Inverter 2. As a result, one of inverters has a resistive impedance output, while the second inverter has inductive impedance.

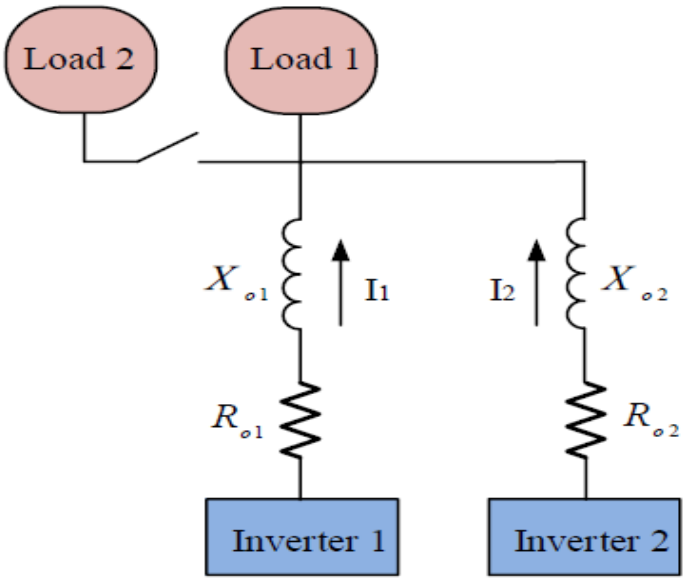

Figure 4.22. Single line diagram of parallel inverters of MG.

Table 4.2. MG system parameters.

Symbol	Description	Value
C	Filter capacitor	30 μF
L_1	Filter inductor (Inverter side)	4 mH
L_2	Filter inductor (Grid side)	4 mH
k_i	The gain of the current control loop	5
k_v	The gain of the voltage control loop	0.01
R_v	Virtual of resistance	20 Ω
L_v	Virtual of inductance	25 mH
n	Voltage droop gain	0.06
m	Frequency droop gain	0.06
f_o	Frequency	50 Hz
V_o	Voltage set point	165 V
L_{o1}, R_{o1}	Equivalent output impedance1	2 mH, 19 Ω
L_{o2}, R_{o2}	Equivalent output impedance2	10 mH, 1.2 Ω
Load 1	Active power	300W
Load 2	Active power	300W

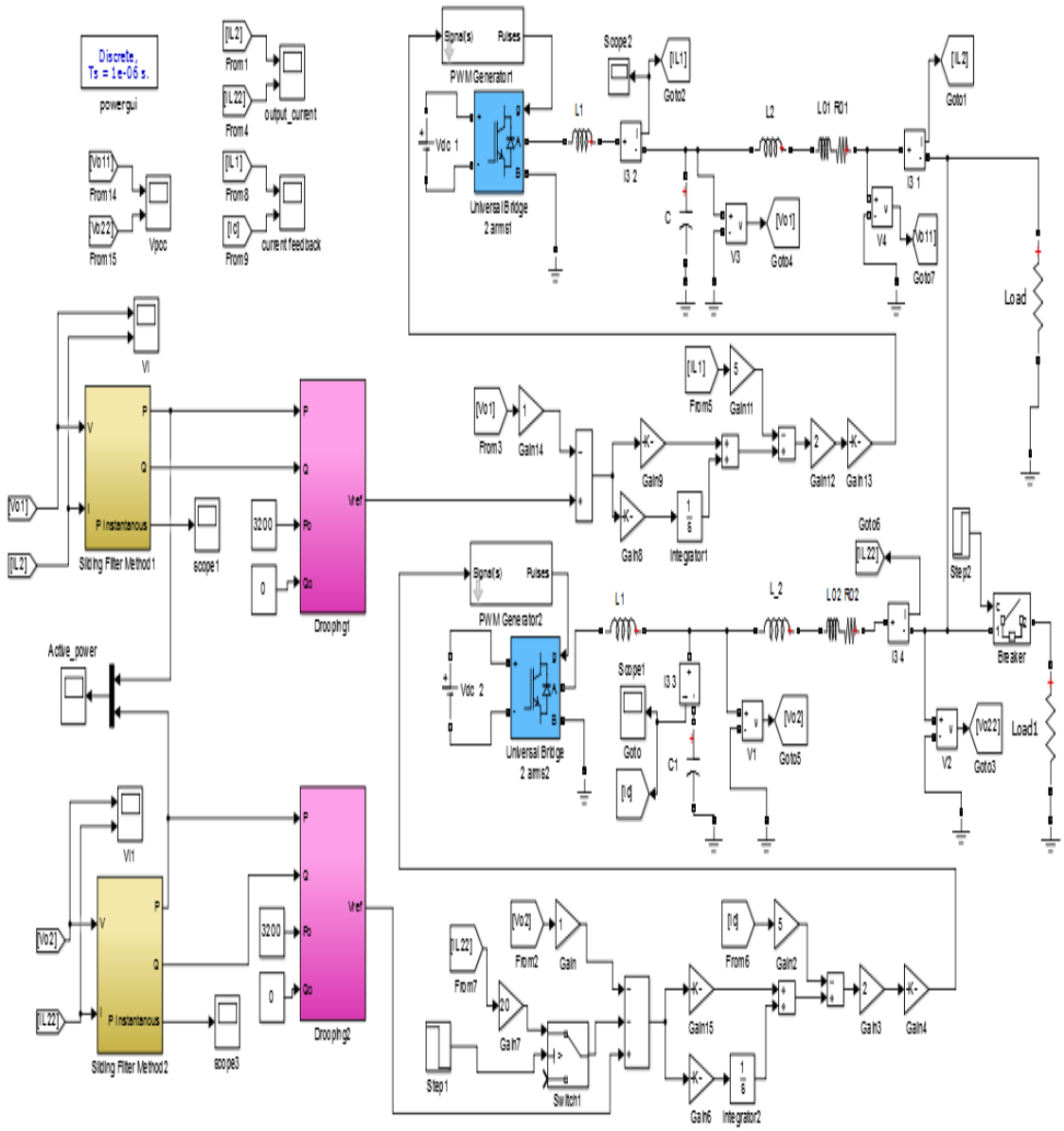

Figure 4.23. MG parallel inverters in MATLAB/Simulink.

The resistive droop controller has applied for sharing power of two inverters. On inverter (2), a virtual impedance was executed because of the large inductive impedance that it has. To make it easier to observe the of Z_v performance, the output power of both inverters is display in Figure 4.24.

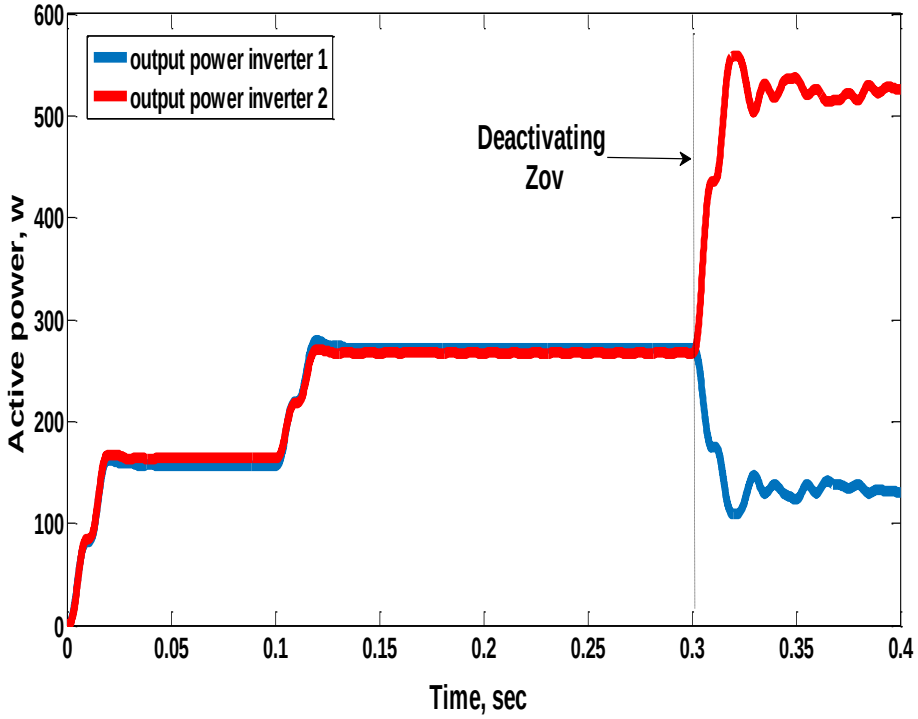

(a) Active power responses

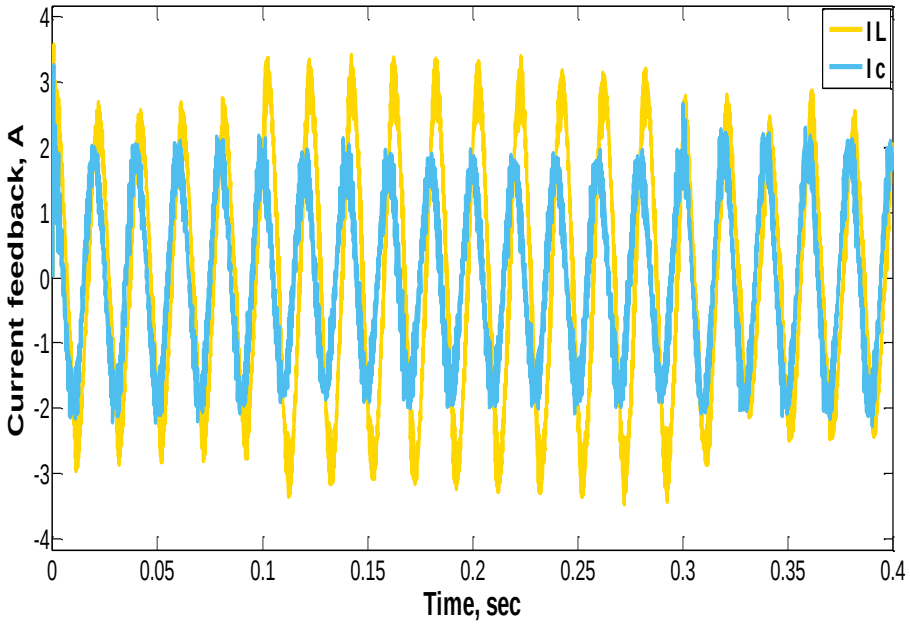

(b) Current feedback responses.

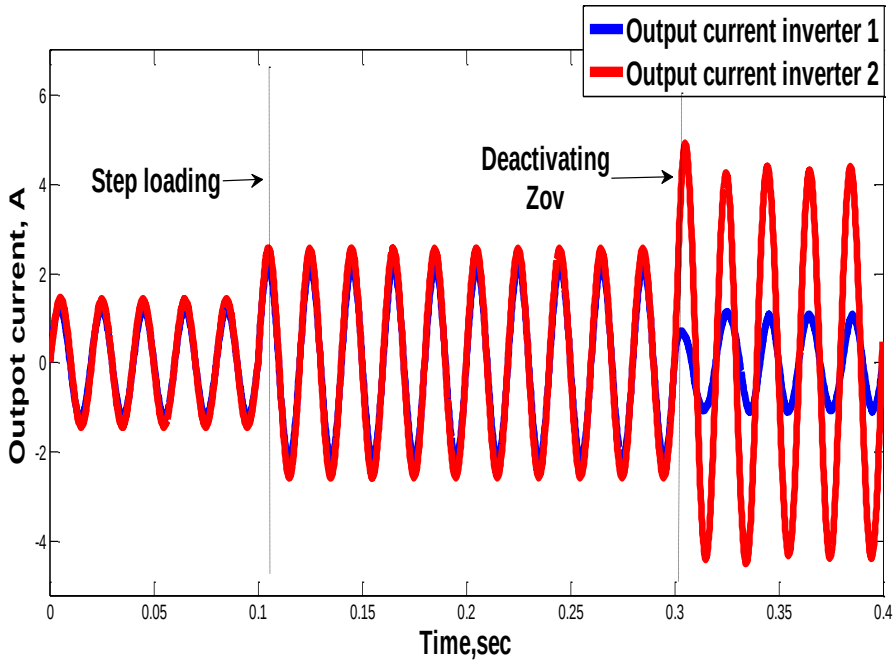

(c) Output current inverters responses.

Figure 4.24. Active power and current responses.

Both inverters are supposed to have operated in parallel and the Z_v is effective. A step loading has been implemented at the time (t=0.1) and it has been noted that each output power is good damped and that the sharing is realized. At the time (t=0.3), the virtual impedance was deactivated that led to the loss of sharing and stability of the power responses. The results appear that the important role of virtual impedance in support of the operation of droop control. The stability could be maintained by low droop gains. That, however, delays the response of power and reduces the precision of sharing. Thus, virtual impedance offers more space for stability with higher gains.

4.8. CONCLUSION

In this chapter, voltage control loops modeling analysis revealed the damping capacity of the resonance by the strategy of dual-loop compared to the strategy of a single loop. Moreover, the results are illustrated the behavior of the output impedance at examining various feedback's signals. For unifying the nature of output impedance of the various controlled inverters as well as for ensuring the appropriate droop control functioning,

the virtual impedance is suggested. The findings of the simulation have been introduced to verify the functioning and efficiency of the suggested controller.

PART 5

IMPROVING ACCURACY REACTIVE POWER SHARING BETWEEN PARALLEL INVERTERS IN ISLANDED MICROGRID

5.1. INTRODUCTION

One of the main issue of parallel inverters working in island mode is the load sharing precision. Several techniques used methods based-communication (Figure 5.1) to realize precise load sharing but those methods require high communication infrastructure bandwidth among all inverters, that raise costs, reduces reliability, addition absence plug-and-play capability that give easily to connect the inverters to the MG without requirements or settings. In addition, losing this link could be very harmful to the controller performance. Droop control technique, which mimics the same synchronous generator's behavior introduced the solution so that the inverters work in parallel with no communication mechanism. To be able the droop controller sharing the reactive power precisely, inverters working in parallel must contain similarly output impedance involving cables impedance and generate similarly output voltage. Even so, in practice, because of the tolerance of parameters in the LC output filter of an inverter, the different lengths of the connection cables, and the inaccuracy of the output voltage control, this cannot be assured. For these reasons, conventional drop control has known for its weak *Q*-sharing performance. This chapter provides an improved method of controlling reactive power-sharing. It uses separate voltage measurements at the PCC bus to estimate output impedance between the PCC bus and the inverters, after that readjusting the gains of the voltage droop control according. Then the controller returns to the conventional controller utilizing a new calculated gain. That enhances controller robustness versus any loss of communication bonds between inverters and central controller. The ability of the suggested controller was shown in the simulation.

.

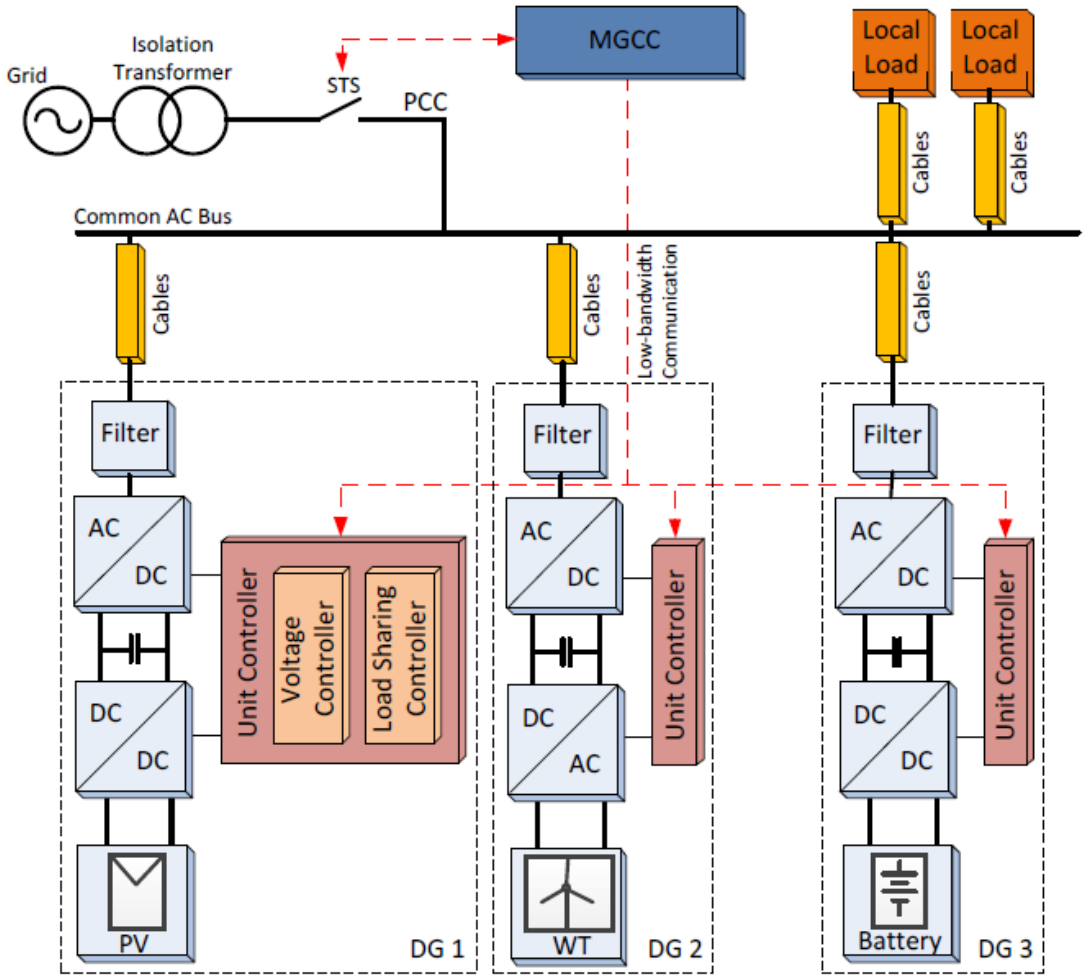

Figure 5.1. Structure of microgrid, including converters.

5.2. ANALYSIS OF SMALL-SIGNAL OF SHARING REACTIVE POWER

A simple MG comprised of 2 inverters is shown in Figure 5.2. Both of them are modeled by their equivalent circuit diagram with two Thevenin terminal, where X_o and V represent impedance Thevenin and the voltage Thevenin successively [4]. A droop control Q-ω and P-V is usually utilized for dominantly resistive impedance of output, while Q-V and P-ω are usually utilized for the dominantly inductive impedance of output [54]. In this chapter, A virtual inductive impedance is used to ensure the output impedance is inductive as indicated in [77], and therefore the Q-V and P-ω droop control is used, see in Figure 5.3. Both inverters are linked to each other via different impedances of the feeder X_{L1} and X_{L2}. The equations of the inverter's conventional droop control (j) become presented through,

$$V_j = V^* - n_j Q_j \tag{5.1}$$

$$\omega_j = \omega^* - m_j P_j \tag{5.2}$$

Where: V_j , ω_j – output voltage & frequency;

V^*, ω^* – Voltage & frequency setpoints;

n_j , m_j – droop coefficients;

P_j , Q_j – Active power & reactive power.

Deviation of small signal of the output voltage (indicate with "~") at (5.1) is giving by,

$$\tilde{V}_j = -n_j \tilde{Q}_j \tag{5.3}$$

This means to the small deviation from V_j relative to the small deviation from Q_j (around the equipoise point) is a linearity relation with a slope $-n_j$, hence the behavior of V_j is specified by,

$$V_j = V_{eq} + \tilde{V}_j \tag{5.4}$$

When selecting the equipoise point V_{eq} as V^*, the expression of the small signal is,

$$V_j = V^* - n_j \tilde{Q}_j \tag{5.5}$$

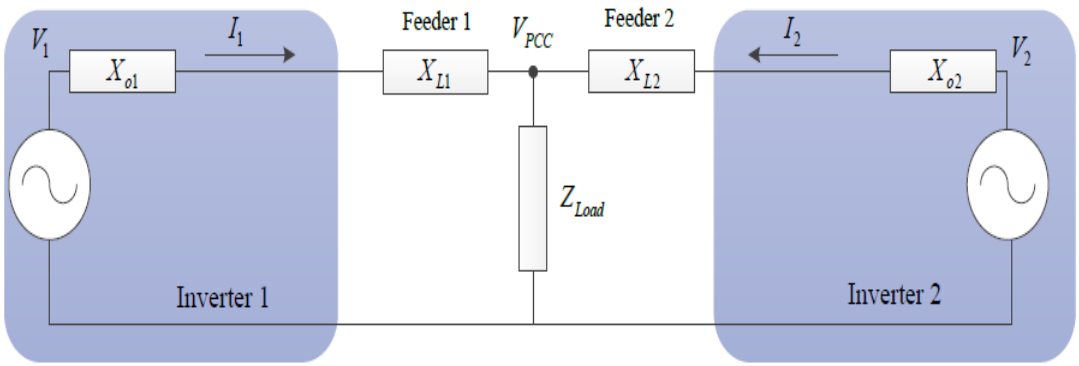

Figure 5.2. Simple islanded-microgrid consisting of two inverters parallel.

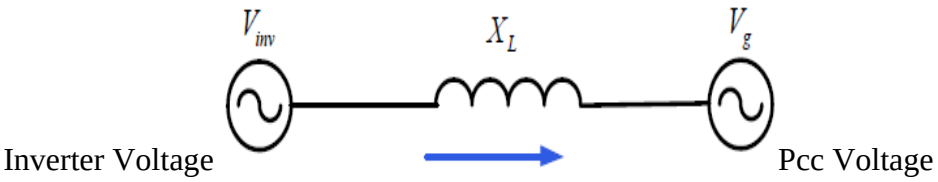

Figure 5.3. Case of the supposition of inductive output impedance for droop control.

There are voltage drops across X_0 and X_L due to the current flow through them, therefore the voltage at V_{PCC} differs from V_1 and V_2. As known that inverter (j) total impedance is $X_j = X_{oj} - X_{Lj}$, it can be shown that the Q-power produced via inverter j is given by:

$$Q_j = \frac{V_j^2 - V_j V_{pcc} \cos \delta_j}{X_j} \tag{5.6}$$

Here δ_j is power angle among V_{pcc} & Vj. With tiny δ_j, the cos $\delta_j \approx 1$ and therefore Q-power is rounded accordingly,

$$Q_j \approx \frac{V_j \Delta V_j}{X_j} \tag{5.7}$$

Where

$$\Delta V_j = V_j - V_{pcc} \tag{5.8}$$

Caused by voltage alter, a little alter (indicate with "~") in Q-power is given as follows,

$$\tilde{Q}_j \approx \frac{1}{X_j} (\Delta V_{eq} \cdot \tilde{V}_j + V_{eq} \cdot \Delta \tilde{V}_j) \tag{5.9}$$

Where V_{eq} and ΔV_{eq} are the equipoise voltage difference ΔV_j and output voltage of inverter V_j where the small disturbance of the signal is carried out. The symbol $\Delta \tilde{V}_j$ indicates a little change in ΔV_j; that is to say $\Delta \tilde{V}_j = \tilde{V}_j - \tilde{V}_{pcc}$. Since $\Delta V_{eq} \ll V_{eq}$ and

the selection of the equipoise point is $V_{eq} = V^{\star}$, the little alter in the Q-power is rounded accordingly,

$$\tilde{Q}_j \approx \frac{V^*}{X_j}\Delta\tilde{V}_j \tag{5.10}$$

Through deviation ΔV_j in (5.8), substituting in (5.10) and rearrangement, the behavior of the output voltage for inverter around equipoise point may be expressed accordingly

$$V_j = V_{eq} + \tilde{V}_j = V^* + \tilde{V}_{pcc} + \frac{X_j}{V^*}\tilde{Q}_j \tag{5.11}$$

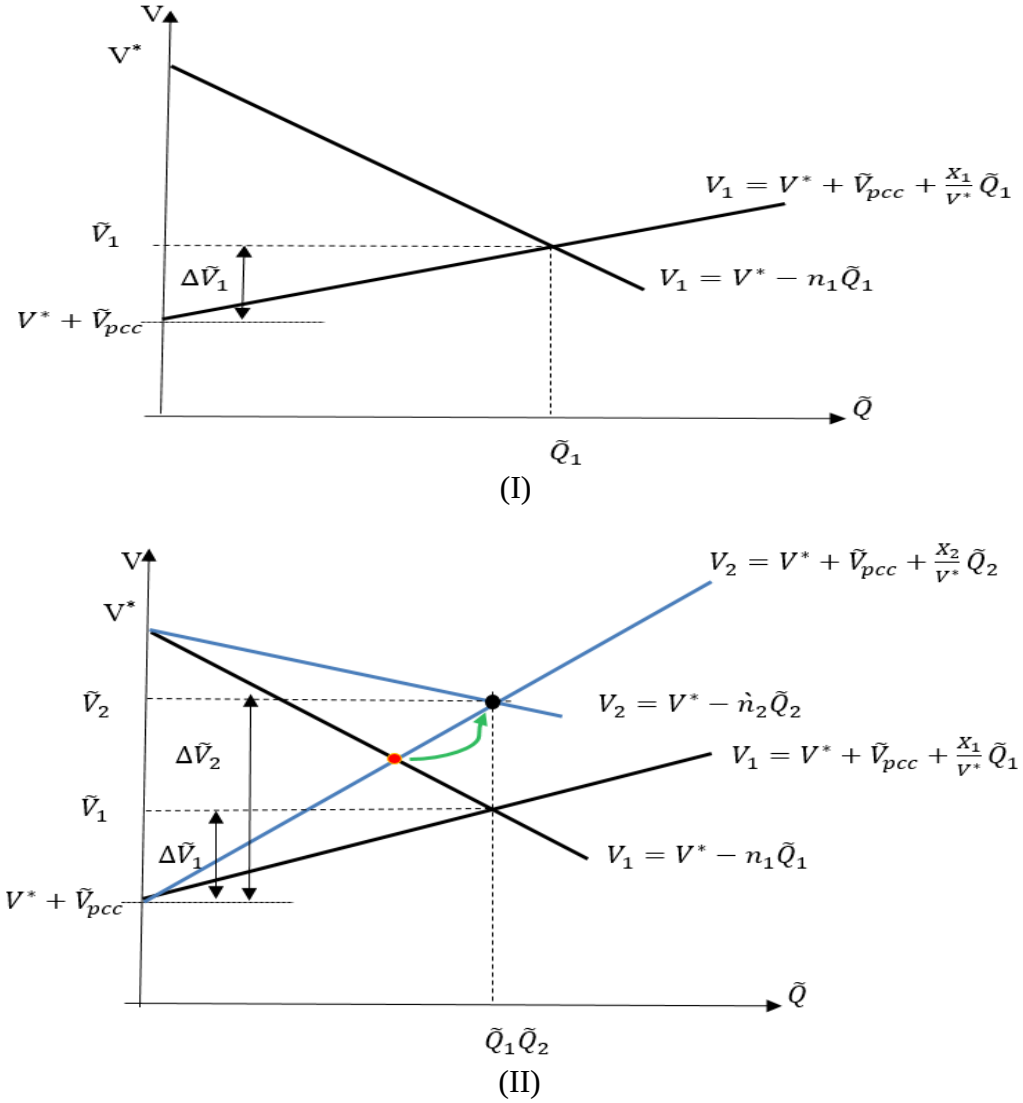

Figure 5.4. Influence the sharing of reactive power through voltage drop.

Equations (5.5) & (5.11) identify relation between V_j and $\tilde{Q}_j$ around the equipoise. Concerning inverter 1, Figure 5.4 (I) equations (5.5) and (5.11) is graphically represented by two lines. Through the intersection of the two lines, *Q*-power output is given. If one of the inverters contains a bigger impedance X_j , slope X_j/V^* in (5.11) would be greater and so as to provide a similar *Q*-power like other inverter, coefficient of voltage droop n_j in (5.5) should be decreased. This is shown in Figure 5.4 (II), in which the total impedance of inverter 2 is greater than that of inverter 1. Consequently, to share *Q*-power equally by both inverters, it is important to minimize Inverter 2 droop coefficient accordingly.

Via substituting (5.5) into (5.11) we get

$$\tilde{Q}_j = \frac{-\tilde{V}_{pcc}}{n_j + X_j/V^*} \tag{5.12}$$

Consequently, for sharing the two inverters reactive power evenly the subsequent condition must be fulfilled,

$$n_1 + \frac{X_1}{V^*} = n_2 + \frac{X_2}{V^*} \tag{5.13}$$

To get reactive power sharing equally, the droop gain n_j must be adjusted in relation to $1/X_j$. In this manner, the inverters that have larger output impedance will decrease voltage drop gain. It is proposed to compute the new droop gain $\grave{n}_j$ as

$$\grave{n}_j = n_j \frac{X_{oj}}{X_j} \tag{5.14}$$

Where X_{oj} is the inverter nominal output impedance, X_j is output impedance which includes connection cable impedances X_{Lj} plus X_{oj} such as $X_j = X_{oj} + X_{Lj}$ (see Figure 5.2). X_{oj} need to be defined to every inverter, whereas X_j could be estimated as follows:

$$X_j = \frac{V^*.\Delta V_j}{Q_j} \tag{5.15}$$

The value X_j is required to compute the doop gain and eventually for improving the reactive power-sharing. At the time all inverters sufficiently share *Q*-power, then X_j value must be calculated. And hence, the output *Q*-power is measured once a precise *Q*-power sharing is achieved utilizing V_{PCC} [67], then the X_j is estimated. Hence, after estimate operation, the conventional droop control unit is recovered but by using newly calculated droop gain, then similarly power-sharing will be given again without V_{PCC}.

By resetting the droop gain such as in (5.14), it could be ensured newly calculated droop gain is less than or equal the previous one. The aforementioned is very significant as instability can occur if new droop gain is excessed the original design value [33].

5.3. THE PROPOSED CONTROLLER

Figure 5.5 displays scheme suggested control. It is composed of 2 phases; In phase 1, the V_{PCC} is utilized by the controller to get a precise sharing value for both inverters, estimating and calculating new voltage drop gain $\grave{n}_j$. In phase 2, the *Q*-power control utilizes the conventional droop, which contains the new droop gain $\grave{n}_j$. The phases are both illustrated in the following.

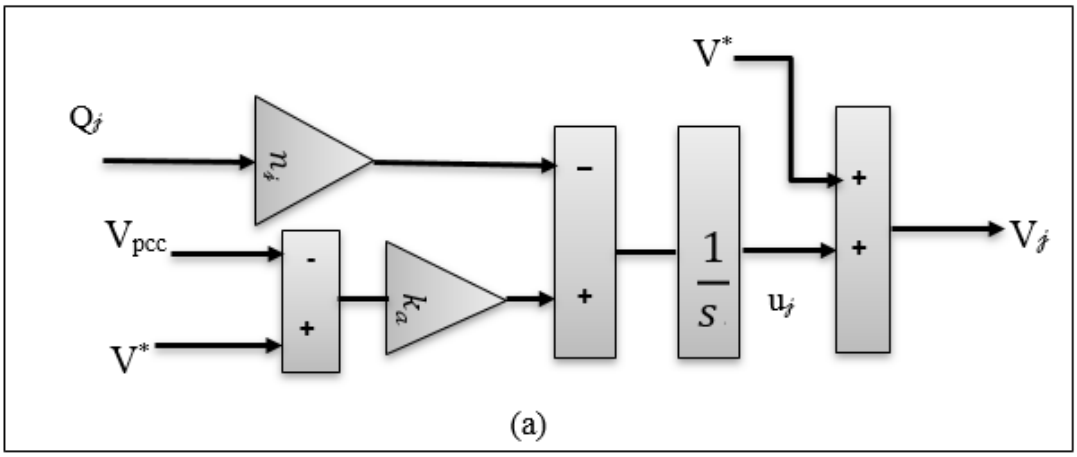

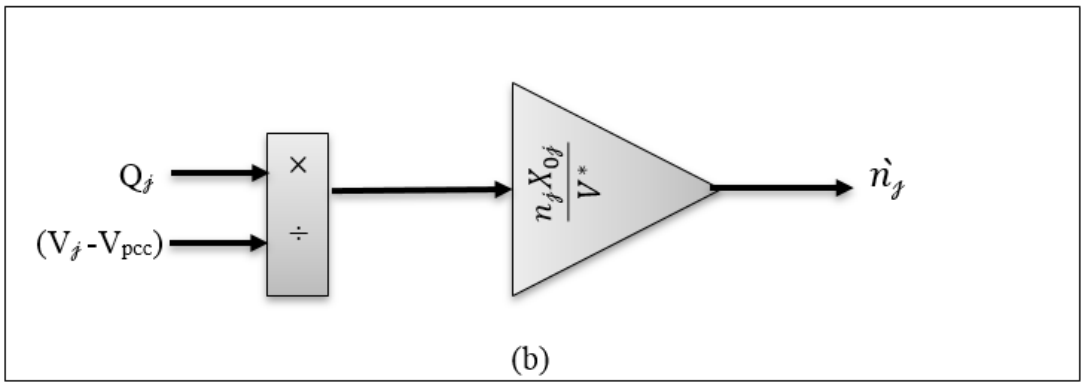

(a) Phase 1

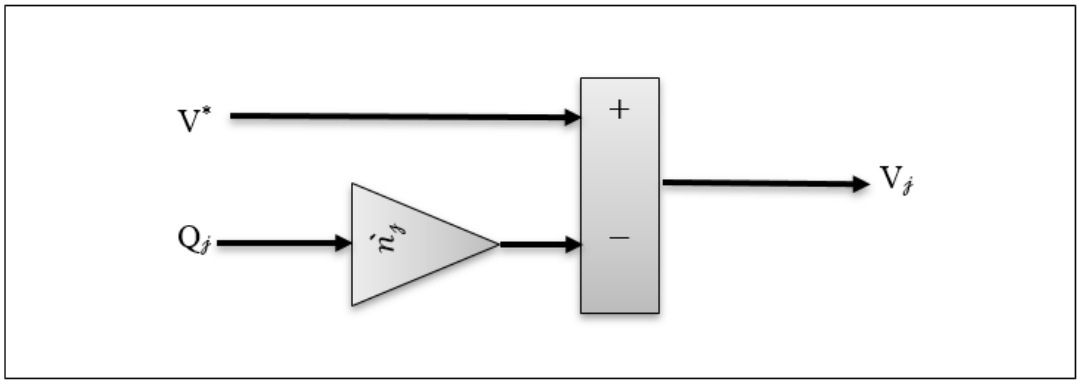

(b) Phase 2

Figure 5.5. Proposed controller scheme: (a) Phase 1; (b) Phase 2.

- **Phase 1**

Within phase 1, $(V * -Vpcc)$ is computed and compared with $n_j * Q_j$, and error is sent by feedback into the controller via the integrator, as suggested in [73], as indicated by Figure 5.5i. Ka is utilized for accelerating a transient signal response if necessary.

The integrator's input will be zero at steady-state case, that implies the *Q*-power can be provided as:

$$Q_j = \frac{K_a(V^* - V_{pcc})}{n_j} \tag{5.16}$$

The right side of (5.16) is equal in both inverters, if each inverter has the same n. Therefore, even if output impedances vary, equal sharing is obtained. The X_j will be estimated utilizing (5.15) when steady-state is achieved, and the n_{new} will be computed with (5.14). All n_{new} are readjusted proportionally with $1 / X_j$ and therefore conventional droop control could be utilized with non-utilizing V_{PCC}.

- **Phase 2**

Within phase 2, there is the transition from control closed-loop which includes measuring the V_{PCC} to conventional control utilizing $\acute{n}_{new}$ computed. with ending of phase 1, (reaching steady-state terms), the V_{out} of the inverter is giving as follows:

$$V_{j(phase\ 1)} = V^* + u_j \tag{5.17}$$

After the new droop gain n' has been adopted by the conventional controller, the V_{out} of the inverter is giving as follows:

$$V_{j(phase\ 2)} = V^* - \grave{n_j} Q_j \tag{5.18}$$

The proposed control can be implemented utilizing a low band-width communication linkage to connect every inverter to MGCC, see Figure 5.6. This linkage submits V_{PCC} to both inverters at the same time (phase 1a) for precise *Q*-sharing. When steady state case is reached (phase 1b), which is signaled to the integrator by a zero input, the new droop gain n ' is calculated. With the ending of phase 1, the synchronous signal submits so both inverters energize (phase 2) simultaneously. in this phase, the $\acute{n}_{new}$ computed is utilized in place of the n_{old} .

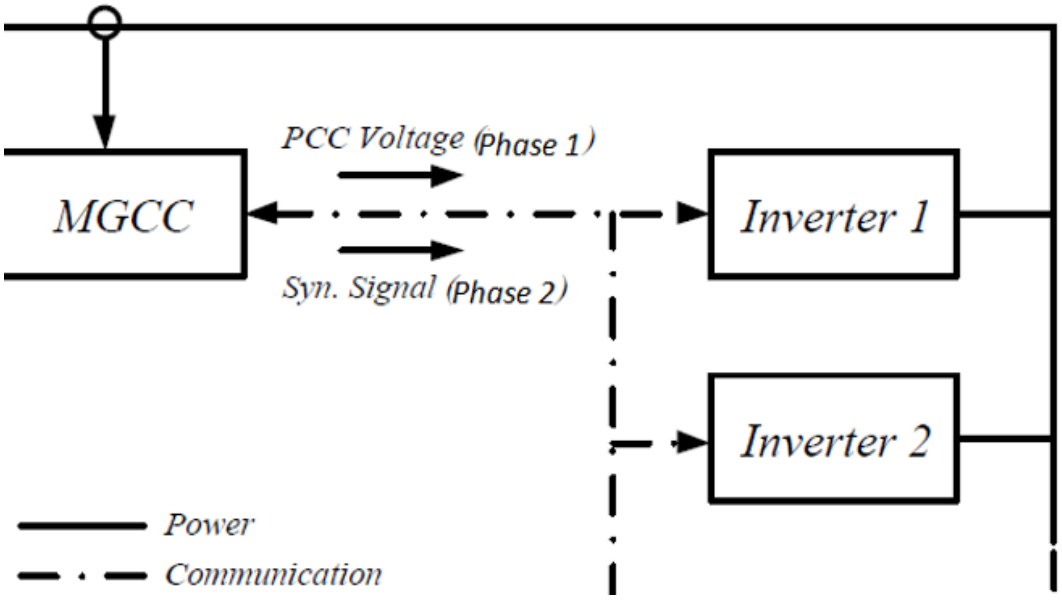

Figure 5.6. Scheme of communication for proposed controller.

5.4. RESULTS OF SIMULATION

As presented in Figure 5.7, the MG consists of two power inverters, which were constructed at MATLAB/Simulink. Each inverter has modeled as the ideal electrical voltage source and an inductive series output impedance (see Figure 5.2). System parameters appear within Table 5.1. Both inverters have the same parameters. Even so, for modeling long interconnecting cable impedance, an additional impedance is entered between PCC and inverter 2 (indicating unequal cable impedances between interconnecting inverters). This simulation is done below various load conditions to validate the suggested controller and compare its performance to the conventional droop control performance.

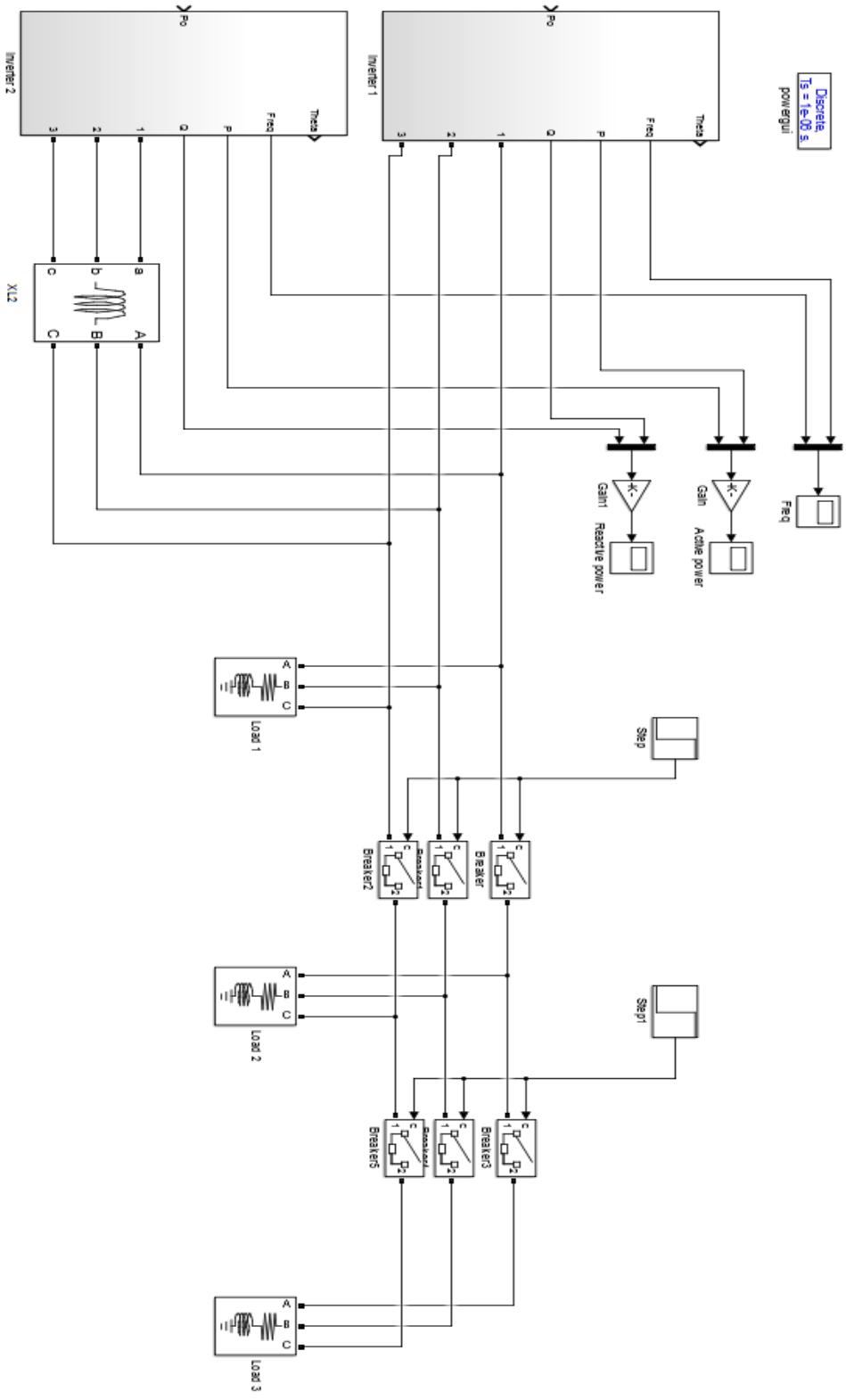

Figure 5.7. Simulation network.

Table 5.1. Parameter values of the Simulation.

Symbols	Detailing	Values
n	Voltage's droop gain	0.002
m	Frequency's droop gain	0.002
f_o	Frequency setpoint	50 Hz
V_o	Voltage setpoint	230 V
X_{o1} R_{01}	Output impedance of inverter 1 (for Simulation only)	2500μH 0.08Ω
X_{o2} R_{02}	Output impedance of inverter 2 (for Simulation only)	2500μH 0.08Ω
X_{L1}	Feeder line impedance of inverter 1	0μH
X_{L2}	Feeder line impedance of inverter 2	500μH
Ka	loop gain	2.64
P_{max}	maximum active power of Inverter	14kW
Q_{max}	maximum reactive power of Inverter	11kVAR

Figure 5.8 shows the reactive power-sharing for two inverters using conventional droop control at various load conditions as follows, low, medium, and high such as 10%, 50%, and 100% of maximum rating *Q*-power of this MG (22 KVAR). It could be seen that the *Q*-power of both inverters is not evenly shared. The steady-state values of simulation outcomes are summarized in Table 5.2.

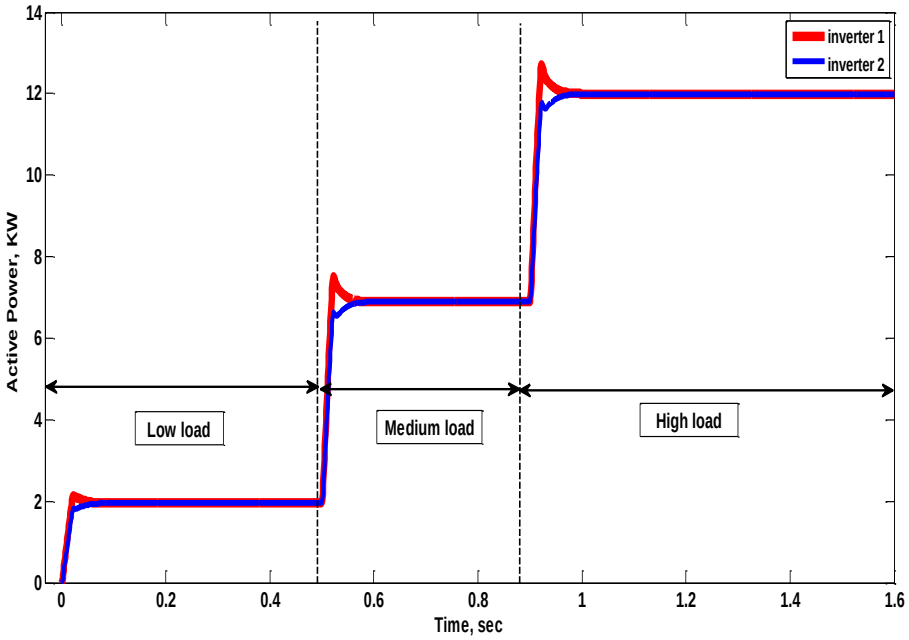

(a) Active power sharing.

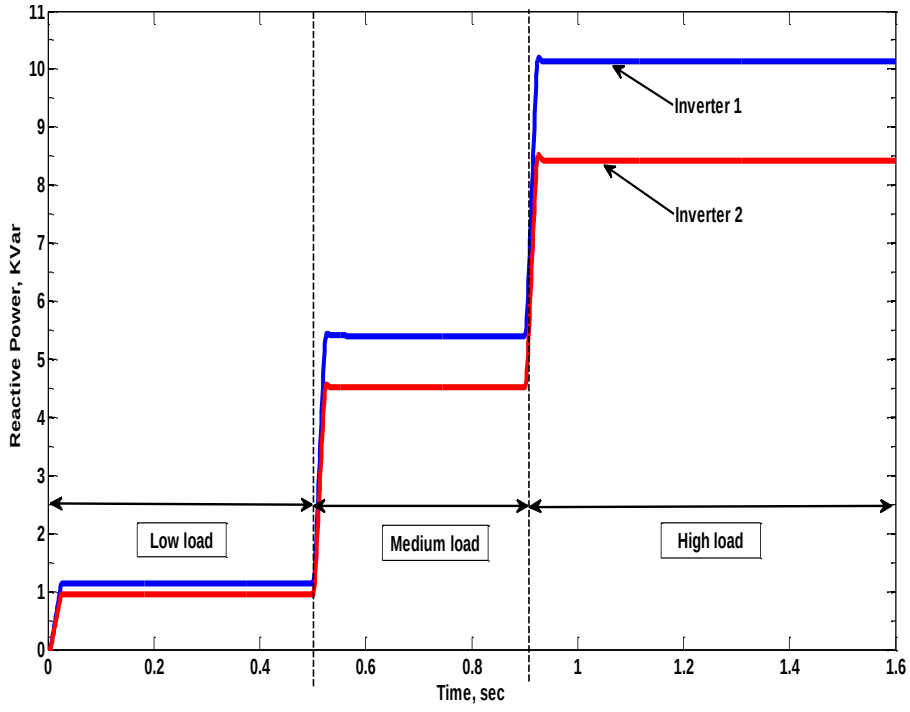

(b) Reactive power sharing.

Figure 5.8. Power-sharing of inverters utilizing conventional droop control for high, medium and low loads.

Reactive power using the suggested control unit below various load terms is presented in Figure 5.9. The conventional droop control is applied up to the Period of simulation

t = 0.3 seconds at which phase 1 is energized, then $\acute{n}_{new}$ is being computed after which energizing phase 2, the controller returns to conventional droop controller but using the $\acute{n}_{new}$. Once the controller has stabilized, then at the time of simulation t = 0.8 s, an unexpected reactive load alter is implemented to check the proposed controller's capacity to preserve well *Q*-sharing,

- A proposed controller is activated at a low reactive load (500 VAR), follow it an unexpected load alters Low to a high level (9200 VAR) as Figure 5.9*a*.
- A proposed controller is activated at a medium reactive load (5000 VAR), follow it an unexpected load alters medium to a high level (12300 VAR) as Figure 5.9*b*.
- A proposed controller is activated at a high reactive load (11200 VAR), follow it an unexpected load alters high to a medium level (5100 VAR) as Figure 5.9*c*.
- A proposed controller is activated at a high reactive high (11200 VAR), follow it an unexpected load alters high to a low level (900 VAR) as Figure 5.9*d*.

All outcomes of the simulation are summed up inside Table 5.2 and that demonstrates enhancement of added proposed controller to share reactive power accurately, compared to conventional control performance results below various load terms.

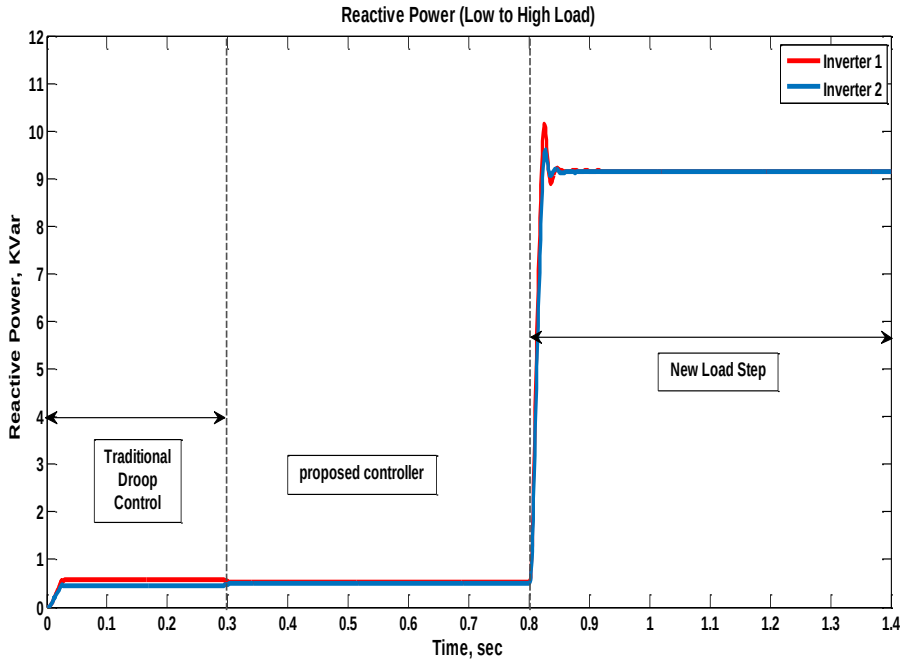

(*a*) Low to high

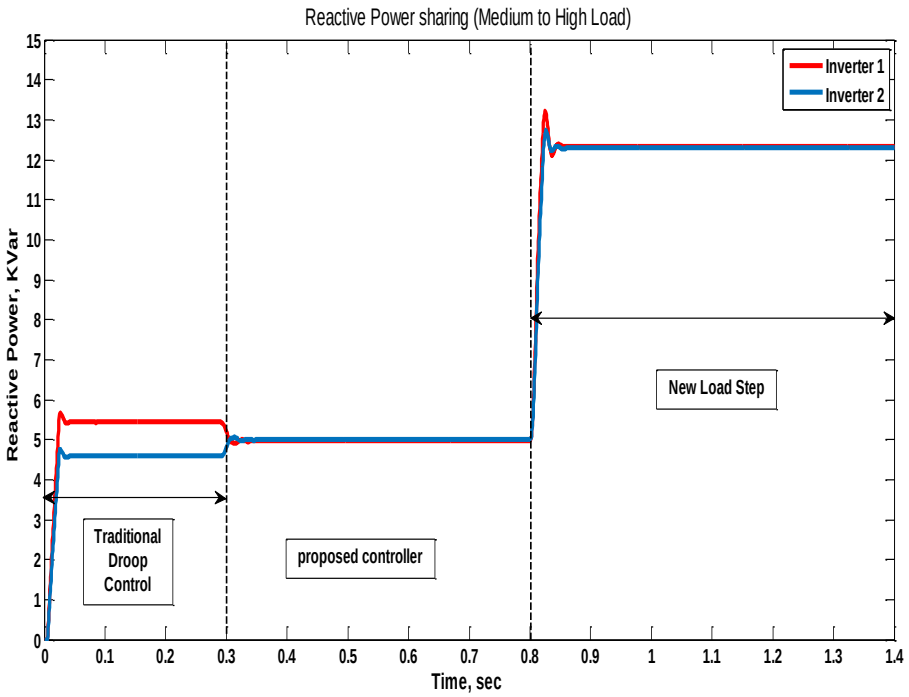

(*b*) Medium to high

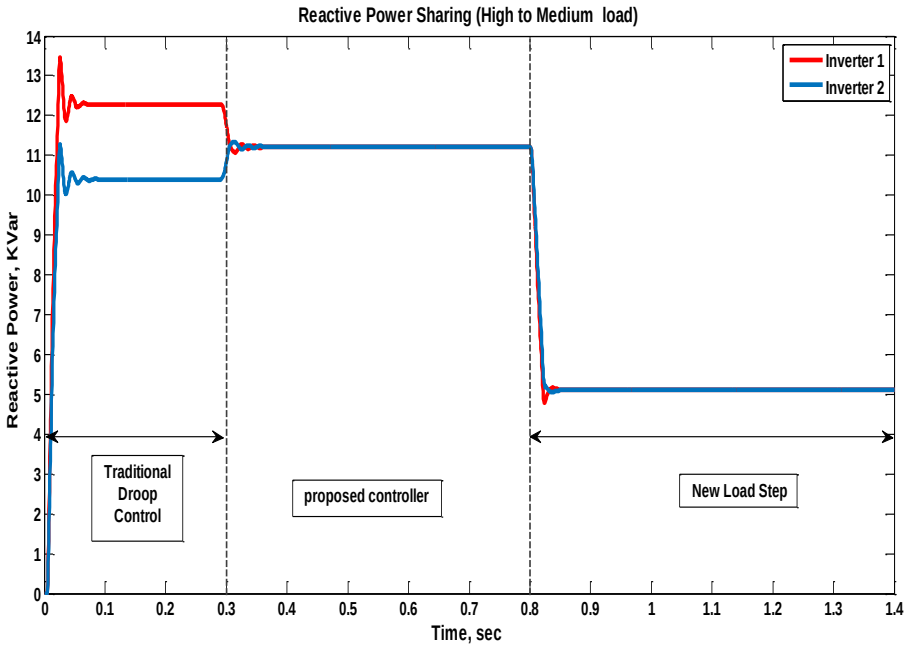

(*c*) High to medium

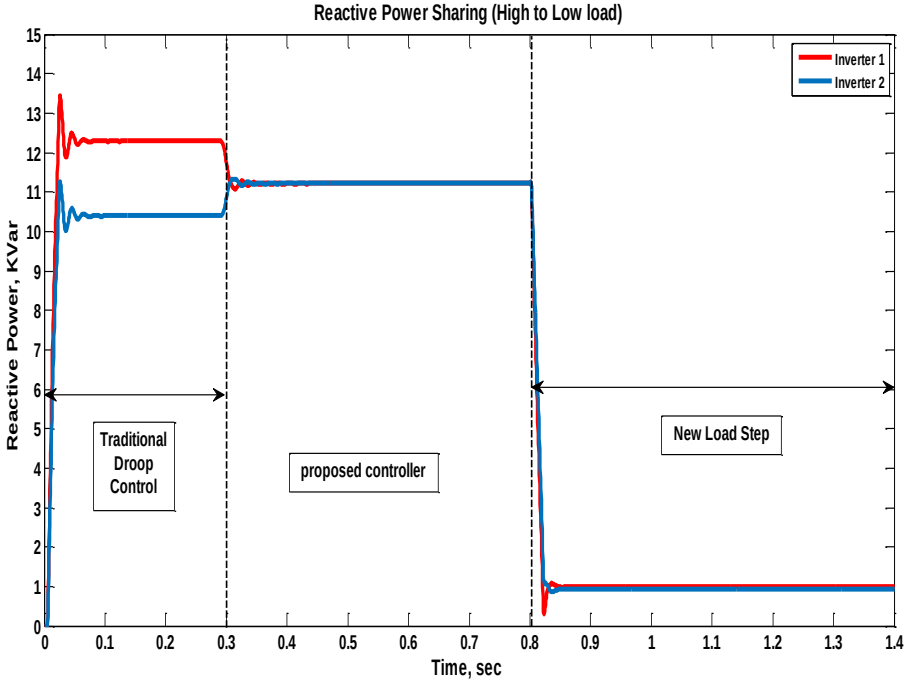

(*d*) High to low

Figure 5.9. Proposed controller simulation outcomes with new loading steps.

Table 5.2. Summary of comparing simulation results between the traditional controller and proposed controller for reactive power sharing.

Droop-control conventional				
State of load		VAR sharing for Inverter 1	VAR sharing for Inverter 2	Error percentage
Low		1130	945	8.9 %
Medium		5405	4510	9 %
High		10120	8420	9.2 %
Proposed Controller				
State of load		VAR sharing for Inverter 1	VAR sharing for Inverter 2	Error percentage
While implementing algorithm (Present load)	After implementing algorithm (New load)			
Low	High	9160	9145	0.08 %
Medium	High	12335	12295	0.16 %
High	Medium	5115	5105	0.09 %
High	Low	988	930	3.0 %

5.5. CONCLUSION

In this chap, a good algorithm of *Q*-power sharing has been proposed between the paralleled inverters in island-mode. To achieve enhanced *Q*-power sharing, the suggested method utilizes measurement intermittently of V_{pcc}. Through this requirement, the output impedance value (mainly supposed to be inductive) of inverters, including cables value, can be estimated. The estimated impedance value is then utilized to compute the new gain of a conventional droop controller that controls *Q*-power sharing during V_{pcc} measurement is unavailable. This new droop control form enhances *Q*-power without the Vpcc having to be measured continuously. This raises system's reliability and stability against the loss of communicating link. However, because the suggested controller supposes that Impedance of inductive output predominates, this could reduce the accuracy of the sharing if it has a significant resistance value. Moreover, the interrupted measurement of the V_{pcc} is managed

according to the development of the microgrid structure (inverters number, cable lengths and loads). Finally, the results of the simulation were displayed to verify the proposed controller performance and efficiency.

PART 6

6.1. CONCLUSION

The thesis studies the control strategies of droop control-based parallel inverters which are used in island microgrid. Thesis' general conclusions summarize as follows:

1. The latest technologies for the interaction between renewable energy and technologies of microgrid control in island mode have surveyed. The literature review shows that the droop control technique is a popular power-sharing method in primary level of control strategy. However, it has many deficiencies and is being improved by research works.
2. In literature, the emphasized effect of various feedback signals on voltage control's loop and on the shape of output impedances is not well explained. The voltage controllers for single and double loops and their effect on stability are studied and system behavior analyzed by utilizing the Bode plot technique when the capacitor/inductor currents are utilized as feedback. Furthermore, differences in the type of output impedance (inductor/resistor) of parallel inverters can affect the accuracy of power-sharing and thus destabilize. A virtual impedance has therefore proposed to reach the system stability and power-sharing by unifying the nature of output impedances. The results appeared that the important role of virtual impedance is to support the operation of droop control.
3. Several techniques adopted methods based on communications to realize good sharing but losing this link could be very harmful to the controller performance. This thesis proposes improving the droop control method of controlling reactive power-sharing. It uses separate voltage measurements at the PCC bus to estimate Z_{out} between the PCC bus and the inverters, after that readjusting the gains of the voltage droop control according. Then the controller returns to the conventional controller utilizing a new calculated gain. That enhances controller robustness versus any loss of communication bonds between inverters and central controller.

The results for proposed method have compared with a conventional method. The comparison reveals that proposed method has better accuracy.

6.2. FUTURE WORK

Since the suggested controller supposes that impedance of inductive output predominates, this could reduce the accuracy of the sharing if it has a significant resistance value. Moreover, the interrupted measurement of the V_{pcc} is managed according to the development of the microgrid structure (inverters number, cable lengths and loads). Thus, this proposed method needs more research and experiments for further development of this research, which will reveal new challenges.

REFERENCES

1. Bert, B. & Stephen, H. T., "Air pollution and health", ***Air Pollut.*** Heal, 115-148 (1999).

2. Hussain, B., Sharkh, S. M., & Hussain, S., "Impact studies of distributed generation on power quality and protection setup of an existing distribution network", ***In SPEEDAM 2010,*** 2(3): 1243-1246 (2010).

3. Carvalho, P. M., Correia, P. F., & Ferreira, L. A., "Distributed reactive power generation control for voltage rise mitigation in distribution networks", ***IEEE transactions on Power Systems,*** 23(2): 766-772 (2008).

4. Abusara, M. A., Guerrero, J. M., & Sharkh, S. M., "Line-interactive UPS for microgrids", ***IEEE Transactions on Industrial Electronics,*** Pisa, Italy, 1292-1300 (2013).

5. Shahid, A., "Smart grid integration of renewable energy systems", **In *2018 7th International Conference on Renewable Energy Research and Applications (ICRERA),*** Paris, France, 944-948) (2018).

6. Justo, J. J., Mwasilu, F., Lee, J., & Jung, J. W., "AC-microgrids versus DC-microgrids with distributed energy resources: A review", ***Renewable and Sustainable Energy Reviews***, 2(4): 387-405 (2013).

7. Mahmoud, M. S., Hussain, S. A., & Abido, M. A., "Modeling and control of microgrid: An overview", ***Journal of the Franklin Institute,*** 351(5): 2822-2859 (2014).

8. Issa, W., & Elkhateb, A., "Virtual Impedance Impact on Inverter Control Topologies", ***In 2018 7th International Conference on Renewable Energy Research and Applications (ICRERA),*** Paris, France, 1423-1428 (2018).

9. Guerrero, J. M., Hang, L., & Uceda, J., "Control of distributed uninterruptible power supply systems", ***IEEE Transactions on Industrial Electronics,*** 55(8): 2845-2859 (2008).

10. Issa, W., Sharkh, S., Mallick, T., & Abusara, M., "Improved reactive power sharing for parallel-operated inverters in islanded microgrids", ***Journal of Power Electronics,*** 16(3): 1152-1162 (2016).

11. Mariam, L., Basu, M., & Conlon, M. F., "A review of existing microgrid architectures", ***Journal of Engineering,*** 20(13): 1-8 (2013).

12. Shoeiby, B., "Current regulator based control strategy for islanded and grid-connected microgrids", ***RMIT University Australia, School of Electrical and Computer Engineering College of Science, Engineering and Health RMIT University Australia,*** Australia, 45-56 (2015).

13. Motjoadi, V., Bokoro, P. N., & Onibonoje, M. O., "A review of microgrid-based approach to rural electrification in South Africa: Architecture and policy framework", ***Energies,*** 13(9): 2193 (2020).

14. Ped, G., Airi, R. and Vasquez, J. C., "Hierarchical Control of an AC Microgrid," ***Master Thesis, Aalborg University Department of Energy Technology,*** Denmark, 66 (2018).

15. Mastromauro, R. A., "Voltage control of a grid-forming converter for an AC microgrid: A real case study", ***In 3rd Renewable Power Generation Conference (RPG 2014),*** Naples, 1-6 (2014).

16. Jiayi, H., Chuanwen, J., & Rong, X., "A review on distributed energy resources and MicroGrid", ***Renewable and Sustainable Energy Reviews,*** 12(9): 2472-2483 (2008).

17. Fu, Q., Nasiri, A., Solanki, A., Bani-Ahmed, A., Weber, L., & Bhavaraju, V., "Microgrids: architectures, controls, protection, and demonstration", ***Electric Power Components and Systems,*** 43(12): 1453-1465 (2015).

18. Lede, A. M. R., Molina, M. G., Martinez, M., & Mercado, P. E., "Microgrid architectures for distributed generation: A brief review", ***In 2017 IEEE PES Innovative Smart Grid Technologies Conference-Latin America***, Quito, Ecuador, 1-6 (2017).

19. Patrao, I., Figueres, E., Garcerá, G., & González-Medina, R., "Microgrid architectures for low voltage distributed generation", ***Renewable and Sustainable Energy Reviews,*** 4(3): 415-424 (2015).

20. Unamuno, E., & Barrena, J. A., "Hybrid ac/dc microgrids—Part I: Review and classification of topologies", ***Renewable and Sustainable Energy Reviews,*** 5(2): 1251-1259 (2015).

21. Guerrero, J. M., Vasquez, J. C., Matas, J., De Vicuña, L. G., & Castilla, M., "Hierarchical control of droop-controlled AC and DC microgrids—A general approach toward standardization", ***IEEE Transactions on Industrial Electronics,*** 58(1): 158-172 (2010).

22. Shafiee, Q., Guerrero, J. M., & Vasquez, J. C., "Distributed secondary control for islanded microgrids—a novel approach", ***IEEE Transactions on Power Electronics,*** 29(2): 1018-1031 (2013).

23. Jadeja, R., Ved, A., Trivedi, T., & Khanduja, G., "Control of power electronic converters in AC microgrid", ***Springer,*** Cham, 329-355 (2020).

24. Luo, F., Lai, Y. M., Chi, K. T., & Loo, K. H., "A triple-droop control scheme for inverter-based microgrids", **In *IECON 2012-38th Annual Conference on IEEE Industrial Electronics Society***, Montreal, Canada, 3368-3375 (2012).

25. Abusara, M. A., & Sharkh, S. M., "Control of line interactive UPS systems in a Microgrid", ***In 2011 IEEE International Symposium on Industrial Electronic****s*, Gdansk, Poland, 1433-1440 (2011).

26. Liang, J., Green, T. C., Weiss, G., & Zhong, Q. C., "Hybrid control of multiple inverters in an island-mode distribution system", ***In IEEE 34th Annual Conference on Power Electronics Specialist, 2003. PESC'03***. 1(2): 61-66 (2003).

27. Vaidya, S., Somalwar, R., & Kadwane, S. G., "Review of various control techniques for power sharing in micro grid", ***In 2016 International Conference on Global Trends in Signal Processing, Information Computing and Communication***, Jalgaon, 438-443 (2016).

28. Katiraei, F., & Iravani, M. R., "Power management strategies for a microgrid with multiple distributed generation units", ***IEEE Transactions on Power Systems,*** 21(4): 1821-1831 (2006).

29. Lopes, J. P., Moreira, C. L., & Madureira, A. G., "Defining control strategies for microgrids islanded operation", ***IEEE Transactions on Power Systems,*** 21(2): 916-924 (2006).

30. Mohd, A., Ortjohann, E., Morton, D., & Omari, O., "Review of control techniques for inverters parallel operation", ***Electric Power Systems Research,*** 80(12): 1477-1487 (2010).

31. Pedrasa, M. A., & Spooner, T., "A survey of techniques used to control microgrid generation and storage during island operation", ***AUPEC2006,*** 2(1)*:* 15 (2006).

32. Guerrero, J. M., Matas, J., De Vicuna, L. G. D. V., Castilla, M., & Miret, J., "Wireless-control strategy for parallel operation of distributed-generation inverters", ***IEEE Transactions on Industrial Electronics,*** 53(5): 1461-1470 (2006).

33. Guerrero, J. M., De Vicuna, L. G., Matas, J., Castilla, M., & Miret, J., "A wireless controller to enhance dynamic performance of parallel inverters in distributed generation systems", ***IEEE Transactions on Power Electronics,*** 19(5): 1205-1213 (2004).

34. Xinchun, L., Feng, F., Shanxu, D., Yong, K., & Jian, C., "The droop characteristic decoupling control of parallel connected UPS with no control interconnection", ***In IEEE International Electric Machines and Drives Conference, 2003. IEMDC'03****,* 3(2): 1777-1780) (2003).

35. Engler, A., & Soultanis, N., "Droop control in LV-grids", ***In 2005 International Conference on Future Power System****s*, Amsterdam, Netherlands, 6 (2005).

36. Guerrero, J. M., Vásquez, J. C., Matas, J., Sosa, J. L., & De Vicuña, L. G., "Parallel operation of uninterruptible power supply systems in microgrids", ***In 2007 European Conference on Power Electronics and Applicatio****ns*, Aalborg, Denmark, 1-9 (2007).

37. Yajuan, G., Weiyang, W., Xiaoqiang, G., & Herong, G., "An improved droop controller for grid-connected voltage source inverter in microgrid", ***In The 2nd International Symposium on Power Electronics for Distributed Generation System****s*, Hefei, China, 823-828 (2010).

38. Majumder, R., Chaudhuri, B., Ghosh, A., Majumder, R., Ledwich, G., & Zare, F., "Improvement of stability and load sharing in an autonomous microgrid using supplementary droop control loop", ***IEEE transactions on Power Systems,*** 25(2): 796-808 (2009).

39. Avelar, H. J., Parreira, W. A., Vieira, J. B., de Freitas, L. C. G., & Coelho, E. A. A., "A state equation model of a single-phase grid-connected inverter using a droop control scheme with extra phase shift control action", ***IEEE Transactions on Industrial Electronics,*** 59(3): 1527-1537 (2011).

40. Coelho, E. A. A., Cortizo, P. C., & Garcia, P. F. D., "Small-signal stability for parallel-connected inverters in stand-alone AC supply systems", ***IEEE Transactions on Industry Applications,*** 38(2): 533-542 (2002).

41. Xinchun, L., Feng, F., Shanxu, D., Yong, K., & Jian, C., "Modeling and stability analysis for two paralleled UPS with no control interconnection", ***In IEEE International Electric Machines and Drives Conference,*** Madison, USA, 1772-1776 (2003).

42. Sanjari, M. J., Kohansal, M., & Gharehpetian, G. B., "An innovative power calculation method to improve power sharing in VSI based Micro Grid", **In** ***Iranian Conference on Smart Grid****s*, Tehran, Iran 1-5 (2012).

43. Gao, M. Z., Chen, M., Jin, C., Guerrero, J. M., & Qian, Z. M., "Analysis, design, and experimental evaluation of power calculation in digital droop-controlled parallel microgrid inverters", **Journal** ***of Zhejiang University Science,*** 14(1): 50-64 (2013).

44. Kang, H. K., Ahn, S. J., & Moon, S. I., "A new method to determine the drop of inverter-based DGs", ***In 2009 IEEE Power & Energy Society General Meetin****g*, USA, 1-6 (2009).

45. Guerrero, J. M., de Vicuna, L. G., Matas, J. S., Miret, J., & Castilla, M., "A wireless load sharing controller to improve dynamic performance of parallel-connected UPS inverters", ***In IEEE 34th Annual Conference on Power Electronics Specialist, 2003. PESC'03****,* Acapulco, Mexico, 1408-1413 (2003).

46. Haddadi, A., Shojaei, A., & Boulet, B., "Enabling high droop gain for improvement of reactive power sharing accuracy in an electronically-interfaced

autonomous microgrid", In ***2011 IEEE Energy Conversion Congress and Exposition***, Phoenix, USA, 673-679 (2011).

47. De Brabandere, K., Bolsens, B., Van den Keybus, J., Woyte, A., Driesen, J., & Belmans, R., "A voltage and frequency droop control method for parallel inverters", ***IEEE Transactions on power electronics,*** 22(4): 1107-1115 (2007).

48. Vásquez, J. C., Guerrero, J. M., Gregorio, E., Rodríguez, P., Teodorescu, R., & Blaabjerg, F., "Adaptive droop control applied to distributed generation inverters connected to the grid", ***In 2008 IEEE International Symposium on Industrial Electronics***, Cambridge, UK, 2420-2425 (2008).

49. Palizban, O., & Kauhaniemi, K., "Hierarchical control structure in microgrids with distributed generation: Island and grid-connected mode", ***Renewable and Sustainable Energy Reviews,*** 4(4): 797-813 (2015).

50. Davison, A. J., Reid, I. D., Molton, N. D., & Stasse, O., "MonoSLAM: Real-time single camera SLAM", ***IEEE Transactions on Pattern Analysis and Machine Intelligence,*** 29(6): 1052-1067 (2007).

51. Guerrero, M., Berbel, J., Matas, L., and Vicuña J., "Decentralized control for parallel operation of distributed generation inverters in microgrids using resistive output impedance," ***IECON Proc. (Industrial Electron. Conf.),*** 54(2): 5149–5154 (2006).

52. Levi, E., "Multiphase electric machines for variable-speed applications", ***IEEE Transactions on Industrial Electronics,*** 55(5): 1893-1909 (2008).

53. Chai, J., & Peng, Y., "Coordinated Power Control for Islanded DC Microgrids Based on Bus-Signaling and Fuzzy Logic Control", ***In 2018 2nd IEEE Conference on Energy Internet and Energy System Integration***, Beijing, 1-6 (2018).

54. Eid, B. M., Abd Rahim, N., Selvaraj, J., & El Khateb, A. H., "Control methods and objectives for electronically coupled distributed energy resources in microgrids: A review", ***IEEE Systems Journal,*** 10(2): 446-458 (2014).

55. Issa, W. R., Abusara, A., & Sharkh, S. M., "Impedance interaction between islanded parallel voltage source inverters and the distribution network", ***7th IET International Conference on Power Electronics***, Manchester, UK, 23-33 (2014).

56. Guerrero, J. M., Berbel, N., de Vicuña, L. G., Matas, J., Miret, J., & Castilla, M., "Droop control method for the parallel operation of online uninterruptible power systems using resistive output impedance", ***In Twenty-First Annual IEEE Applied Power Electronics Conference and Exposition, 2006. APEC'06,*** Dallas, USA, 7 (2006).

57. Skjellnes, T., Skjellnes, A., & Norum, L. E., "Load sharing for parallel inverters without communication", ***In Nordic Workshop in Power and Industrial***

Electronics, Trondheim, 1-5 (2002).

58. Yao, W., Chen, M., Matas, J., Guerrero, J. M., & Qian, Z. M., "Design and analysis of the droop control method for parallel inverters considering the impact of the complex impedance on the power sharing", ***IEEE Transactions on Industrial Electronics,*** 58(2): 576-588 (2010).

59. Pei, Y., Jiang, G., Yang, X., & Wang, Z., "Auto-master-slave control technique of parallel inverters in distributed AC power systems and UPS", ***In 2004 IEEE 35th Annual Power Electronics Specialists Conferenc****e,* Aachen, Germany, 2050-2053 (2004).

60. Lee, W. C., Lee, T. K., Lee, S. H., Kim, K. H., Hyun, D. S., & Suh, I. Y., "A master and slave control strategy for parallel operation of three-phase UPS systems with different ratings", **In *Nineteenth Annual IEEE Applied Power Electronics Conference and Exposition, 2004. APEC'04****,* Anaheim, USA, 456-462 (2004).

61. Cheng, Y. J., & Sng, E. K. K., "A novel communication strategy for decentralized control of paralleled multi-inverter systems", ***IEEE Transactions On Power Electronics,*** 21(1): 148-156 (2006).

62. Tan, J., Lin, H., Zhang, J., & Ying, J., "A novel load sharing control technique for paralleled inverters", ***In IEEE 34th Annual Conference on Power Electronics Specialist, 2003. PESC'03.*** Acapulco, Mexico, 1432-1437 (2003).

63. Tuladhar, A., Jin, H., Unger, T., & Mauch, K., "Control of parallel inverters in distributed AC power systems with consideration of line impedance effect", ***IEEE Transactions on Industry Applications,*** 36(1): 131-138 (2000).

64. Lee, C. T., Chu, C. C., & Cheng, P. T., "A new droop control method for the autonomous operation of distributed energy resource interface converters", ***IEEE Transactions on Power Electronics,*** 28(4): 1980-1993 (2012).

65. Micallef, A., Apap, M., Staines, C. S., & Zapata, J. G., "Secondary control for reactive power sharing and voltage amplitude restoration in droop-controlled islanded microgrids", **In *2012 3rd IEEE International Symposium on Power Electronics for Distributed Generation Systems (PEDG),*** Aalborg, Denmark, 492-498 (2012).

66. Li, Y. W., & Kao, C. N., "An accurate power control strategy for power-electronics-interfaced distributed generation units operating in a low-voltage multibus microgrid", ***IEEE Transactions on Power Electronics,*** 24(12): 2977-2988 (2009).

67. Zhong, Q. C., "Robust droop controller for accurate proportional load sharing among inverters operated in parallel", **IEEE *Transactions on industrial Electronics,*** 60(4): 1281-1290 (2011).

68. He, J., & Li, Y. W., "An enhanced microgrid load demand sharing strategy", ***IEEE***

Transactions on Power Electronics, 27(9): 3984-3995 (2012).

69. He, J., Li, Y. W., Guerrero, J. M., Vasquez, J. C., & Blaabjerg, F., "An islanding microgrid reactive power sharing scheme enhanced by programmed virtual impedances", ***In 2012 3rd IEEE International Symposium on Power Electronics for Distributed Generation Systems (PEDG)***, Aalborg, Denmark, 229-235 (2012).

70. He, J., Li, Y. W., Guerrero, J. M., Blaabjerg, F., & Vasquez, J. C., "An islanding microgrid power sharing approach using enhanced virtual impedance control scheme", ***IEEE Transactions on Power Electronics,*** 28(11): 5272-5282 (2013).

71. Amir, A., Che, H. S., Amir, A., El Khateb, A., & Abd Rahim, N., "Transformerless high gain boost and buck-boost DC-DC converters based on extendable switched capacitor (SC) cell for stand-alone photovoltaic system", ***Solar Energy,*** 17(1): 212-222 (2018).

72. Attia, H. A., Freddy, T. K. S., Che, H. S., Hew, W. P., & El Khateb, A. H., "Confined band variable switching frequency pulse width modulation (CB-VSF PWM) for a single-phase inverter with an LCL filter", ***IEEE Transactions on Power Electronics,*** 32(11): 8593-8605 (2016).

73. El Khateb, A., Abd Rahim, N., Selvaraj, J., & Uddin, M. N., "Fuzzy-logic-controller-based SEPIC converter for maximum power point tracking", ***IEEE Transactions on Industry Applications,*** 50(4): 2349-2358 (2014).

74. Abusara, M. A., Jamil, M., & Sharkh, S. M., "Repetitive current control of an interleaved grid-connected inverter", ***In 2012 3rd IEEE International Symposium on Power Electronics for Distributed Generation Systems (PEDG),*** Aalborg, Denmark, 558-563 (2012).

75. Escobar, G., Mattavelli, P., Stankovic, A. M., Valdez, A. A., & Leyva-Ramos, J., "An adaptive control for UPS to compensate unbalance and harmonic distortion using a combined capacitor/load current sensing", ***IEEE Transactions on Industrial Electronics,*** 54(2): 839-847 (2007).

76. Ortega, R., Figueres, E., Garcerá, G., Trujillo, C. L., & Velasco, D., "Control techniques for reduction of the total harmonic distortion in voltage applied to a single-phase inverter with nonlinear loads", ***Renewable and Sustainable Energy Reviews,*** 16(3): 1754-1761 (2012).

77. Guerrero, J. M., De Vicuna, L. G., Matas, J., Castilla, M., & Miret, J., "Output impedance design of parallel-connected UPS inverters with wireless load-sharing control", ***IEEE Transactions on Industrial Electronics,*** 52(4): 1126-1135 (2005).